The origin of novelties in evolution: evolution of the protoconch II of planktotrophic gastropod larvae

by

Alison Mary Page
B.Sc. Animal Biology, University of Alberta, 2006

A Thesis Submitted in Partial Fulfillment
of the Requirements for the Degree of

MASTER OF SCIENCE

in the Department of Biology

Supervisory Committee

The origin of novelties in evolution: evolution of the protoconch II of planktotrophic gastropod larvae

by

Alison Mary Page
B.Sc., University of Alberta, 2006

Supervisory Committee

Dr. Louise R. Page, (Department of Biology)
Supervisor

Dr. S. Kim Juniper (Department of Biology and School of Earth and Ocean Sciences)
Departmental Member

Dr. Steve Perlman (Department of Biology)
Departmental Member

Abstract

Supervisory Committee
Dr. Louise R. Page (Department of Biology)
Supervisor

Dr. S. Kim Juniper (Department of Biology and School of Earth and Ocean Sciences)
Departmental Member

Dr. Steve Perlman (Department of Biology)
Departmental Member

My research tested hypotheses about the evolutionary origin of a novel feature by modification of development. The novelty is the growing larval shell of gastropod molluscs, which emerged when gastropod larvae acquired the ability to feed. One hypothesis states that the growing larval shell in the Heterobranchia is a continuation of the embryonic phase of shell secretion. The second hypothesis states that the larval shell in the Caenogastropoda may be a precocious juvenile shell. These hypotheses implicate heterochrony. To test these hypotheses, I examined ultrastructural features of the shell-secreting cells of two or three life history stages in a member of each of four clades of gastropods: the Patellogastropoda, Vetigastropoda, Caenogastropoda, and Heterobranchia. My results are consistent with the first hypothesis, but I found no ultrastructural support for the second hypothesis. These results provide the most comprehensive comparative data set on the ontogeny of shell-secreting cells for the Gastropoda.

Table of Contents

List of Tables

List of Figures

Acknowledgments

I would like first to acknowledge the support and encouragement of my supervisor, Dr. Louise R. Page, without which this thesis would certainly not have been possible. Her knowledge, guidance, patience and understanding has helped me time and time again during my time here at the University of Victoria. I would like to thank the staff in the Aquatics Facility: Brian Ringwood, Amy Hoare and Brendon Campbell for their advice, assistance with feeding and aquaria set-up, friendship, and patience with me when I have called with "aquatic emergencies" these past three years. Many thanks to Brent Gowen in the Electron Microscopy Lab for his patience and advice with sectioning and the electron microscopes, for loaning me his killer BBC DVD collection and for his sense of humour, that made the hours I spent in the EM lab memorable! Thanks to my committee members Dr. Kim Juniper and Dr. Steve Perlman. Many thanks to my lab-mates over the years: Will Duguid and Heather Stewart (my fellow GastroGirl). Finally I would like to thank my friends and family, without whom I never would have made it through this alive: my parents Bill and Carol Page and my brother Ian, my husband Ryan Nelson and sister-in-law Michelle Nelson, my best friend and invertebrate-partner-in-crime Erin Pemberton, and bffs Pam Mah, Matthew Boeckner, and Karyn Suchy.

Dedication

I would like to dedicate this thesis to my parents, Bill and Carol Page, who have always supported and encouraged me, no matter what I've set out to do. I remember when I was 10 years old, telling my Dad (a microbiologist), "I'll never study anything that I have to use a microscope to see!" I was wrong.

Introduction

1.1 Definition and evolutionary origin of novelties

It is the mystery and beauty of organic form that sets the problem for us.

-Ross Harrison, embryologist (1913)

Novelties incite our curiosity as biologists and prompt us to ask the question: How do novelties arise during evolution? Development may hold the key to explaining the origin of novelties, because evolution of morphology must occur by changes to the developmental events that generate morphology during each new generation. The mechanics of development is where the origin of evolutionary novelties should be investigated (Müller and Wagner, 1991; Hall, 1999; True and Haag, 2001; Müller and Newman, 2005).

What is the exact definition of a novelty or a novel trait? Can a single definition encompass all parameters of the concept of novelty? Moczek (2008) recently reviewed several historical and modern definitions of the term novelty and pointed-out shortcomings of each. Ultimately, Moczek (2008) concluded that the debate about the definition of novelty is closely related to the long-standing debate about the definition of homology.

A classical definition of an evolutionary novelty, as suggested by Ernst Mayr (1960), is “any newly acquired structure or property that permits the assumption of a new function” (Mayr, 1960). This definition seems straightforward and should make it simple to identify and characterize a novelty. Moczek (2008) provides the example of colour patterns on the wings of Lepidoptera (butterflies and moths), which are produced by

coloured scales secreted by wing epithelial cells. Coloured scales give wings the novel function of mate recognition. These scales are homologous to wing setae on the closest insect relatives of Lepidoptera, but wing setae do not serve the function of mate recognition (Silberglied, 1984). Wing scales of Lepidoptera would therefore fit Mayr's concept of a novelty. However, the problem with coupling function to a definition of novelty is that function provides no insight into the origin of novel traits. Function cannot be selected until the trait serving the function already exists in some form. Selection can act only on pre-existing traits and therefore selection cannot explain origin.

Another definition of a novelty that was reviewed by Moczek (2008) is that given by Gerd Müller (1990), who described novelty as "a qualitatively new structure with a discontinuous origin, marking a relatively abrupt deviation from the ancestral condition". Under Müller's definition, a novel trait can have homologues within related organisms, but the trait can be judged as novel if it is sufficiently different from the range of variation exhibited in close relatives (Moczek, 2008; Müller, 1990). This, however, still presents a limitation - how different from the average variation in a sister group must a trait be in order to be considered a true novelty? How can qualitative and quantitative parameters be distinguished in order to apply this definition of novelty?

Müller and Wagner (1991) subsequently proposed the most rigorous definition to date for an evolutionary novelty. They stated that: "A morphological novelty is a structure that is neither homologous to any structure in the ancestral species nor homonomous to any other structure in the same organism". Moczek (2008) points out that traits conforming to this last definition of novelty are the most challenging to explain under evolutionary theory and he goes on to explore the possibility that developmental

canalization, plasticity, and threshold responses may ultimately provide an explanation for novelties that appear to have no homologues in related organisms. However, he also points out that developmental studies can also hold the key to understanding mechanisms that have allowed emergence of dramatic change to homologous traits; that is, novelties under the second definition of Müller (1990).

My study focused on the growing larval shell of feeding (planktotrophic) gastropod larvae as a novel feature within the life history of these molluscs. Current phylogenetic hypotheses for gastropods suggest that the ancestral life history pattern consisted of three stages: an embryo that secreted an embryonic shell (protoconch), a pelagic larval stage that did not feed or grow and therefore did not have a growing shell, and a post-metamorphic stage that did secrete a shell to accommodate body growth. When larvae acquired the ability to feed, they grew in body size prior to metamorphosis, and growth of soft tissues required a larval shell that could also grow. The insertion of a phase of larval shell growth is a novelty under the second definition described above, because the shell-secreting tissues in all life history stages of gastropods are ontogenetic homologues (Haszprunar, 1992). I have explored the possibility that shell growth by feeding gastropod larvae originated as either a developmentally extended phase of embryonic shell growth or as a precociously initiated phase of post-metamorphic shell growth. Justification for these hypotheses requires background information about the process of shell biomineralization in molluscs and further information about life history evolution and phases of shell secretion during the development of gastropod molluscs.

1.2 Shell biomineralization in adult molluscs

The formation of biomineralized structures among metazoans has facilitated many aspects of the adaptive radiation and diversification of these taxa since the Cambrian Explosion. The molluscan shell is a well-studied biomineralized exoskeletal structure that has remarkable biomechanical properties (Wilt *et al*., 2003). The process of biomineralization involves the incorporation of ions from solution into a framework of organic macromolecules to form a solid material that is a composite of mineral and organic matrix (Simkiss and Wilbur, 1989; Lowenstam and Weiner, 1989). The gastropod shell consists of multiple layers that may differ in mineral type and crystal orientation and is covered externally by a proteinaceous outer layer, the periostracum (Wilt *et al.*, 2003). The adult sclerotized periostracum functions as a protective layer over the shell and may serve to prevent dissolution of mineral ions of the shell (Saleuddin and Petit, 1983).

Both the shell and periostracum of molluscs is secreted by the mantle, which is the epithelium covering the dorsal surface or visceral mass. Mantle epithelium forms an inward fold, the mantle fold, that delineates the mantle cavity (Fig. 1). The mantle cavity houses one or more gills (ctenidia), one or more osphradia (sensory structures) and receives the discharge openings of the digestive tract and metanephridia. The periostracum is secreted by a discrete population of cells located at the periphery of the mantle fold in adult molluscs. The exact organization and ultrastructure of cells responsible for the formation and secretion of the growing periostracum varies amongst species, but their location at the edge of the mantle fold is consistent (Saleuddin and Petit, 1983).

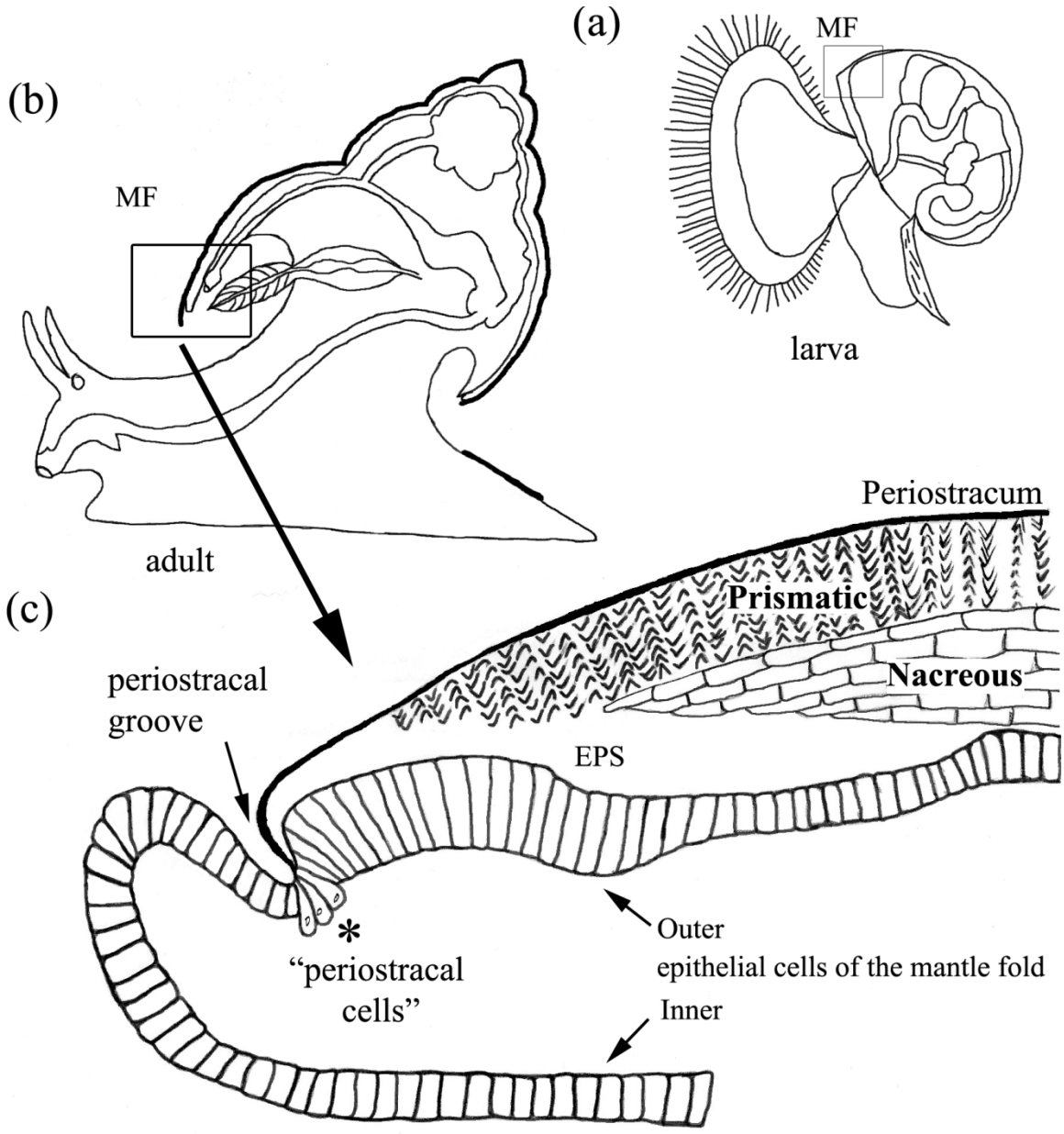

Figure 1. Site of new shell formation in larval and adult gastropods. **(a)** Veliger larva, highlighted region is the mantle fold (MF) where periostracum and shell secretion occurs. Adapted from Ruppert *et al.* (2004). **(b)** Generalized adult shelled gastropod, highlighted region is the mantle fold tissue (MF), the region where new shell and periostracum material is formed and added to the aperture of the shell. Adapted from Pearse *et. al.* (1987). **(c)** Detail of MF showing the layers of the adult gastropod shell, the first outer organic layer the periostracum, followed by the prismatic calcitic layer, and finally the inner aragonitic nacreous layer. The growing edge of the periostracum inserts into the "periostracal groove" and is formed by the "periostracal cells". Cells of the inner mantle epithelium face the outer environment (water within the mantle cavity) and cells of the outer mantle epithelium face the extrapallial space (EPS). Adapted from Saleuddin and Petit (1983) and Wilt *et al.* (2003).

The biomineral component of the shell is deposited at the peripheral margin of the pre-existing shell within a space delineated by the periostracum and the outer epithelium of the mantle fold (Saleuddin and Petit, 1983; Simkiss and Wilbur, 1989) (Fig. 1). This space is known as the extrapallial space (EPS). The extrapallial space is sealed-off from the surrounding seawater only if the periostracum is tightly bound to the periphery of the mantle fold epithelium.

The first step of biomineral formation is secretion of organic macromolecules, the so-called organic matrix, within the delineated space for biomineralization. Although the organic matrix is a minor component of the total make-up of the shell (1-5% per unit weight), while calcium carbonate accounts for 95-99%, the organic matrix is essential for determining the mineral composition (calcite or aragonite), the crystal orientation, and the overall shape of the shell biomineral (Simkiss and Wilbur, 1989; Marin and Luquet, 2004; Addadi *et al*., 2006). It also contributes substantially to the biomechanical properties of molluscan shell (Currey, 1980). Matrix material may vary between taxa, however common components have been identified as ß-chitin, silk fibroin similar to spider silk, and a complex of hydrophilic acidic proteins (Simkiss and Wilbur, 1989; Addadi *et al*., 2006).

The initial model for the relationship between mineral and organic components of the mollusc shell was proposed by Weiner *et. al.* (1984) and was known as the epitactic matrix model. According to this model, the insoluble ß-chitin and silk fibroin macromolecules of the matrix form a scaffold upon which the soluble, hydrophilic proteins form a nucleating surface for the mineral phase. The soluble matrix proteins are often negatively charged, polyanionic proteins (enriched with aspartic and glutamic acid

residues) whose anionic groups bind calcium cations and control the polymorph formed (either calcite or aragonite) (Falini *et al.,* 1996) and the orientation of the crystal polymorph (Shen *et al.*, 1997). As biomineral is deposited, the soluble proteins become entombed within the growing biomineral (Shen *et al.,* 1997). This highly packed network of both soluble and insoluble matrix proteins, together with the layers of biomineral, strengthens the integrity of the shell as a whole (Simkiss and Wilbur, 1989; Falini *et al*., 1996; Shen *et al.*, 1997).

The epitactic matrix model has been slightly modified in recent years, in that the silk proteins are no longer believed to exist as a coating on the ß-chitin prior to mineral nucleation. Instead, the silk fibroin is thought to be a highly hydrated gel that fills the envelopes of ß-chitin scaffolding prior to mineral deposition (Addadi *et al*., 2006). The silk gel may maintain the spacing between adjacent crystal layers during the mineralization process. Presumably, the silk proteins become progressively dehydrated and compressed between the sheets of ß-chitin and the mineral layers as biomineralization proceeds (Addadi *et al.*, 2006).

The calcium and carbonate ions necessary for shell formation are taken up from seawater by the inner epithelium of the mantle fold. Seawater bathing this epithelial layer is continuously replenished as water is circulated through the mantle cavity for gas exchange across the gills. Calcium ions may also be absorbed across the wall of the gut and carbon dioxide generated by respiration may contribute to formation of carbonate ions (Marin and Luquet, 2004; Addadi *et al*., 2006).

Although it has long been believed that the calcium carbonate mineral of molluscan shells, either aragonite or calcite, is precipitated from a supersaturated solution

of calcium within the extrapallial space described above, a perplexing aspect of this hypothesis comes from the result of calculations indicating that the volume of saturated $CaCO_3$ solution needed would be 10^5 larger than the mineral volume deposited (Addadi *et al*., 2006). A possible solution to this enigma, at least for aragonitic shell layers, comes from relatively recent data suggesting that aragonitic shells of both larval and adult molluscs may be initially deposited as amorphous (non-crystalline) calcium carbonate (Weiss *et al*., 2002; Marin and Luquet, 2004). Evidence suggests that concretions of amorphous calcium carbonate may be initially deposited within intracellular vesicles of the shell-secreting mantle, and then deposited onto the organic matrix where they subsequently transform to aragonite crystals.

1.3 Life history evolution in gastropods

The majority of marine invertebrates have a complex life cycle that includes two free-living stages after an initial period of embryogenesis. These two stages are a pelagic larva and a benthic juvenile-adult (pelagobenthic life cycle). There have been opposing views on the evolutionary origin of this pelagobenthic life history within the Mollusca and in marine invertebrates in general (reviewed by Degnan and Degnan, 2006; Page, 2009).

Under the terminal addition hypothesis, ancestral metazoans were holopelagic and resembled feeding larvae of extant marine invertebrates. The benthic adults of extant marine invertebrates originated as a terminal addition to the ancestral, holopelagic life history (Jägersten, 1972; Nielsen and Nørrevang, 1985; Davidson *et al*., 1995). Under this hypothesis, the initial pelagobenthic life history included a feeding larva that

recapitulated the former adult stage, but sexual maturity was shunted to the added-on benthic stage. Alternatively, under the intercalation hypothesis, the ancestral life history was direct development; eggs became embryos that developed directly into benthic juveniles then adults. A free-living pelagic larval stage was subsequently intercalated into this life history (Wolpert, 1999; Collins and Valentine, 2001). According to the intercalation hypothesis, the larval stage of the first metazoans with a complex life cycle was a pelagic embryo that did not feed. Pelagic larvae that were able to feed were then a secondary evolutionary emergence.

For gastropod molluscs, phylogenetic analyses based on morphological (Ponder and Lindberg, 1997) and molecular data (Aktipis *et al*., 2008) and interpretations of the gastropod fossil record (Nützel *et al.,* 2006) have suggested that the ancestral life history included a pelagic, but non-feeding larva (Haszprunar *et al*., 1995; Ponder and Lindberg, 1997; Page, 2009). Pelagic but non-feeding larvae of the Patellogastropoda (true limpets) and Vetigastropoda (abalone, key hole limpets, trochids) may be the best, extant representatives of the ancestral gastropod larval type. If this is correct, then feeding larvae among the Caenogastropoda and Heterobranchia represent a derived life history stage. Eggs that develop into feeding (planktotrophic) larvae are small relative to those of non-feeding (lecithotrophic) larvae, because they are provisioned with relatively little yolk. Planktotrophic larvae must capture and digest microalgae over an extended pelagic period to fuel the growth and development necessary to achieve metamorphic competence, defined as the stage when larvae can undergo the morphological transformation that will allow them to assume the lifestyle of the benthic juvenile (Hadfield *et al*., 2001).

A gastropod larva that undergoes considerable growth of soft tissues before it reaches metamorphic competence must also be capable of enlarging its shell during the larval stage. This is because the shell of gastropods evolved as a protective retreat. The shell not only encases the visceral mass, but it must also be large enough to accommodate the head and foot during protective withdrawals.

Shell growth by gastropods occurs by accretion of new shell material to the apertural rim of the shell. Previous studies have shown that the shell secreted during each of the life history stages of a gastropod, including the embryo, larva, and juvenile-adult, often has distinctive sculptural and morphometric characteristics. As a result, the shell of adult gastropods chronicles its previous life history (Thorson, 1950; Jablonski and Lutz, 1983). The shells of species that lack a free-living larva have only an embryonic shell (protoconch) and a post-metamorphic shell (teleoconch). By contrast, shells of species that have two phases of shell secretion prior to the post-metamorphic teleoconch: the embryonic shell, called the protoconch I, and the shell secreted during the feeding larval stage, called the protoconch II. To date there is no information about possible differences in the mechanisms underlying shell secretion during each of these ontogenetic phases of shell secretion.

1.4 Morphological features of shell formation during gastropod development

Although the molluscan shell is arguably one of the most widely recognized biomineralized structures made by animals, information about its early formation and the cells responsible for its secretion is limited to only a few representatives from the

Bivalvia, the Polyplacophora and the Gastropoda. The embryonic shell, known as the protoconch I in gastropods (prodissoconch I in bivalves), is secreted in the early embryo by a group of ectodermally derived cells collectively known as the "shell field" (Kniprath, 1981). The shell field becomes recognizable at the completion of gastrulation as a thickening of the dorsal ectoderm (Kniprath, 1981; Wilt *et al.*, 2003).

The "shell field" invaginates to form what has been historically termed the "shell gland" because all cells that formed the invagination were thought to be directly involved in secretion of biomineral precursors. However, more recent studies have questioned this interpretation, so a preferable term for the invagination is simply "shell field invagination" or SFI (Eyster, 1983). The shell field invagination subsequently evaginates and extends around the future visceral mass of the embryo. During this phase of evagination and subsequent anterior growth of the shell field, the first components of the embryonic shell are formed, initially as a delicate sheet of organic material that Eyster (1983; 1986) called the "organic shell". This sheet appears to be a developmental precursor of the periostracum covering the shell in later developmental stages. Based on studies on the heterobranchs *Aeolidia papillosa* and *Coryphella salmonacea*, Eyster (1983; 1985) hypothesized that the function of the invagination of the shell field may be to bring together the circle of periostracum-secreting cells that form the peripheral border of the shell field. These cells were called "growing edge cells" (GE cells) by Eyster (1983). At full invagination of the shell field, these growing edge cells border the pore of the invagination and their secretory activity therefore produces an initial disc of periostracum over the pore. The SFI evaginates concurrent with continued secretion from the growing edge cells at the peripheral rim of the shell field so that the sheet of

periostracum enlarges as an expanding sheet around the visceral mass of the embryo. Mouëza *et al.* (2006) studying embryos of the bivalve *Chione cancellata* also observed a close association between the edge of the embryonic periostracum and the apical surface of the GE cells [termed the T1 cells by Mouëza *et al.* (2006)].

The GE cells of *A. papillosa, C. salmonacea*, and *C. cancellata* contain many electron dense granules associated with the Golgi apparatus. Eyster (1983) hypothesized that these granules might be involved in the production of shell or periostracum-like material. Similar "granules" are also evident in association with the Golgi apparatus of cells near the "pore" of the SFI in the embryonic stage of the pulmonate heterobranch *Biomphalaria glabrata* (Bielefeld and Becker, 1991). Observations by Eyster (1985) on embryonic shell formation in *Coryphella salmonacea* are interesting because this direct developing species of nudibranch never forms a mineralized shell. Despite this, an organic, embryonic periostracum was secreted by a conventional shell field that invaginated then evaginated and growing edge cells contained electron dense granules. These observations suggest that the electron dense granules of growing edge cells may be precursor of the periostracum-like organic sheet, rather than any component (organic or mineral) of the biomineral. Nevertheless, in Kniprath's (1977) study on shell secretion in *Lymnaea stagnalis*, he suggested that calcium may be attached to the electron dense granules for transport through the cell and ultimate incorporation into the growing shell. However, the chemical composition of electron dense granules within GE cells has yet to be determined.

The cells directly neighbouring the GE cells under the periostracum were given the name "proximal cells" by Eyster (1983; 1985). These cells occasionally contain

electron dense granules, similar to those observed in the GE cells. Eyster (1983; 1985) consistently noted an "intercellular space" between the proximal cells of *Aeolidia papillosa* and *Coryphella salmonacea,* which was created by interdigitating microvilli or cytoplasmic extensions from neighbouring cells that associate with the inner surface or overlap the growing edge of the shell material or periostracum, to create this open space between the proximal and GE cells.

The cells bordering the other side of the row of GE cells, are "microvilli-bearing cells" or MV cells [in *C. cancellata* these were termed T2 cells by Mouëza *et al*. (2006)], as they characteristically bear long, densely packed microvilli extending from their apical surface. Eyster (1983) noted that microvilli of the MV cells often extended over the GE cells and the growing edge of the sheet of periostracum.

After the evaginated shell field has evaginated and spread over the visceral mass of the embryo to form the embryonic shell, it becomes the mantle epithelium underlying the shell (Weiss *et al.*, 2002; Wilt *et al*., 2003). The periphery of the mantle fold contains the cells that secrete the periostracum and the biomineral that enlarges the shell.

1.5 Phases of shell growth in major gastropod clades

The Patellogastropoda and the Vetigastropoda have a life history that is currently interpreted as the ancestral pattern for gastropods (Haszprunar *et al*., 1995; Ponder and Lindberg, 1997; Page, 2009). Members of these clades produce a pelagic but non-feeding larva and they have two distinct phases of shell secretion. The first phase occurs during the embryonic stage and the shell produced is known as the embryonic shell or the protoconch (Jablonski and Lutz, 1980; Haszprunar *et al.*, 1995). The protoconch does not

enlarge during the short, non-feeding larval phase of patellogastropods and vetigastropods, but shell secretion resumes with the production of the teleoconch following metamorphosis. During the larval stage, when the shell does not grow, the periphery of the mantle fold retracts from the apertural rim of the protoconch (Page, 1997; Collin and Voltzow, 1998).

The more derived groups of gastropods, the Caenogastropoda and the Heterobranchia, have three phases of shell secretion when the life history includes a feeding larval stage. The shell produced before hatching from the egg capsule is known as the embryonic shell or protoconch I (Jablonski and Lutz, 1980; Haszprunar *et al.*, 1995). After hatching, the feeding larva of caenogastropods and heterobranchs secrete a larval shell, also called the protoconch II. After metamorphosis, the juvenile and later adult produce the post-metamorphic shell or teleoconch. Although the protoconch II of caenogastropods grows continuously throughout larval life and even continues to grow when metamorphosis is delayed (Lesoway and Page, 2008), the protoconch II of the Heterobranchia stops growing during the last part of larval development (Kempf, 1981; Hadfield and Miller, 1987). Arrest of protoconch II growth in larval heterobranchs is correlated with retraction of the periphery of the mantle fold from the apertural rim of the shell, much as occurs during the arrest of larval shell growth in patellogastropod and vetigastropod larvae.

1.6 Objectives

As previously mentioned, the current hypothesis for gastropod molluscs suggests that the ancestral life history included a pelagic, but non-feeding larva. Pelagic but non-

feeding larvae of the Patellogastropoda and Vetigastropoda may be the best, extant representatives of this ancestral larval type for the Gastropoda. Feeding larvae among the Caenogastropoda and Heterobranchia appear to represent a derived life history stage, which has allowed for the acquisition of energy to build the complex locomotory and predatory feeding structures required for life after metamorphosis. The evolution of the growing shell in feeding larvae represents an important pre-requisite to accommodate for these complex structures. Although previous research has provided information on the ultrastructure of shell-secreting tissues in embryonic and adult molluscs, very little ultrastructural information is available on shell-secreting mantle cells in molluscan larvae. One such study was recently published by Mouëza *et al*. (2006) on embryonic and larval stages of the bivalve *Chione cancellata*.

The goal of this research will be to investigate the following hypotheses:

(a) The larval shell of the Heterobranchia (the protoconch II) is a continuation and elaboration of the protoconch I, the embryonic shell. Under this hypothesis, the cellular phenotype of the shell-secreting cells of the larva will resemble that of the embryo in the process of secreting the protoconch I. This hypothesis is put forward because the mantle fold retracts from the shell rim coincident with arrest of shell growth in embryonic patellogastropods and vetigastropods, and also in larval heterobranchs.

(b) The growing shell secreted during the larval phase in the Caenogastropoda (the protoconch II) is a precocious juvenile shell. Under this hypothesis, the phenotype of the shell-secreting cells in larvae of caenogastropods will resemble that of the teleoconch-secreting cells in the juvenile. This hypothesis is suggested by the fact that the larval shell

of caenogastropods does not have a phase of growth arrest and its form and surface sculpturing is often (although not always) similar to that of the teleoconch.

I have examined the cellular phenotypes of different ontogenetic stages of one representative each from the Patellogastropoda, Vetigastropoda, Caenogastropoda and Heterobranchia to test the predictions under these two hypotheses.

Materials and Methods

2.1 Collection of adults, fertilization of gametes, and culture of embryos and larvae

Patellogastropoda

Developmental stages of *Tectura scutum* (Rathke, 1833) that I sectioned for this study were obtained previously by L.R. Page. Adult specimens were collected by hand from the rocky intertidal zone off Victoria, British Columbia during low tides of August and September in 1998 and 2001. The animals were placed into separate, sea water-filled glass cups and maintained in a 12^{o}C incubator, where some of the animals spawned spontaneously late in the evening after collection. Spawned eggs were placed in 1 L of Millipore-filtered sea water (0.45 µm pore size; MPFSW). Sperm were added to 500 ml of MPFSW until the suspension was slightly opaque and 1 – 2 ml of the sperm suspension was gently stirred into the egg suspension to achieve fertilization. Fertilized eggs were rinsed after approximately 30 minutes and were distributed into glass beakers containing 500 ml of MPFSW at a density of not more than 0.2 egg ml^{-1}. Culture water was replaced daily by gently pouring cultures through a sieve placed within a shallow bowl of seawater. The sieve was constructed by replacing the bottom of a Nalgene cup with Nitex cloth having a pore size of 49 µm. Larvae retained within the partially immersed sieve were then pipetted into a beaker of fresh MPFSW. It was not necessary to add food to these cultures because the larvae do not feed.

Vetigastropoda

Adults of *Calliostoma ligatum* (Gould, 1849) were collected at low tides of -0.3 m and 0.0 m on July 2, 2008 and July 20, 2009, respectively, from tidepools and surge

channels in the rocky intertidal zone at Clover Point, Victoria, B.C.. Snails were spawned according to a protocol outlined by Strathmann (1992), where individuals were inverted in a small cup containing coarse-filtered (Pall Corporation, type A/E 47 mm glass fibre filter) seawater (CFSW) at 10˚C and allowed to warm to 18˚C. If the snail righted itself (foot flat on substrate), it was inverted immediately. Gametes from males and females were shed. Three Pasteur pipets of sperm were collected directly from the male gonopore and diluted to make a slightly opaque solution of sperm, and kept in an 11˚C incubator. A wide-bore pipet was used to transfer spawned eggs into a bowl containing MPFSW at 18˚C, which was then placed in the sea-table to cool prior to the addition of sperm. Approximately 50 eggs were added to each of seven 1L beakers and the beakers were placed in the sea-table to stay cool. Each beaker of eggs was fertilized using the 11˚C sperm dilution. Approximately 200 ml of seawater in the beakers was carefully decanted (as the eggs were very buoyant) and replaced after 10 minutes had elapsed to prevent polyspermy. Fertilization was confirmed by the appearance of the first polar body after about 1 hour following addition of sperm. Larval cultures were changed every day by filtering culture water through a 64 µm pore size Nitex sieve supported by a shallow cup. Larvae collected in the sieve were rinsed with freshly filtered seawater, and returned to fresh MPFSW water by pipet. During later development, streptomycin sulfate (Sigma Chemical Company) was added to the culture water at a concentration of 50 µg/ml to control bacterial growth. At the first evidence of crawling (a requirement for metamorphosis) at 15 days post fertilization, larvae were transferred to custard cups and rocks with a layer of biofilm collected from Clover Point were added to the custard cups

to induce metamorphosis. Culture seawater was subsequently replaced every other day by pipetting off the old water and replacing it with new, so as to not disturb the snails.

Caenogastropoda

Adults of *Nassarius mendicus* (Gould, 1850) were collected from a sandy mudflat (adjacent to the Institute of Ocean Sciences), in Patricia Bay, Saanich, B.C. at a low tide of 0.2 m on May 24, 2009. The snails were brought to the University of Victoria, placed in an aquarium provided with flow-through seawater and a lid to prevent escape. They were fed krill by the Aquatics staff every other day. Fragments of algae *(Gracilariopsis* sp.) were provided daily as a substrate onto which snails could lay their egg masses. The algal fragments were collected at the end of each day from the aquarium and were placed in small cups containing 100 ml CFSW seawater maintained at 12˚C in an incubator. Seawater was replaced daily.

Larvae hatched from their egg capsules after an average of 17 days, and were cultured at an initial density of 0.3 larvae/ml and maintained at 12 ^{o}C. Larvae were pipetted into 500 ml of CFSW with 5 ml of streptomycin antibiotic (50 µg/ml), and fed 5 x 10^{4}cells ml^{-1} of a 1:1 mixture of *Isochrysis galbana* (CCMP 1323) and *Pavlova lutheri* (CCMP 1323). Algal inocula were obtained from the Provasoli –Guillard National Center for Culture of Marine Phytoplankton (CCMP). Algal cultures were grown in Guillard's f/2 enrichment medium (Guillard, 1975) without silicates in a 17˚C incubator and provided with constant aeration and illumination. Cetyl alcohol flakes were sprinkled on the surface of each larval culture to prevent the larval shells from being trapped on the surface tension. Larvae were transferred to fresh culture medium

every other day, by the same method used for cultures of *T. scutum* and *C. ligatum*, except algal food was added at each culture change.

Once larva reached metamorphic competency, as determined by the capacity for intermittent crawling, they were placed in small glass custard cups with a few pinches of sediment collected from Patricia Bay to induce metamorphosis. Larvae were checked daily for the loss of the velum, and once this occurred, these newly metamorphosed, carnivorous juveniles were placed in custard cups with small pieces of krill.

Heterobranchia

Developmental stages of *Siphonaria denticulata* Quoy & Gaimard, 1833 that I sectioned for this study were obtained previously by L.R. Page. The distinctive jelly egg masses of this species were collected from intertidal rock pools at Mona Vale, just north of Sydney Australia, during October 2006. Larvae held in seawater aquaria in the laboratory began hatching within a week of collection and were cultured using the same method described above for *Nassarius mendicus*, except the culture temperature was 21 – 25 ^{o}C.

(The representative species for the four groups chosen for this research were selected based on their ease of collection and in the case of the heterobranch *S. denticulata*, because of its retention of the shell after metamorphosis. Species were not chosen based on their phylogenetic position within their respective groups.)

2.2 Preparation for transmission electron microscopy

The method used to anaesthetize embryos and larvae has been described by Page (1997) and the method for chemical fixation and decalcification of larval shells was described by Page (1995). The procedures are briefly described below.

Later embryos, larvae, and juveniles of gastropods must be anaesthetized prior to chemical fixation to prevent retraction of the head, mantle fold, and foot into the shell. For this purpose, specimens were placed in MPFSW within 8 ml specimen vials sitting on scant crushed ice. The seawater was gradually replaced with artificial seawater containing increased Mg^{2+} and reduced Ca^{2+} concentrations. Once relaxed, all but 1 ml of the artificial seawater was removed and 3 drops of a cold, saturated solution of Chlorobutanal in seawater was added every 1.5 min for a total of 6 additions. At this point, the anaesthetizing solution was replaced with the primary fixative of 2.5% gluteraldehyde in Millonig's phosphate buffer (0.4 M, pH 7.6) and sodium chloride (0.34 M) solution. Primary fixative was replaced once and fixed embryos were placed in an 8˚C refrigerator overnight.

After the primary fixation, specimens were decalcified using a 1:1 solution of primary fixative and a 10% solution of ethylene diaminotetraacetic acid (EDTA; dissolved from disodium salt). Time for full decalcification varied greatly depending on the size and thickness of the shell; it ranged from 1 hour for embryos of *T. scutum* and *C. ligatum* to overnight for juveniles of *N. mendicus*. During prolonged incubations for decalcification, the mix of fixative and EDTA was periodically replaced with fresh solution.

After decalcification, specimens were rinsed in 3 – 4 changes of 2.5% sodium bicarbonate (pH 7.2) for 15 min each and were post-fixed in a 1:1 mix of 4% osmium tetroxide and 2.5% sodium bicarbonate. Specimens were then dehydrated in an acetone dilution series, embedded in Embed-812 resin and were sectioned with a Leica Ultracut ultramicrotome. Reference histological sections of 0.75 µm thickness were cut with glass

knives and stained with Richardson's stain (Richardson *et al.*, 1960) for light microscopy and 80 nm ultra-thin sections were cut with a Diatome diamond knife and mounted on 150 mesh copper grids. Ultra-thin sections were stained for 1.25 hour in aqueous 2% uranyl acetate, rinsed in double distilled water (ddH_2O), and stained for 6.5 min in 0.2% lead citrate, then rinsed again in ddH_2O. Grids were examined using a Hitachi H-7000 transmission electron microscope (TEM).

Three developmental stages of the patellogastropod *T. scutum*, the vetigastropod *C. ligatum*, and the caenogastropod *N. mendicus* were fixed, sectioned, and examined by transmission microscopy. These three stages represented an embryo, larva, and juvenile stage of the life history of each. For the heterobranch *S. denticulata*, only a larval and juvenile stage was examined. Details of the fixed stages are given in the following table:

Table 1. Examined developmental stages for four gastropod species

Species	Higher Taxon	Develop. Stage	No. of individuals sectioned	Age (Temp)	Comments
Tectura Scutum	Patellogastropoda	embryo	2	49 hpf (12°C)	Protoconch I approaching end of secretion
		larva	2	10 dpf (12 °C)	Approaching or achieved metamorphic competence; no shell secretion
		juvenile	2	1 mpm (12 °C)	Teleoconch undergoing secretion
Calliostoma ligatum	Vetigastropoda	embryo	2	29.5 hpf (11 °C)	Protoconch I undergoing secretion
		larva	3	13 dpf (11 °C)	Approaching or achieved metamorphic competence; no shell secretion
		juvenile	3	1 mpm (11 °C)	Teleoconch undergoing secretion
Nassarius mendicus	Caenogastropoda	embryo	3	8 dpo (12°C)	Protoconch I undergoing secretion
		larva	3	20 dph (12°C)	Protoconch II undergoing secretion
		juvenile	2	1 mpm (12°C)	Teleoconch undergoing secretion
Siphonaria denticulata	Heterobranchia	Pre-hatch embryo not obtained	--	--	--
		young larva	1	6dph	Protoconch II undergoing secretion
		older larva	3	14 dph (21-25°C)	No shell growth
		juvenile	2	1 mpm (21-25°C)	Teleoconch undergoing secretion

Abbreviations: dpf, days post-fertilization; dph, days post-hatching; dpo, days post-oviposition; hpf, hours post-fertilization; mpm, month post-metamorphosis.

2.3 Preparation of shells for scanning electron microscopy

At each stage and for each species that was fixed and embedded for sectioning and transmission electron microscopy, specimens of the same stage and species were prepared for examination with the scanning electron microscope (SEM). Embryonic stages without the capacity to retract into their shells were not anaesthetized, but larval and juvenile stages were anaesthetized for varying amounts of time in artificial seawater containing high Mg^{2+} and low Ca^{2+}. Shells were prepared by rinsing specimens in distilled water three times, then rinsing for varying amounts of time (30 minutes to three hours) in a dilute solution of sodium hypochlorite until the soft tissue had successfully been removed. Once the tissue was removed, shells were rinsed three times in distilled water and dehydrated in a graded series of acetone. Shells were pipetted out onto lens paper (with filter paper underneath to absorb excess acetone) and the acetone was allowed to evaporate. Shells were transferred to a small square of double-sided adhesive tape on a SEM stub using a cactus spine held by cross-closing forceps. Colloidal silver paste was smeared along the boundary between tape and metal SEM stub to ensure electrical conductivity between tape and stub. Mounted specimens were sputter-coated with gold and viewed with a Hitachi S3500N SEM. All micrographs and composite images were arranged and adjusted for contrast and brightness, and edited for size using Adobe Photoshop CS3 (v. 10.0.1) software.

Results

3.1 Patellogastropoda – *Tectura scutum*

3.1.a *Tectura scutum* – overview of development and ontogeny of shell form

Embryos of *Tectura scutum* hatched from the vitelline envelope and jelly coat at about 15 hours after fertilization when cultured at 12°C. The embryonic shell (protoconch) first appeared as a transparent, lens-shaped disc on the posterior-dorsal side of the embryo at approximately 30 hours after fertilization (Fig. 2a) and it enlarged over the next 20 - 22 hours until it entirely encompassed the visceral lobe (Fig. 2b). The protoconch reached its final size by the time the embryos began ontogenetic torsion at approximately 52 hours post-fertilization (hpf). Ontogenetic torsion is a morphogenetic movement whereby the head and foot rotate by 180° relative to the shell, mantle, and visceral lobe (compare Figs. 2b and 2c).

The enlarging, lens-shaped protoconch of *T. scutum* gradually acquired a distinctive patterning of wavy, parallel ridges (Figs. 2b, c and 3a). This pattern was due to deposition of biomineral, because the same pattern was observed on shells of post-torsional larvae that had been completely cleaned of the organic periostracum by incubation in a weak solution of sodium hypochlorite (household bleach) (Fig. 2d). However, although the distinctive patterning indicative of biomineral deposition was evident over most of the protoconch by the time larvae approached the onset of ontogenetic torsion, biomineralization of the apertural rim was not complete at this time because the rim disintegrated when these embryos were placed in sodium hypochlorite solution (Fig. 2d inset).

I define the larval stage of *T. scutum* as the period between the onset of ontogenetic torsion at 52 hpf and the onset of metamorphosis at approximately 9 days post-fertilization (dpf). Although the protoconch did not enlarge during the larval stage, the foot grew dramatically and was used for the crawling behaviour that preceded metamorphosis. The most obvious event of metamorphosis was loss of the ciliated velar cells, which the larva used for swimming. Within several days after the velar cells were lost, the juvenile began to secrete the teleoconch, or post-metamorphic shell. The teleoconch was deposited as a visor-like rim added to the apertural margin of the protoconch (see section 3.1.d below). The shape and surface sculpturing of the teleoconch differed from that of the protoconch.

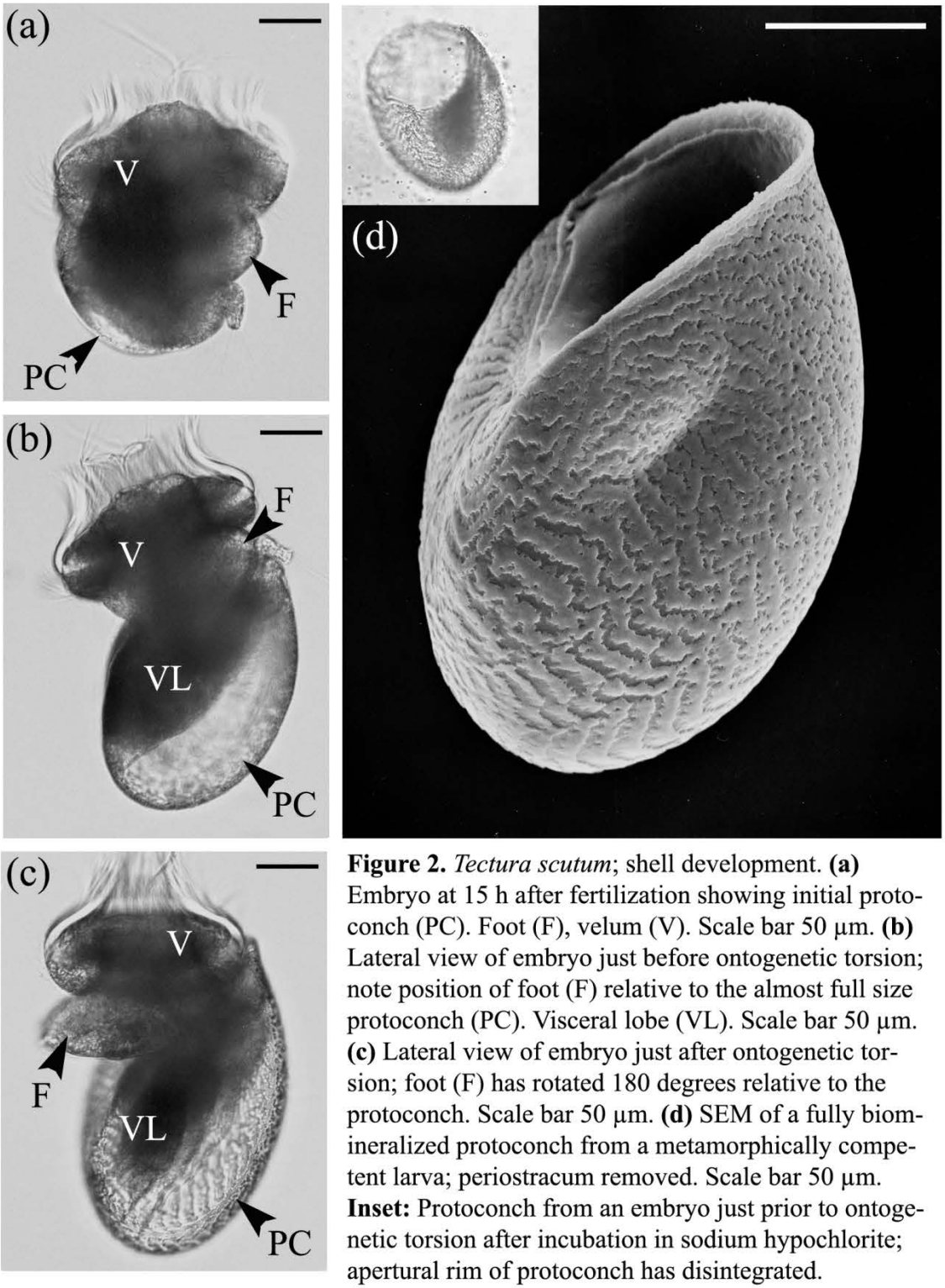

Figure 2. *Tectura scutum*; shell development. **(a)** Embryo at 15 h after fertilization showing initial protoconch (PC). Foot (F), velum (V). Scale bar 50 µm. **(b)** Lateral view of embryo just before ontogenetic torsion; note position of foot (F) relative to the almost full size protoconch (PC). Visceral lobe (VL). Scale bar 50 µm. **(c)** Lateral view of embryo just after ontogenetic torsion; foot (F) has rotated 180 degrees relative to the protoconch. Scale bar 50 µm. **(d)** SEM of a fully biomineralized protoconch from a metamorphically competent larva; periostracum removed. Scale bar 50 µm. **Inset:** Protoconch from an embryo just prior to ontogenetic torsion after incubation in sodium hypochlorite; apertural rim of protoconch has disintegrated.

3.1.b *Tectura scutum* – embryonic stage (pre-torsion)

Embryos of *T. scutum* at 49 hours post-fertilization were fixed, decalcified, embedded and sectioned to describe the cells of the mantle epithelium at the periphery of the mantle fold (PMF). At this stage, the protoconch was close to attaining its final size (Fig. 3a), but the apertural rim of the protoconch was not fully mineralized. Histological longitudinal sections showed more anatomical detail than could be discerned from external views of live larvae at this stage. The mid-sagittal section in Fig. 3b shows the foot and the fold of mantle epithelium delineating the mantle cavity. Although the protoconch had been decalcified in this specimen, a sheet of organic material remained that surrounded the visceral mass and terminated at the periphery of the mantle fold. I interpret this sheet of organic material as periostracum (Fig. 3b). In life, the periostracum covered the exterior of the biomineral of the protoconch. However, as a result of the decalcification procedure, the organic periostracum was not supported by rigid biomineral and it was often folded and distorted to some degree in sectioned material (Figs. 3c, d). Transmission electron microscopy of sectioned embryos showed that the periostracum at the apertural rim of the protoconch was closely applied to the PMF (Figs. 3c, d, 4).

The terminology that I use throughout this thesis to describe the cells within the “shell growth region” of the PMF is based on the terminology of Eyster (1983). The different cell types were identified on the basis of their association with the peripheral edge of the periostracum and on distinctive ultrastructural characteristics of the cells. The periostracum was identified by its electron dense, lamellar structure (Fig. 3d), although the lamellar structure became somewhat fragmented and fibrillar where the periostracum

was attached to the PMF (Fig. 4). The cells within the "shell growth region" of the PMF were identified as proximal cells (Pr), growing edge cells (GE), and the microvilli-bearing cell (MV) (Figs. 3d, 4)

Individual longitudinal sections through the PMF of *T. scutum* typically showed profiles of more than one GE cell, suggesting that several rows of these cells are embedded within the PMF. The GE cells occurred at the peripheral edge of the periostracum. Apical cytoplasmic extensions (C) originating from the GE cells loosely interdigitated so as to form an irregular subsurface crypt or what Eyster (1983) has observed and describes as an intercellular space (ICS) (Fig. 4). In addition, the apical region of GE cells contained a few electron dense granules and many, small electron-lucent vesicles (Fig. 4). The Pr cell ran adjacent to the GE cells and microvilli arising from the Pr cell were intimately associated with the newly formed periostracum at the apertural rim of the protoconch (Fig 4). The Pr cell in the embryo had shorter microvilli than the MV cell and had a small number of electron dense granules and mitochondria in its apical region (Fig. 3d, 4). The MV cells neighboured the other side of the GE cells; they were the first row of cells forming the inner mantle epithelium lining the mantle cavity. MV cells were characterized by long, erect, and densely packed microvilli (unlike the microvilli arising from Pr cells) (Figs. 3d, 4).

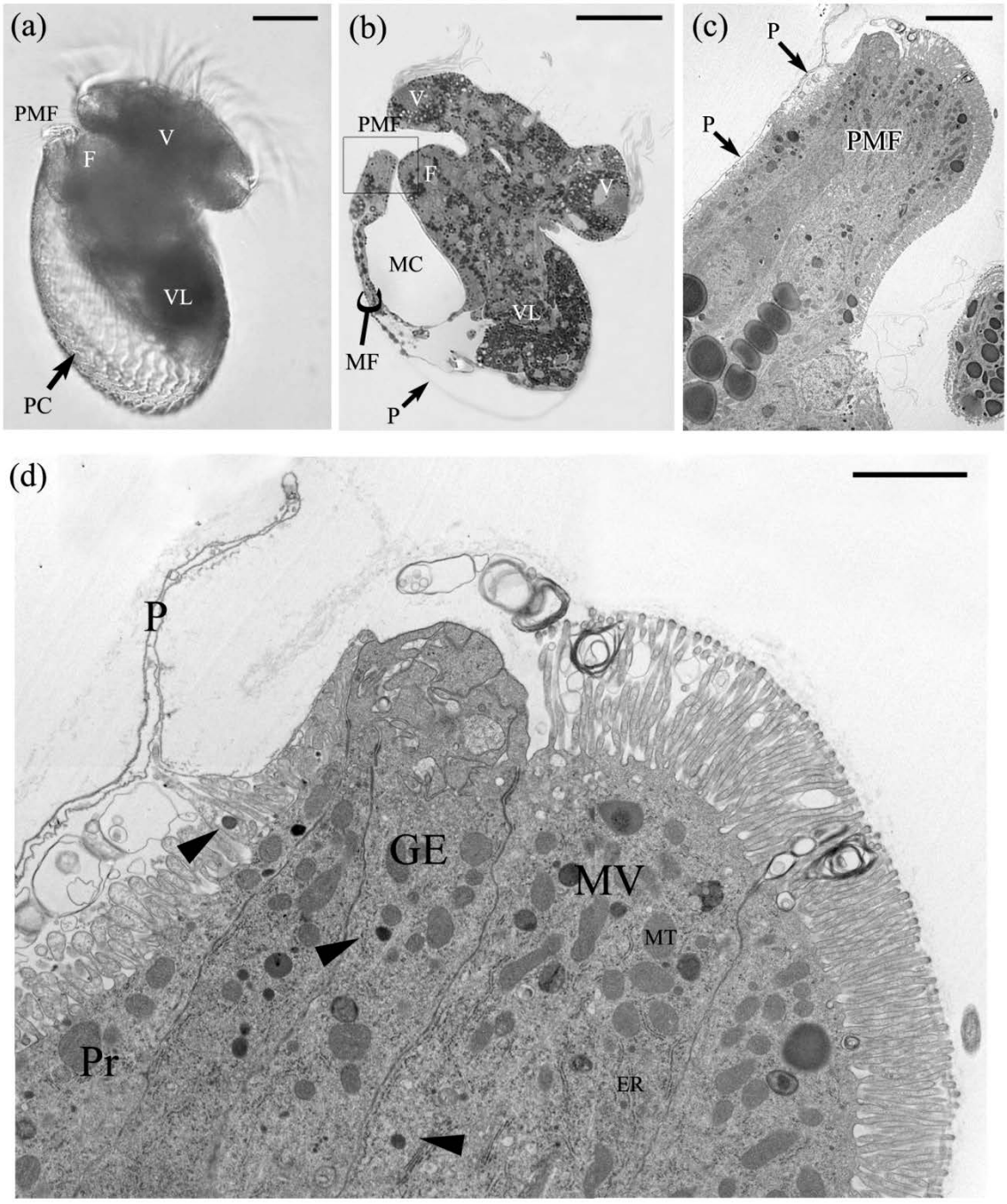

Figure 3. *Tectura scutum*; embryo at 49 h post-fertilization (prior to ontogenetic torsion). **(a)** Light micrograph of live embryo showing periphery of the mantle fold (PMF), protoconch (PC), foot rudiment (F), velum (V), and visceral lobe (VL). Scale bar 50 µm. **(b)** Light micrograph of a mid-sagittal section showing the mantle fold (MF) delineating the mantle cavity (MC); boxed area is the PMF. Note the periostracum (P) of the decalcified embryonic shell. Scale bar 50 µm. **(c)** TEM showing the periphery of the mantle fold (PMF) with attached periostracum (P). Scale bar 10 µm. **(d)** Higher magnification TEM of apical regions of PMF cells; note the proximal cells (Pr), growing edge cells (GE), and microvilli-bearing cells (MV). Scale bar 2 µm.

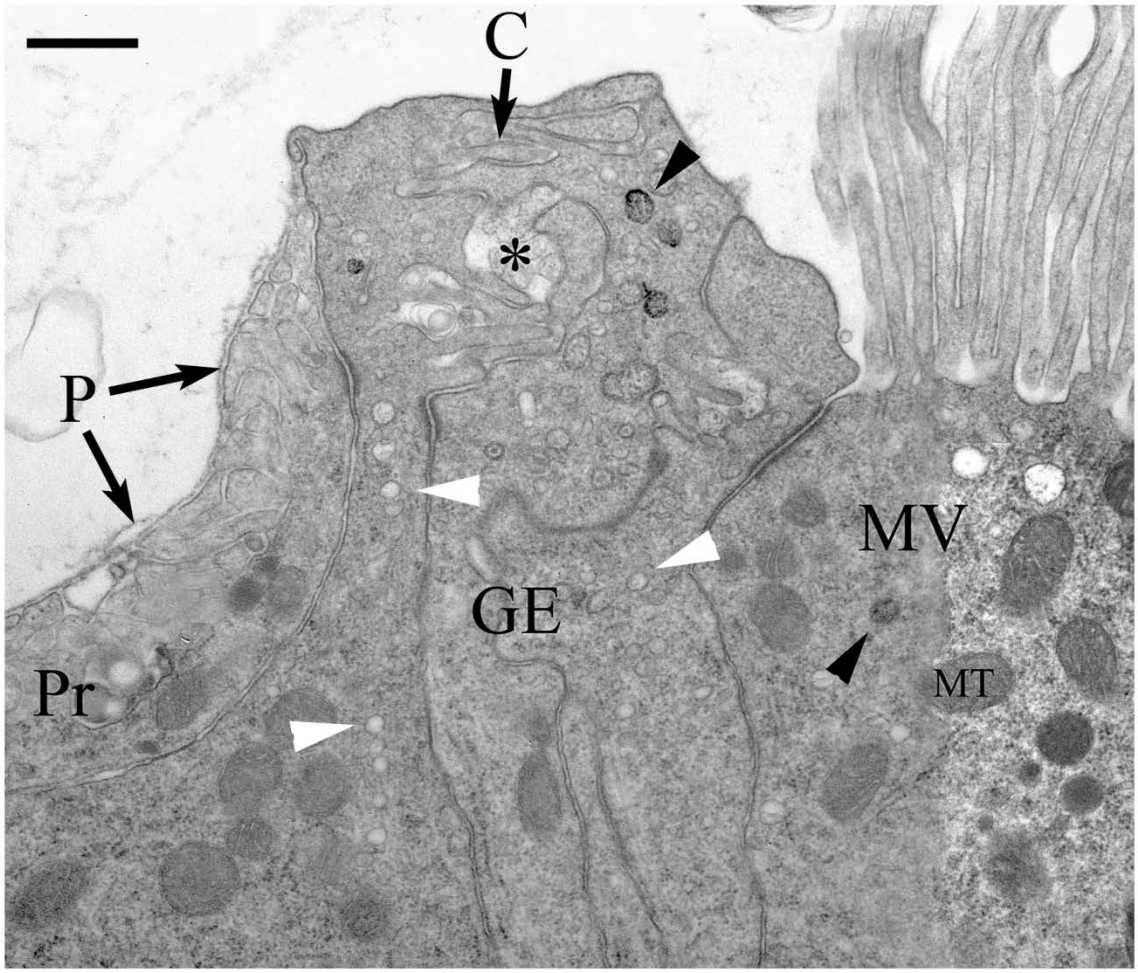

Figure 4. *Tectura scutum*; embryo at 49 h post-fertilization. TEM detail of apical regions of the cells at the periphery of the mantle fold. Note the proximal cell (Pr), growing edge cells (GE), and microvilli-bearing cell (MV). All three cell types contain mitochondria (MT), electron dense granules (black arrowheads) and electron-lucent vesicles (white arrowheads). Elaborate, stacked cytoplasmic extensions (C) originate from the GE cells to form an intercellular space or ICS (asterisk). The organic periostracum (P) is a diffuse fibrillar layer that is closely applied to microvilli of the Pr cell and terminates at the GE cell. Scale bar 0.5 μm.

3.1.c *Tectura scutum* – larval stage (post-torsion)

During the larval stage between ontogenetic torsion and metamorphic competence, the foot enlarged greatly and the ventral surface became ciliated to facilitate crawling behaviour (Fig. 5a, b). However, the protoconch did not enlarge during the larval stage and the periphery of the mantle fold detached and retracted from the apertural rim of the protoconch (Fig. 5a, b). The cells within the "shell growth region" of the PMF retained characteristics observed from the embryonic stage, which made them distinguishable as the Pr, GE and MV cells, but the periostracum was no longer closely applied to the GE cells (Fig. 6). Furthermore, the apices of GE cells appeared shrunken relative to their condition in the embryonic stage and the cytoplasmic extensions originating from the apical surface of the GE cells were much reduced and did not form interdigitations outlining a subsurface crypt or intercellular space as was observed for the embryonic stage (compare Figs. 4 and 6). The Pr cell bears short microvilli and a few electron dense granules (Fig. 6). The Pr, GE and MV cells had a lower density of mitochondria than observed within these cells during the embryonic stage.

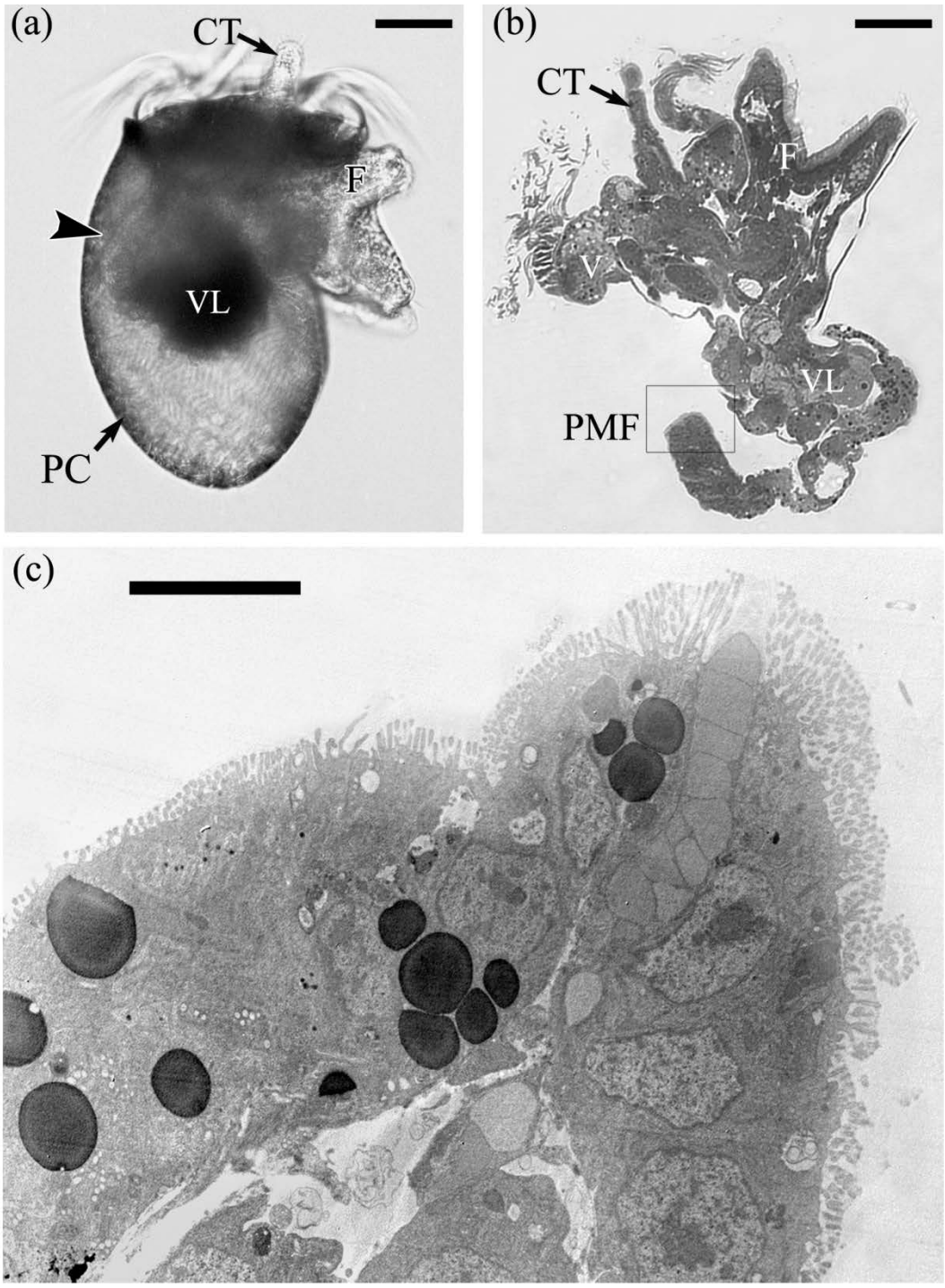

Figure 5. *Tectura scutum*; larva at metamorphic competence. **(a)** Light micrograph of a live larva with foot (F), visceral lobe (VL), ciliated velum (V), and cephalic tentacles (CT); arrowhead indicates periphery of mantle fold retracted from apertural rim of protoconch (PC). Scale bar 25 µm. **(b)** Histological mid-sagittal section through a competent larva with the periphery of the mantle fold (PMF) retracted and detached from the aperture of the protoconch. Scale bar 25 µm. **(c)** TEM of the periphery of the mantle fold detached from the apertural rim of protoconch. Scale bar 4 µm.

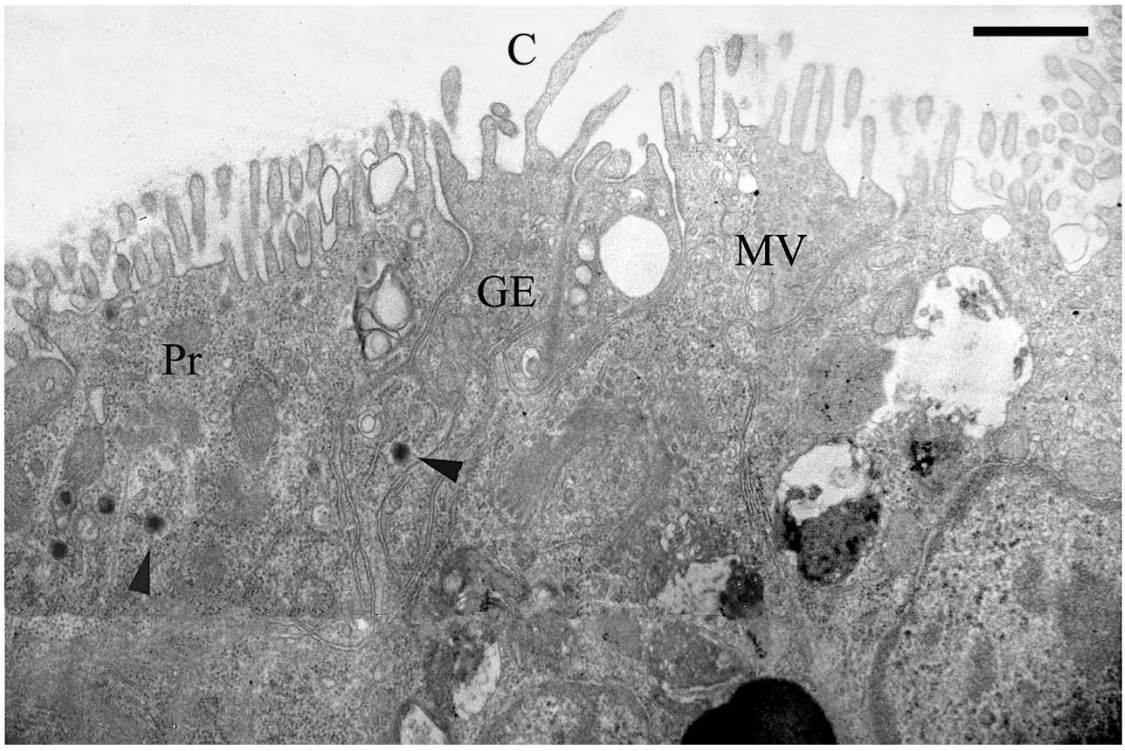

Figure 6. *Tectura scutum*; larva at metamorphic competence (post-torsional). TEM showing apical regions of cells at the periphery of the mantle fold. Arrowheads indicate dense granules of growing edge and proximal cells. Scale bar 0.5 µm.

3.1.d *Tectura scutum* – juvenile stage

The teleoconch of *T. scutum* juveniles became evident within a few days after metamorphic loss of the velum as a visor-like rim extending from the apertural edge of the protoconch (Fig. 7a). Sections through juveniles at one month after metamorphosis showed the edge of the periostracum connected to the periphery of the mantle fold (Fig. 7b). The fibrillar organic matrix material of the teleoconch of decalcified specimens was very conspicuous within the extrapallial space between the periostracum and outer mantle epithelium (Figs. 7c, 8a, b). The Pr, GE and MV cells were all extremely elongated apically, and elaborate cytoplasmic extensions of the GE cell were attached to the edge of the periostracum (Fig. 7c, 8b). The extensions from the GE cells delineated an intercellular space (Figs. 8a, b). Small electron dense granules were present in all three cell types of the PMF, but were particularly abundant within the apices of GE cells (Fig. 8a). The MV cells formed a type of cleft at the edge of the inner mantle epithelium (Fig. 7c).

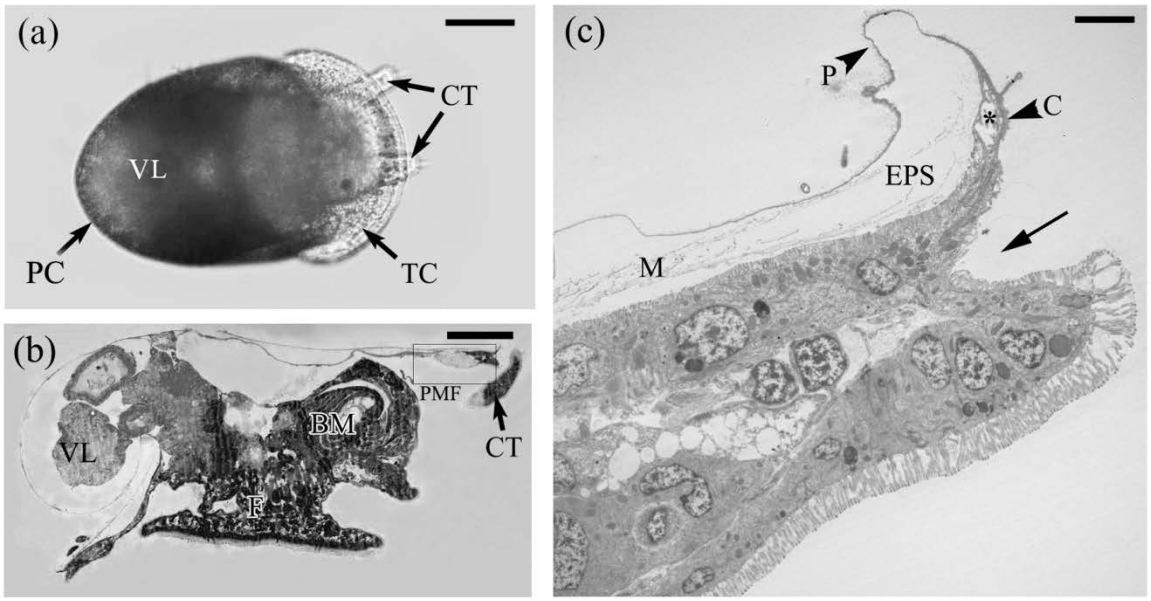

Figure 7. *Tectura scutum*; juveniles. **(a)** Light micrograph of a live juvenile in dorsal view showing the rim of teleoconch (TC) added to the protoconch (PC). Cephalic tentacles (CT), visceral lobe (VL). Scale bar 50 µm. **(b)** Mid-sagittal section of a juvenile at 1 month after metamorphosis that passes through the buccal mass (BM), a cephalic tentacle (CT), and the visceral lobe (VL). The boxed area is the periphery of the mantle fold (PMF). Scale bar 50 µm. **(c)** TEM of periphery of the mantle fold showing the intimate association between the periostracam (P) and elongate cytoplasmic extensions (C) from the PMF cells forming an intercellular space (asterisk). A distinct cleft is present (arrow) and organic matrix (M) of the teleoconch lies within the extrapallial space (EPS). Scale bar 2 µm.

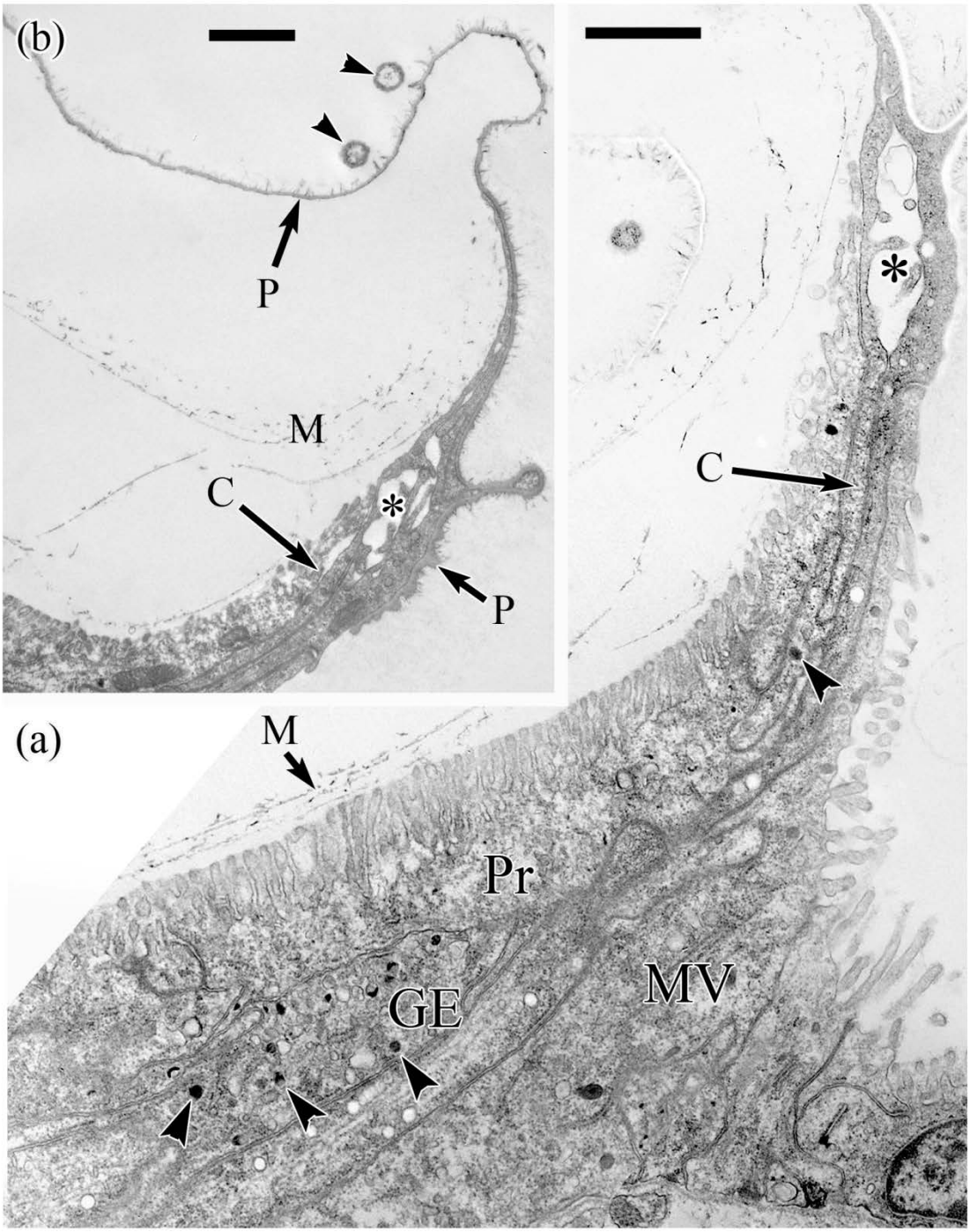

Figure 8. *Tectura scutum*; juvenile at 1 month post-metamorphosis. **(a)** TEM showing detail of the the periphery of the mantle fold. Note the proximal (Pr), growing edge (GE), and microvilli-bearing (MV) cells; the apices of each cell type are drawn-out into narrow cytoplasmic extensions (C) and an intercellular space (asterisk) is present. Arrowheads indicate electron dense granules within the GE cells. Organic matrix of teleoconch (M). Scale bar 2 µm. **(b)** Cytoplasmic extensions (C) of apices of PMF cells attached to periostracum (P). Asterisk indicates intercellular space; arrowheads indicate bacteria. Organic matrix (M). Scale bar 0.5 µm.

3.2 Vetigastropoda - *Calliostoma ligatum*

3.2.a *Calliostoma ligatum* – overview of development and ontogeny of shell form

The pattern of development in *C. ligatum* was similar to that of *T. scutum* in many respects. Both species free-spawned gametes and eggs were fertilized externally. The embryos of both exhibited ontogenetic torsion as a distinct morphogenetic movement and the larvae were non-feeding and required little time before metamorphic competence was achieved. However, unlike *T. scutum*, *C. ligatum* remained within the vitelline envelope and jelly coat until well after ontogenetic torsion was completed. Nevertheless, because these egg investments were transparent, details of embryogenesis could be easily seen in whole mounts of live larvae.

The protoconch of *C. ligatum* was first evident as a transparent, lens-shaped structure that showed no evidence of sculpturing as it grew around the visceral lobe of the embryo (Fig. 9a inset). However, as the protoconch approached final size during the period just before ontogenetic torsion, it acquired a distinct polygonal patterning that began at the first-secreted area of the protoconch and spread toward the apertural region. This patterning was evident in shells cleaned of organic material (Figs. 9, 10), suggesting that it represented deposited biomineral and not secreted periostracum. The protoconch of *C. ligatum*, like that of *T. scutum*, did not enlarge further after ontogenetic torsion.

Juvenile shells of *C. ligatum* consisted of both protoconch and teleoconch, each having a distinct type of patterning (Figs. 9, 10). The protoconch pattern clearly terminated at a prominent, raised ridge that separated the embryonic phase of shell secretion from the juvenile phase of shell secretion (Fig. 9b). The juvenile teleoconch had a sculpturing of raised, radial ridges.

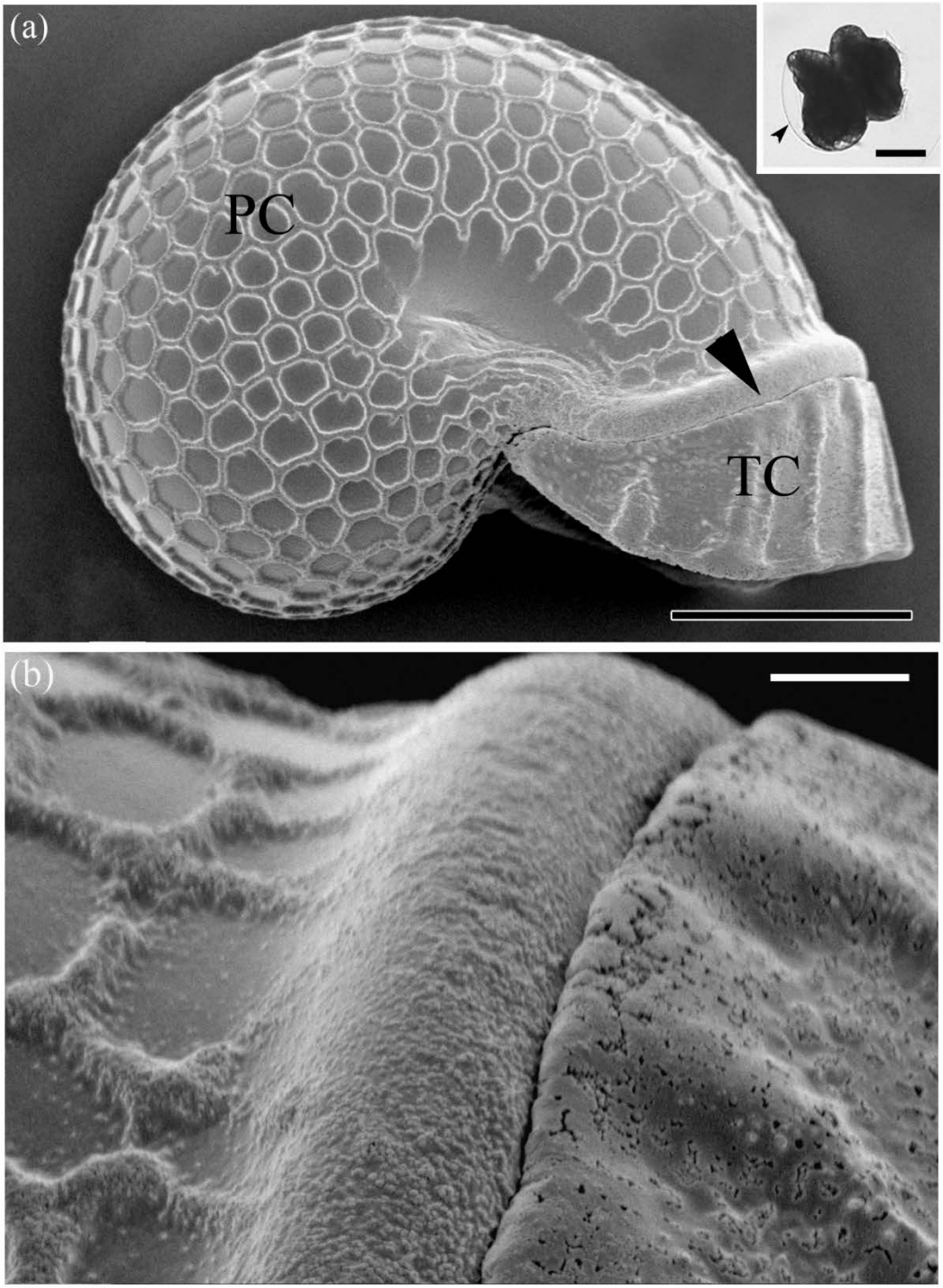

Figure 9. *Calliostoma ligatum*; SEM of shell from a young juvenile. **(a)** Right side of shell showing polygonal patterning of the embryonic protoconch (PC) and radial ridges of the post-metamorphic teleoconch (TC). Arrowhead indicates transition between protoconch and teleoconch. Scale bar 100 μm. **Inset:** Light micrograph of a live embryo showing protoconch (arrowhead) without evidence of patterning. Scale bar 50 μm. **(b)** Detail of transition between protoconch and teleoconch. Scale bar 10 μm.

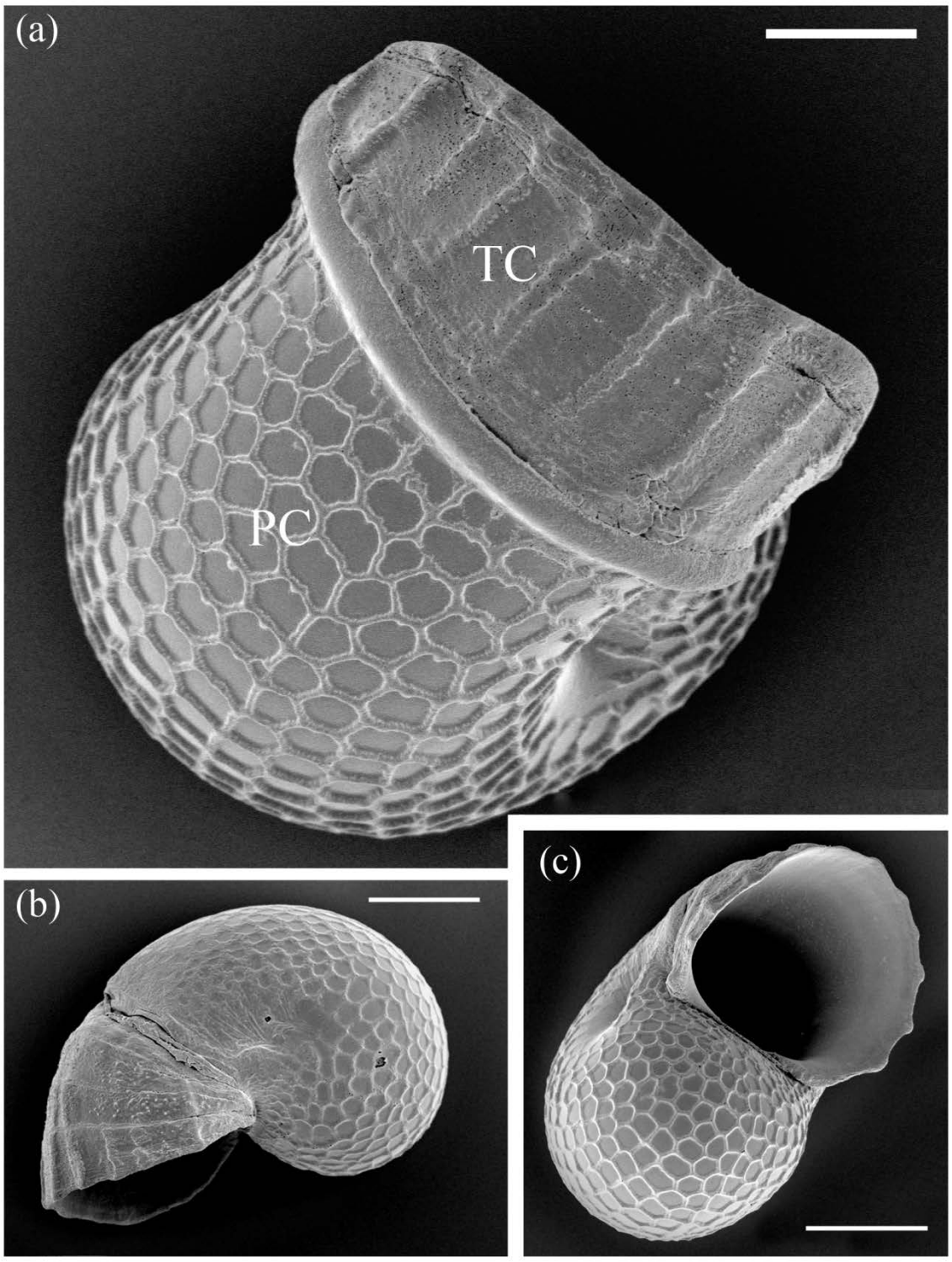

Figure 10. *Calliostoma ligatum*; SEM of a shell from a young juvenile. **(a)** Abapertural view showing embryonic protoconch (PC) and juvenile teleoconch (TC). Scale bar 50 µm. **(b)** Left view of shell. Scale bar 100 µm. **(c)** Apertural view of shell. Scale bar 100 µm.

3.2.b *Calliostoma ligatum* – embryonic stage

The embryonic stage of *C. ligatum*, defined here as the phase of development up to ontogenetic torsion, was fixed and sectioned at 29.5 hours post-fertilization, when individuals were still within the egg investment layers. Longitudinal sections of these embryos showed that the peripheral rim of the periostracum was connected to the periphery of the mantle fold (PMF), which was located just posterior to the foot rudiment (Fig. 11a).

Transmission electron microscopy of *C. ligatum* embryos revealed the same three basic cell types at the periphery of the mantle fold (PMF) as described previously for *T. scutum.* Figure 11b shows an overview of the PMF in a low magnification electron micrograph and Figures 11c, d, and e show higher magnification images of selected regions. The peripheral edge of the periostracum was intimately associated with the apical surface of the growing edge cells (Figs. 11c, d), but ended before the junction between growing edge cells (GE) and the microvilli-bearing cells (MV) (Fig. 11d). Long cytoplasmic extensions arising from GE cells supported the periostracum (Fig. 11c). Furthermore, narrow gaps between the apices of neighbouring GE cells demarcated an irregular intercellular space or subsurface crypt within this zone of cells (Fig. 11d). The apical regions of both the MV and GE cells contained numerous mitochondria. The GE cells contained very few electron dense granules (Figs. 11c, d).

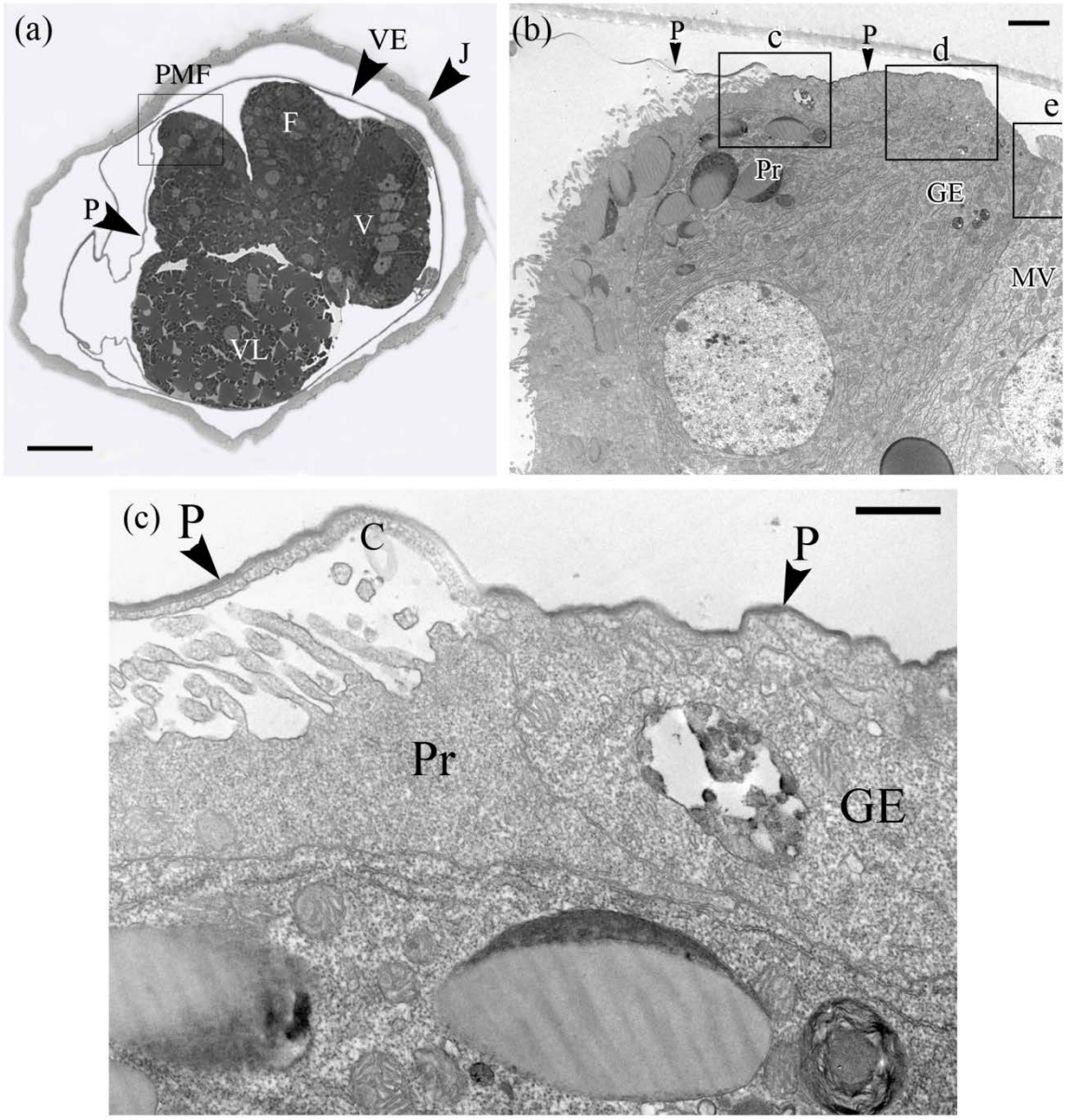

Figure 11. *Calliostoma ligatum*; embryo at 29.5 h post-fertilization. **(a)** Light micrograph of a mid-sagittal section showing periostracum (P) attached to periphery of the mantle fold (PMF). The embryo is enclosed within a vitelline envelope (VE) and jelly coat (J). Foot (F), velum (V), visceral lobe (VL). **(b)** TEM at low magnification showing periostracum (P) attached to PMF with Pr, GE, and MV cells; details of areas within letter-labelled boxes are shown in Figs. 11c, d, & e. Scale bar 2 µm. **(c)** TEM of apical regions of proximal cell (Pr) and growing edge cell (GE); cytoplasmic extension arising from GE cell is closely associated with periostracum (P). Scale bar 0.5 µm.

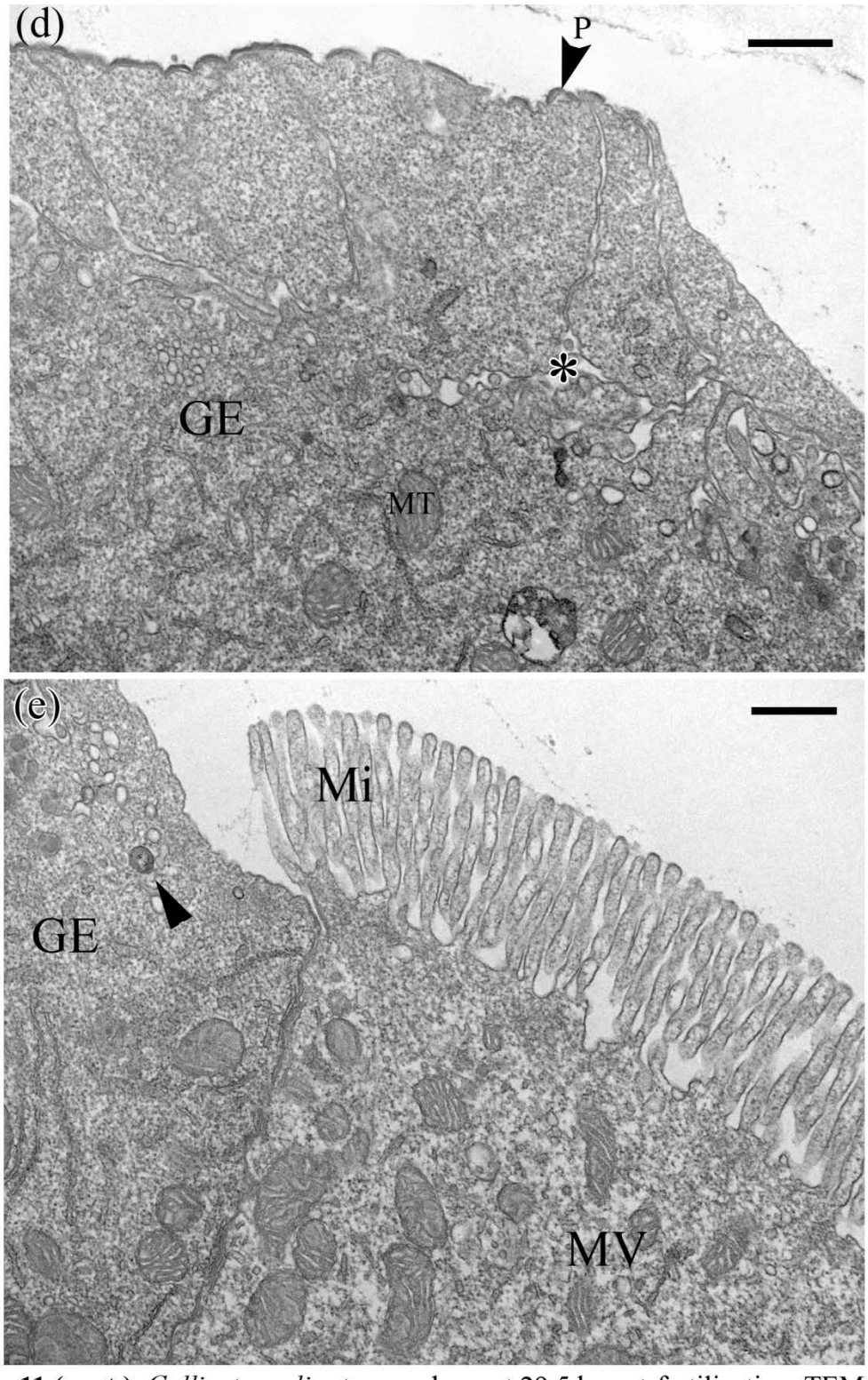

Figure 11 (cont.). *Calliostoma ligatum*; embryo at 29.5 h post-fertilization. TEM micrographs of apices of cells within the PMF. **(d)** Growing edge cells (GE) with closely applied organic periostracum, which terminates prior to the microvilli-bearing cell (MV); asterisk indicates intercellular or subapical space. Scale bar 0.5 µm. **(e)** MV cell with densely packed microvilli (Mi) neighbouring GE cell. Scale bar 0.5 µm.

3.2.c *Calliostoma ligatum* – larval stage

The larval stage of *C. ligatum* was fixed and sectioned at 13 days post-hatching to visualize and describe the cells at the periphery of the mantle fold (PMF). The PMF was detached and retracted from the apertural rim of the protoconch (Figs. 12a, b). Transmission electron microscopy showed that the zone of GE cells was considerably reduced in breadth, relative to the embryonic stage, but these cells contained numerous electron dense granules (Fig. 12b, c). Cytoplasmic extensions originating from the GE cell appeared to create an intercellular space (Fig. 12c).

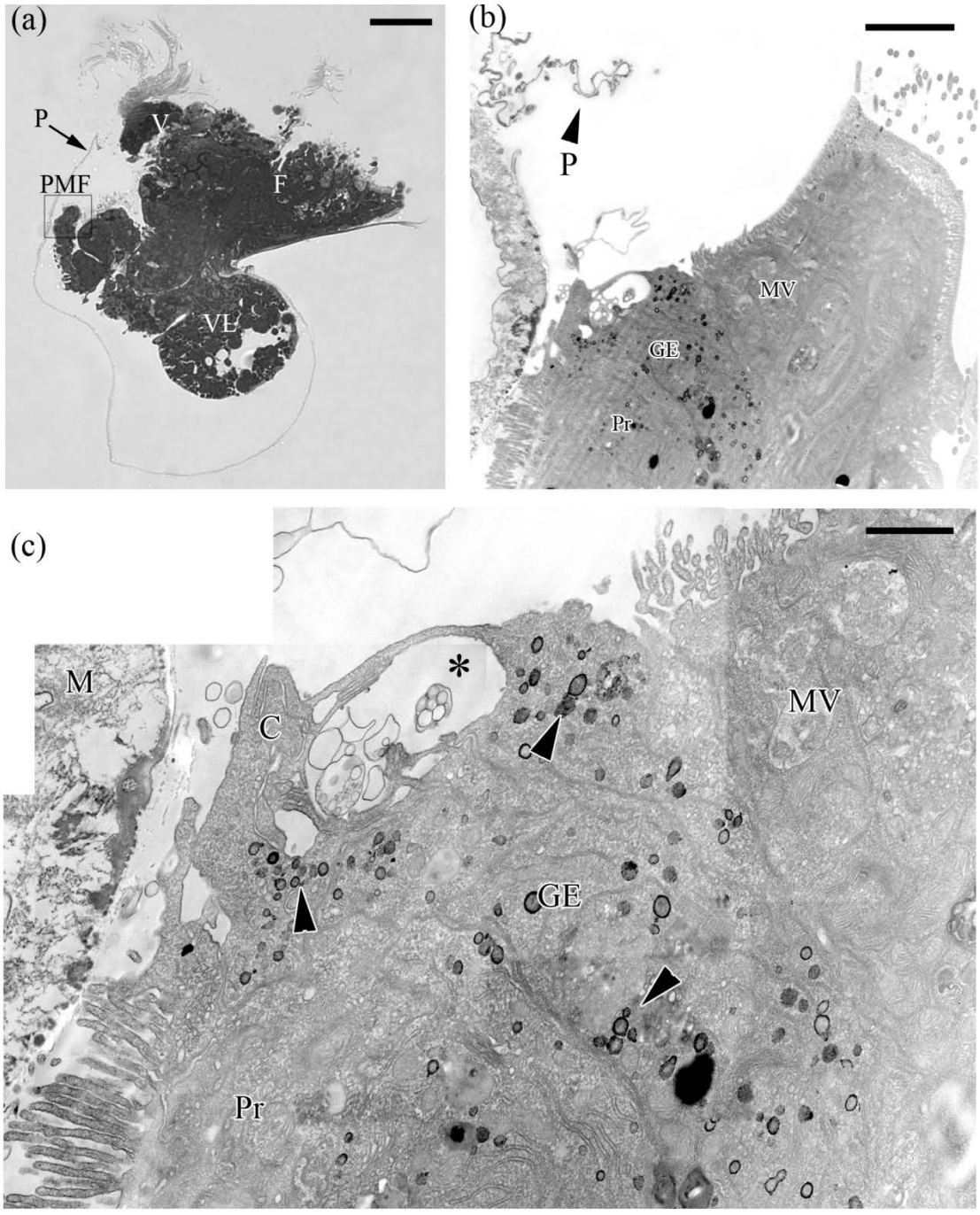

Figure 12. *Calliostoma ligatum*; larva at 13 days post-fertilization. **(a)** Light micrograph of mid-sagittal section showing periphery of the mantle fold (PMF) retracted and detached from apertural rim of the periostracum (P). Scale bar 50 μm. **(b)** TEM of PMF showing organic periostracum (P) detached from the growing edge cells (GE). Scale bar 4 μm. **(c)** TEM of apical regions of the proximal (Pr), growing edge (GE) and microvilli-bearing (MV) cells. Pr and GE cells with elaborate cytoplasmic extensions (C) creating an intercellular space (asterisk). GE cell with numerous electron dense granules (arrowheads). Fibrillar organic matrix (M) of decalcified protoconch. Scale bar 1 μm.

3.2.d *Calliostoma ligatum* – juvenile stage

One month post-metamorphic juveniles of *C. ligatum* were fixed and sectioned to visualize and describe the cells of the outer mantle epithelium at the periphery of the mantle fold (PMF). Although the PMF was close to the peripheral edge of the periostracum, histological sections showed that the two were not physically connected (Fig. 13a). However, in juveniles, fibrillar organic matrix material was present beneath the periostracum and elongate cytoplasmic extensions originating from the GE cells and microvilli arising from the Pr cells were closely associated with this organic matrix of the decalcified teleoconch (Figs. 13b, c, 14). The GE cells contained dense granules (Fig. 14), although not as many as were present within the GE cells of 13 day larvae.
The Pr cells contained many large vacuoles containing unidentified material (Fig. 13c, 14).

A large secretory cell, presumably containing and secreting mucous (to the external environment), was present adjacent to the MV cell (Fig. 13c).

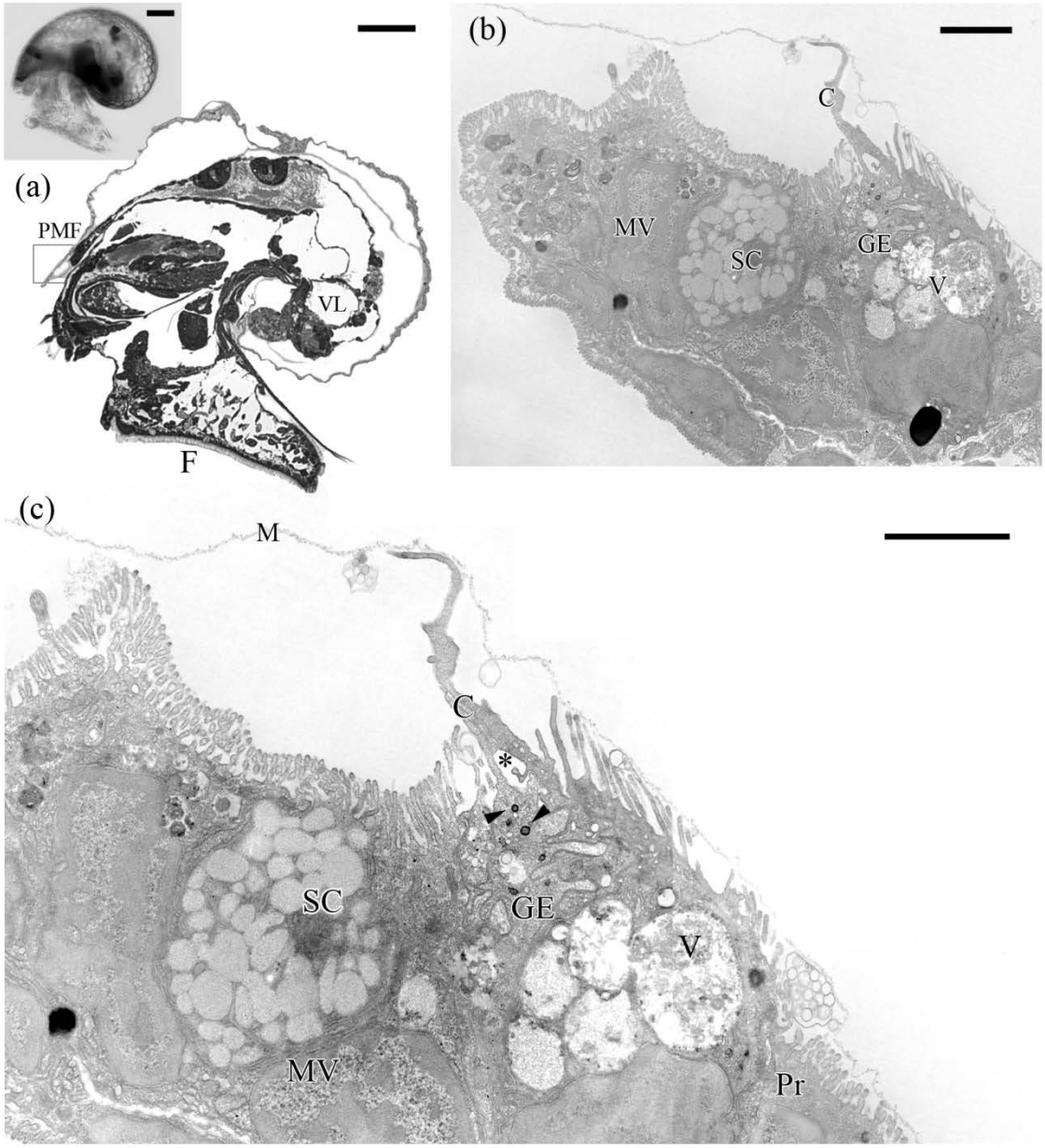

Figure 13. *Calliostoma ligatum*; juveniles at 1 month post-metamorphosis. **(a)** Mid-sagittal section showing periphery of mantle fold (PMF) at the apertural rim of the teleoconch; velum has been lost and juvenile relies on ciliated foot (F) for locomotion. Scale bar 50 µm. **Inset:** Light micrograph of live juvenile in left lateral view. Scale bar 25 µm. **(b)** TEM of PMF, with periostracum (P) overlying the apical surfaces of the growing edge (GE) and proximal (Pr) cells. Secretory cell (SC). Scale bar 2 µm. **(c)** TEM of apical regions of microvilli-bearing (MV), GE and Pr cells. GE cells bear elaborate cytoplasmic extensions (C) that associate with the inner surface of the organic matrix (M) and create an intercellular space (asterisk). Vacuoles (V) containing unidentified material. Secretory cell (SC). Scale bar 2 µm.

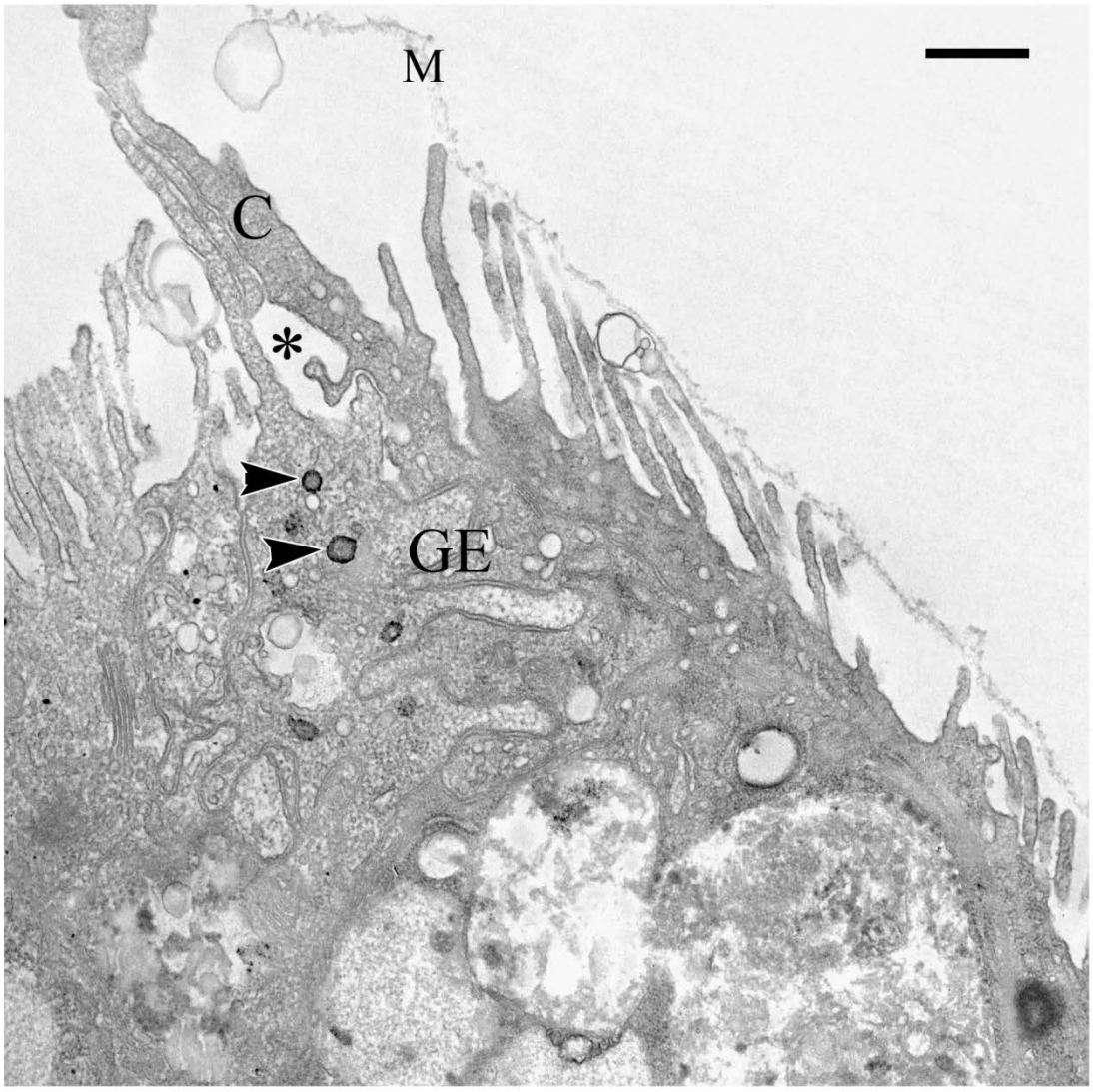

Figure 14. *Calliostoma ligatum*; juvenile at 1 month post-metamorphosis. TEM of apical regions of growing edge cells (GE) showing cytoplasmic extensions (C) in intimate association with the fibrillar organic matrix (M) of the decalcified teleoconch and creating an intercellular space (asterisk). Arrowheads indicate electron dense granules. Scale bar 2 µm.

3.3 Heterobranchia - *Siphonaria denticulata*

3.3.a *Siphonaria denticulata* – overview of development and ontogeny of shell form

Like the eggs of most heterobranchs, those of *Siphonaria denticulata* are internally fertilized and deposited as a benthic egg mass consisting of many, individually encapsulated eggs embedded within a common mass of jelly-like material. I refer to pre-hatching individuals as embryos and embryos secreted a protoconch I (Fig. 15a-c). Embryos became larvae when they hatched from the benthic egg mass at approximately 12 days following oviposition at 17°C. Unlike the larvae of patellogastropods and vetigastropods, which have shells that do not grow during the larval stage, the shells of feeding larvae of heterobranchs do grow; this phase of shell secretion is called the protoconch II (Figs. 16, 17). Swimming larvae fed on microalgae to fuel growth and development to the stage of metamorphic competence at approximately 12 days post-hatching (20-25°C). Shortly before metamorphic competence, when larvae were 10 days post-hatching, growth of the protoconch II arrested. Metamorphosis was induced by small, biofilmed pebbles collected from the adult habitat (high intertidal zone of rocky shores along southwestern Australia). Larvae withheld from the induction cue continued to swim and feed, but neither the protoconch II nor the soft tissues grew or developed further unless the animal underwent metamorphosis.

The completed protoconch I as seen in newly hatched larvae of *S. denticulata* was smooth and without sculpturing, ridges or granules on the surface (Fig. 15a-c). The shells of young juveniles showed the embryonic protoconch I (P1) at the apex of the shell, followed by the larval protoconch II (P2) and the initial portion of juvenile

teleoconch (TC) growing at the apertural edge (Figs. 16, 17). Like the protoconch I, the protoconch II showed no distinctive surface sculpturing, although the two phases of pre-metamorphic shell secretion were demarcated by a slight indentation in the smooth surface of the shell (Figs. 16a, 17a). The transition between the protoconch II and the juvenile teleoconch was marked by a more distinct discontinuity in the form of a prominent raised ridge and adjacent cleft (Fig. 16b). The juvenile teleoconch had subtle transverse ridges that clearly differentiated it from the unsculptured surface of protoconch I and II (Figs. 16, 17).

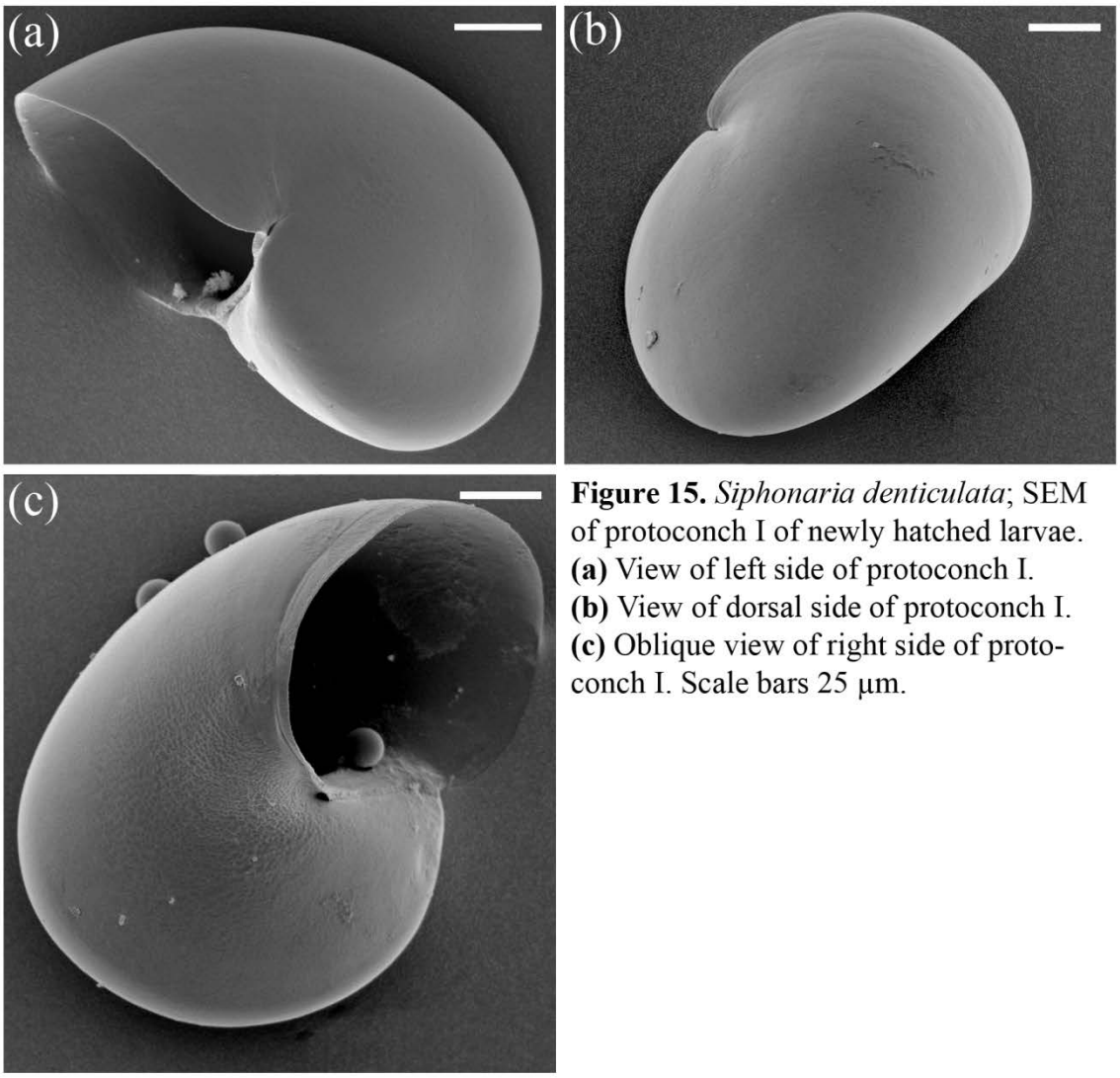

Figure 15. *Siphonaria denticulata*; SEM of protoconch I of newly hatched larvae. **(a)** View of left side of protoconch I. **(b)** View of dorsal side of protoconch I. **(c)** Oblique view of right side of protoconch I. Scale bars 25 µm.

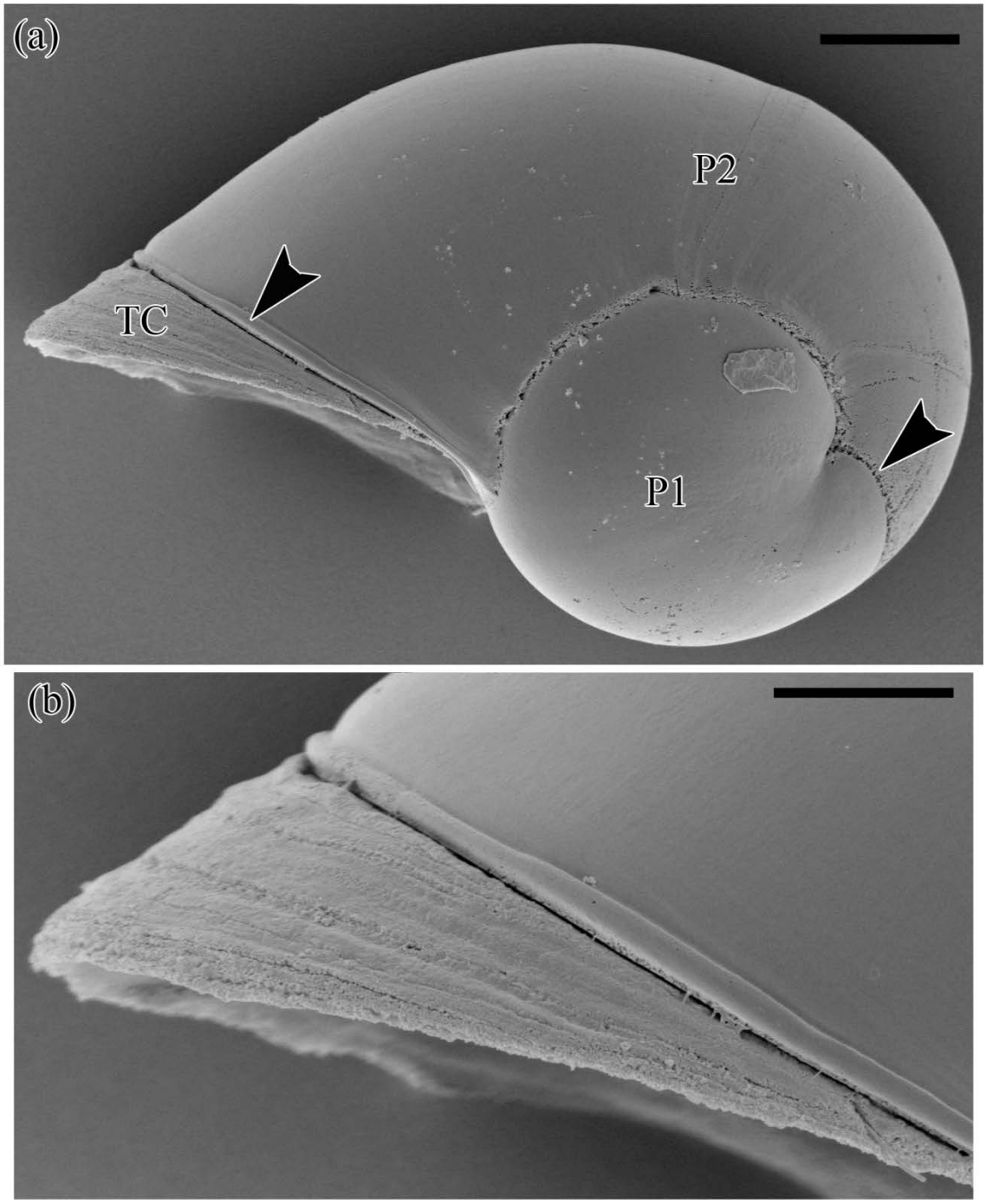

Figure 16. *Siphonaria denticulata*; juvenile shell (teleoconch). **(a)** SEM of shell showing initial teleoconch (TC), the larval protoconch II (P2), and the embryonic protoconch I (P1). Transitions between these shells highlighted by arrowheads. Scale bar 50 µm. **(b)** SEM detail of transition between larval protoconch II and juvenile teleoconch. Scale bar 25 µm.

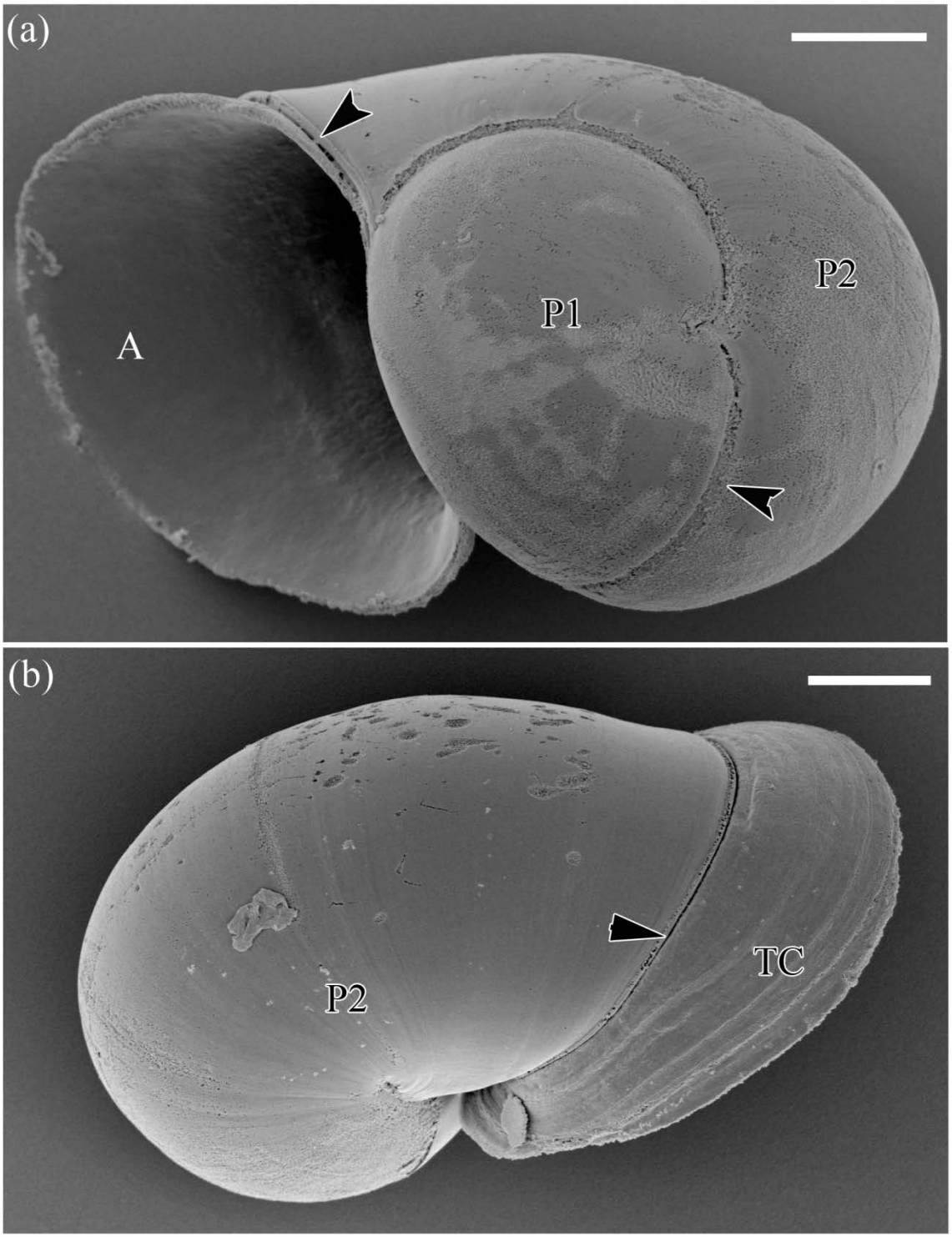

Figure 17. *Siphonaria denticulata*; juvenile shells. **(a)** Basal view showing the embryonic protoconch (P1) and larval protoconch II (P2) and the shell aperture (A). Transition between phases of shell growth marked by arrowhead. Scale bar 50 µm. **(b)** Oblique view of larval protoconch (P2) and juvenile teleoconch (TC). Transition between these shell regions is marked by arrowhead. Scale bar 50 µm.

3.3.b *Siphonaria denticulata* – larva at 6 days post-hatching

Throughout all but the last couple of days of the obligatory larval phase of *S. denticulata*, the periphery of the mantle fold of live larvae appeared to lie immediately adjacent to the apertural rim of the protoconch II (Fig. 18a). At 6 days post-hatching (dph), the protoconch II was growing and larvae at this age that were sectioned showed that the periostracum of the decalcified protoconch II was physically connected to the periphery of the mantle fold (Figs. 18b-c).

The cells of the "shell growth region" were identified based on their morphology and association with the growing edge of the periostracum. The peripheral margin of the periostracum adhered directly to the apices of the proximal (Pr) and growing edge (GE) cells and terminated just before the microvilli-bearing (MV) cell (Figs. 18d, 19a, b). There appeared to be only a single row of GE cells along the periphery of the mantle fold of *S. denticulata*. Nevertheless, the GE cell gave rise to cytoplasmic extensions that loosely interdigitated to form an intercellular space (Fig. 19b). Short microvilli arising from the proximal cell that neighboured the GE cell were also closely associated with the peripheral edge of the growing periostracum (Fig. 19a). The apical region of the GE cell contained a few electron dense granules and mitochondria (Fig. 19b). The MV cell neighbours the GE cell, towards the inner mantle epithelium, and gave rise to longer microvilli than the Pr cell.

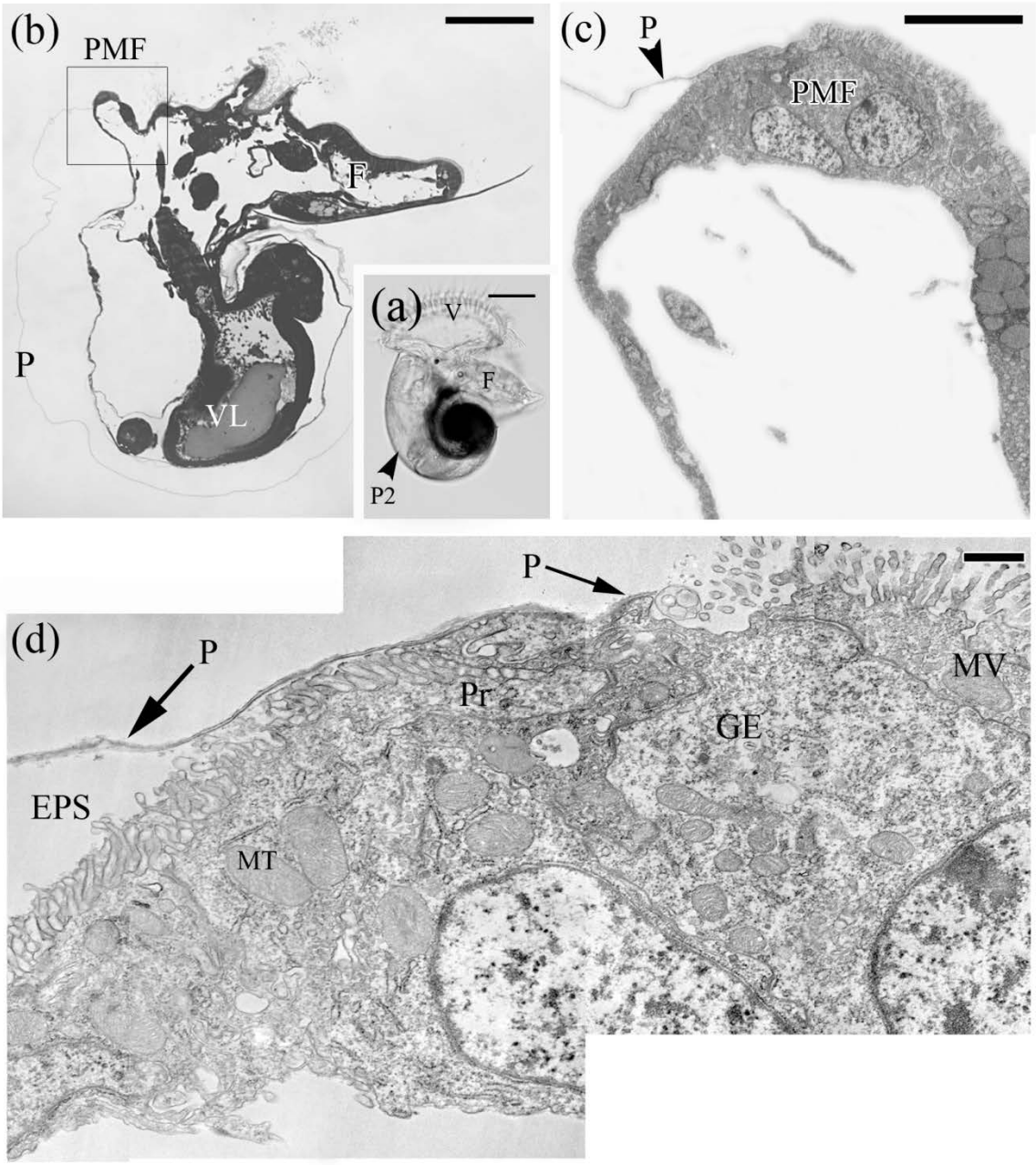

Figure 18. *Siphonaria denticulata*; larva at 6 days post-hatching. **(a)** Live larva showing velum (V), foot (F), and growing protoconch II (P2). Scale bar 100 µm. **(b)** Light micrograph of mid-sagittal section showing the periphery of the mantle fold (PMF) attached to growing edge of the periostracum (P). Foot (F), visceral lobe (VL). Scale bar 50 µm. **(c)** Low magnification TEM of PMF with attached periostracum (P). Scale bar 5 µm. **(d)** Higher magnification TEM of PMF showing apical regions of proximal (Pr), growing edge (GE) and microvilli-bearing (MV) cells. Periostracum (P) overlies microvilli of the proximal cell and terminates at the GE cells. Apical regions of MV, GE and Pr cells have numerous mitochondria (MT). Extrapallial space (EPS). Scale bar 1 µm.

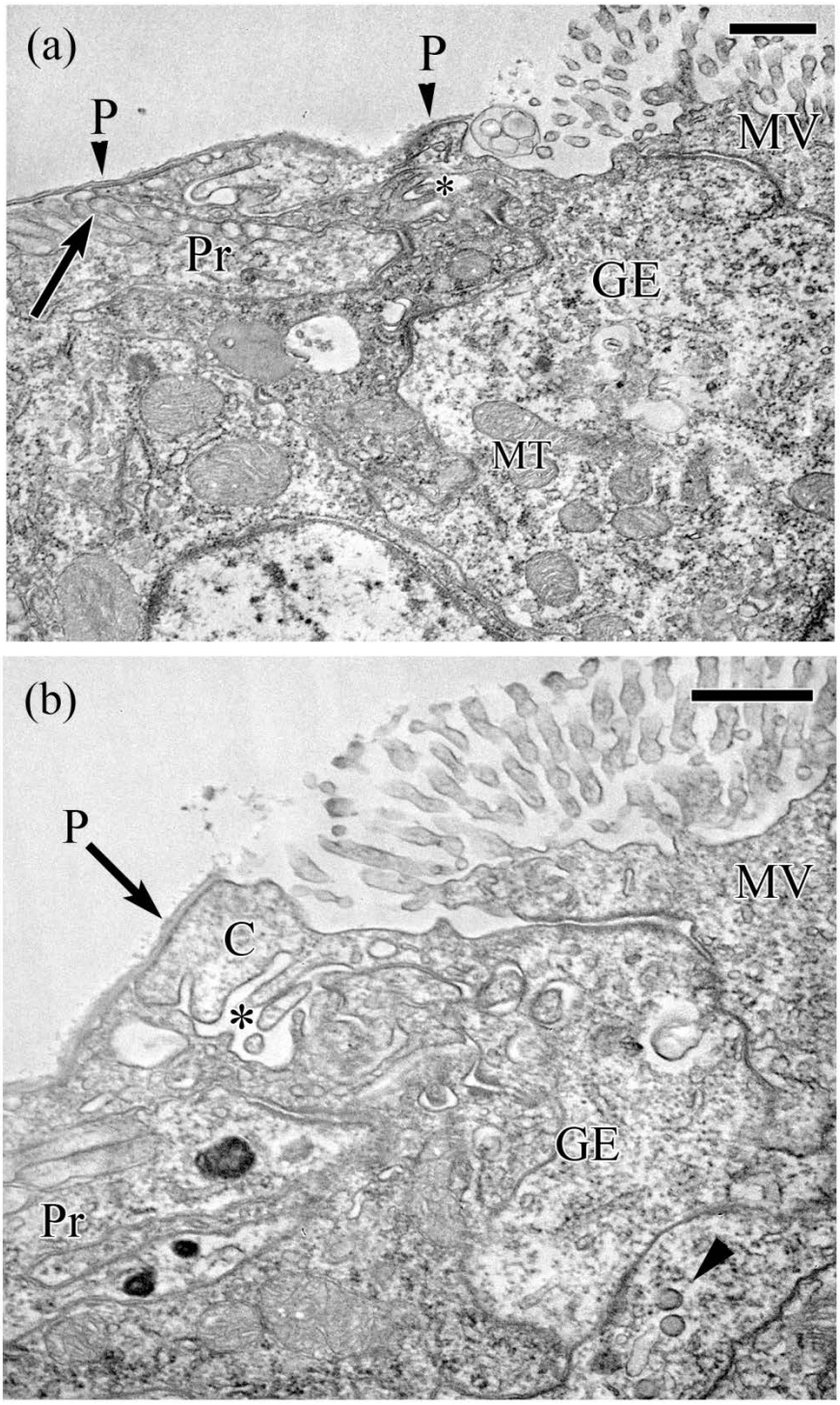

Figure 19. *Siphonaria denticulata*; 6 dph larva. **(a)** TEM detail from Fig. 18d showing apices of proximal cell (Pr), growing edge cell (GE), and microvilli-bearing cell (MV). Asterisk indicates intercellular space of GE cell and arrow indicates microvilli of Pr cell closely applied to periostracum (P). Mitochondria (MT). **(b)** TEM detail of cytoplasmic extensions (C) originating from the GE cell associated with the peripheral edge of the periostracum (P). Asterisk indicates intercellular space created by cytoplasmic extensions and arrowhead indicates electron dense granules within GE cell. Scale bars 0.5 μm.

3.3.c *Siphonaria denticulata* – 14 dph larva (after arrest of protoconch II growth)

Whole mounts of larvae of *S. denticulata* at 14 dph showed that the periphery of the mantle fold had retracted slightly from the apertural edge of protoconch II (Fig. 20a) and sections of larvae at this age showed physical disconnection between the periostracum of the decalcified protoconch II and the PMF (Figs. 20b, c). The cells of the "shell growth region" at the PMF appeared significantly reduced in size and were difficult to identify with certainly. However, a row of cells that gave rise to irregularly-shaped cytoplasmic extensions appeared to correspond to the GE cells of younger larvae that were actively secreting shell material (Figs. 21a, b). No electron dense granules were observed within these presumed GE cells. The Pr cell and MV cells located on either side of the GE cell would not be identifiable without these small extensions originating from the GE cell. The microvilli on the apices of the Pr and MV cells were reduced in size (Figs. 21a, b).

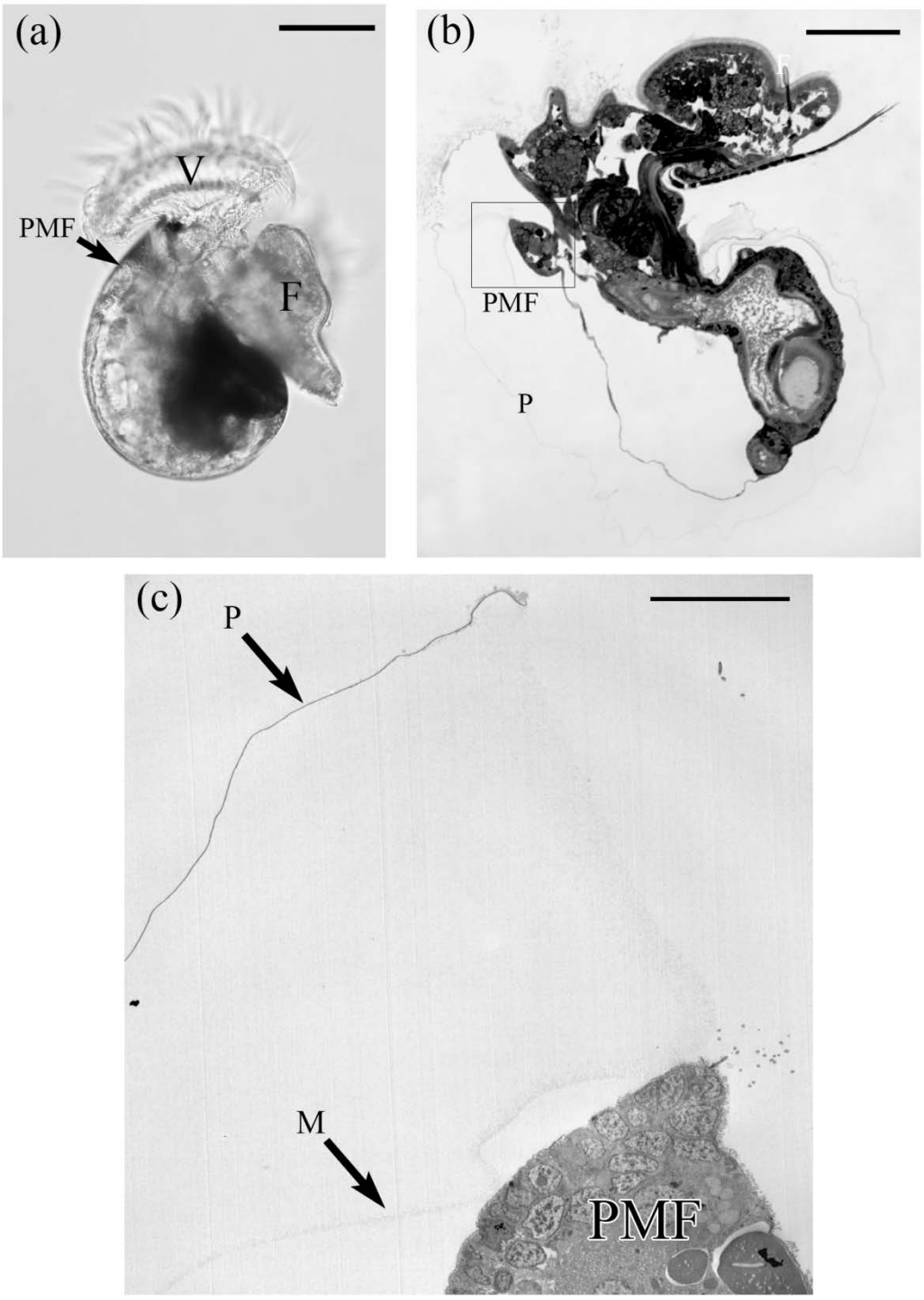

Figure 20. *Siphonaria denticulata*; 14 dph larva. **(a)** Light micrograph of a live larva showing periphery of mantle fold (PMF) detached and retracted from apertural rim of protoconch II. Velum (V), foot (F). Scale bar 100 µm. **(b)** Light micrograph of mid-sagittal section showing the periphery of the mantle fold (PMF). Scale bar 50 µm. **(c)** TEM at low magnification of PMF separated from periostracum (P). Also note layer of fibrillar organic matrix (M). Scale bar 10 µm.

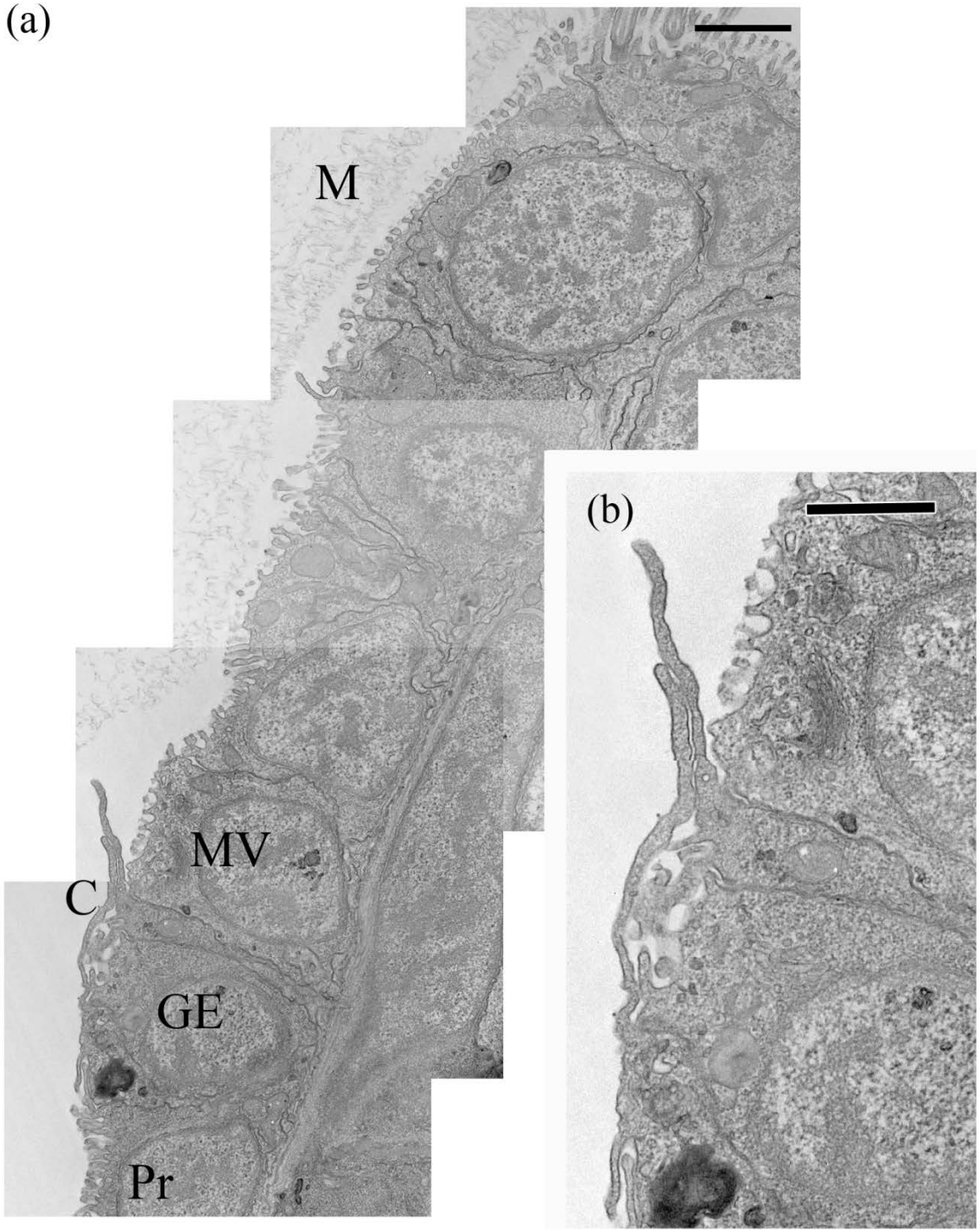

Figure 21. *Siphonaria denticulata*; 14 dph larva. **(a)** TEM detail of retracted periphery of the mantle fold with presumed proximal (Pr), growing edge (GE) and microvilli-bearing (MV) cells. Cytoplasmic extensions (C) originate from the GE cells. Fibrillar organic matrix (M). Scale bar 1 μm. **(b)** TEM detail of apex of presumed GE cell with cytoplasmic extensions. Scale bar 0.5 μm.

3.3.d *Siphonaria denticulata* – one month-old juvenile

Sections through a one month-old, post-metamorphic juvenile of *S. denticulata* showed the growing edge of the periostracum closely associated with the periphery of the mantle fold (Figs. 22a, b). The Pr cell had stubby microvilli, which appeared to be associated with organic matrix material (Figs. 22b, 23). The GE cells gave rise to cytoplasmic extensions that delineated an intercellular space and, in some sections, elongate cytoplasmic extensions from the GE cells reached to the surface of the overlying periostracum (Fig. 23). The GE cells contained a few electron dense granules (Figs. 22c, 23). The cells beyond the MV cell (further along the inner mantle epithelium) formed a cleft that ran parallel to the PMF (Fig. 23). However, the cleft did not appear to associate directly with the peripheral edge of the periostracum or the organic matrix. A thick coating of material on the outer surface of the periostracum of the teleoconch of *S. denticulata* may be biofilm (Fig. 22b, c).

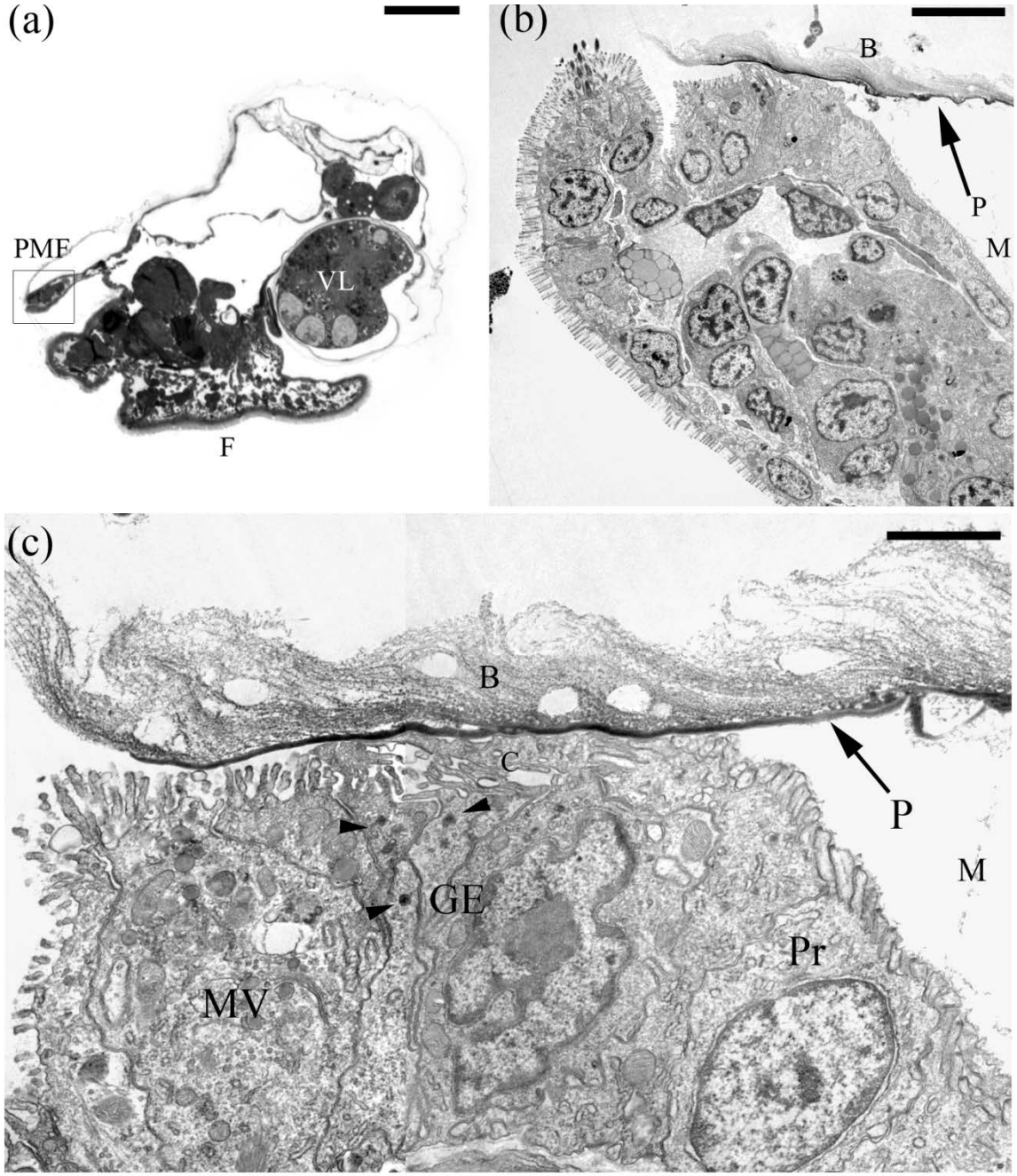

Figure 22. *Siphonaria denticulata*; one month-old juvenile. **(a)** Light micrograph of longitudinal section showing growing edge of the periostracum associated with the periphery of mantle fold (PMF). Visceral lobe (VL), foot (F). Scale bar 50 µm. **(b)** TEM of the PMF with the organic periostracum (P) overlying the apical region of the cells in this region. Fibrillar organic matrix (M), biofilm (B). Scale bar 4 µm. **(c)** TEM of apical region of the proximal (Pr), growing edge (GE) and microvilli-bearing (MV) cells, with periostracum in intimate association. Few electron dense granules (arrowheads) in the GE and MV cells. Elaborate cytoplasmic extensions (C) from the GE cells in contact with inner surface of periostracum (P). Fibrillar organic matrix (M). Scale bar 1 µm.

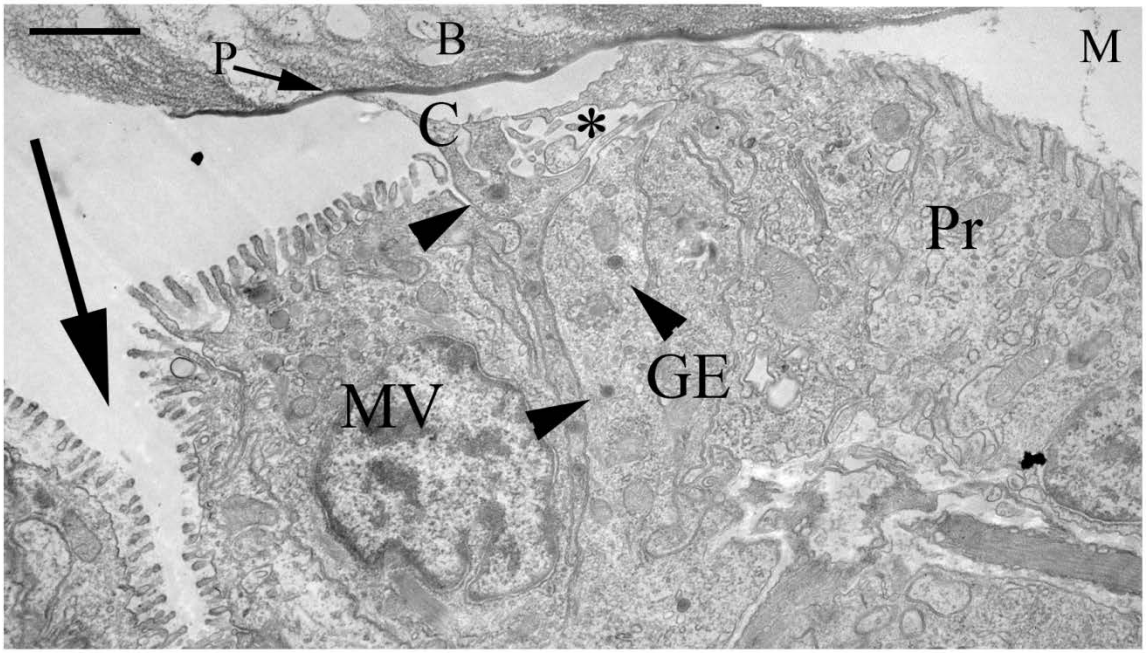

Figure 23. *Siphonaria denticulata*; 1 month-old juvenile. TEM detail of apices of microvilli-bearing (MV), growing edge (GE) and proximal (Pr) cells of the periphery of the mantle fold. The elaborate cytoplasmic extensions (C) originating from the GE cells associate with the inner surface of the periostracum (P) and form an intercellular space (asterisk). GE cells have few electron dense granules (arrowheads). A cleft (large arrow) appears adjacent to the MV cell towards the inner mantle epithelium. Biofilm (B) on outer surface of periostracum, fibrillar organic matrix (M) on inner surface of periostracum. Scale bar 1 μm.

3.4 Caenogastropoda - *Nassarius mendicus*

3.4.a *Nassarius mendicus* – overview of development and ontogeny of shell form

Eggs of the caenogastropod *Nassarius mendicus* are fertilized internally and females deposit batches of eggs into many, pouch-shaped egg capsules that are fastened to a substrate by a short stalk. Embryos inside capsules could be easily seen because the capsule wall was transparent. As with *Siphonaria denticulata*, embryos of *N. mendicus* began secreting a shell prior to hatching, which is known as the protoconch I. After 14 to 16 days at 12°C, an opening appeared at the apex of the egg capsule and swimming larvae emerged. Larvae fed on microalgae for 6 to 7 weeks before acquiring metamorphic competence. Larvae secreted a protoconch II, which grew considerably in size during the larval phase and shell growth was accompanied by growth and differentiation of the soft tissues. Larvae that had reached metamorphic competence were induced to metamorphose by sand particles collected from the habitat of the parents (low intertidal zone of the sandy shore bordering Patricia Bay, Saanich Inlet, southern Vancouver Island) and juveniles began secreting the teleoconch within a few days following metamorphosis. Larvae of *N. mendicus* delayed metamorphosis in the absence of an induction cue. However, unlike larvae of *S. denticulata*, which arrest growth of the protoconch II during delay of metamorphosis, larvae of *N. mendicus* continued to enlarge the protoconch II during a period of delayed metamorphosis.

The embryonic protoconch I of *N. mendicus* at 8 days post-oviposition was delicate and lacked sculpture, except for small, granule-like nodules on the shell surface (Fig. 24a). Secretion of protoconch II among caenogastropods with feeding larvae is traditionally thought to begin at the time of hatching. However, SEM observations of

shells from newly hatched larvae of *N. mendicus* showed that the shell secreted during the period of embryonic encapsulation began to acquire the distinctive sculpturing of the larval shell (protoconch II) well before the time of hatching (Fig. 24b). Unlike the relatively smooth external surface of protoconch I, the protoconch II of *N. mendicus* was characterized by a succession of transverse ridges running parallel to the apertural rim (Figs. 24b, 25a, b). By 20 days post-hatching (dph), the apertural margin of the protoconch II of *N. mendicus* had acquired a sinuous outline, which delineated an apertural beak and two lateral notches (Fig. 25a). By this stage of larval development, the velum of the larvae had enlarged greatly with each lateral lobe being subdivided into two arms. When these large velar lobes were extended, they fit into the lateral notches of the shell aperture; hence they are called 'velar notches'. The juvenile shell of *N. mendicus* shows the embryonic protoconch I at the apex, the larval protoconch II, and the growing juvenile teleoconch (Fig. 26a, b). Surface features of the teleoconch from young juveniles were not markedly different from those of the protoconch II. The velar notches were filled-in by the teleoconch soon after metamorphosis, but there was a siphonal canal on the left side of the apertural margin (Fig. 26c). This siphonal canal is formed by the protoconch II, even before metamorphosis (not shown).

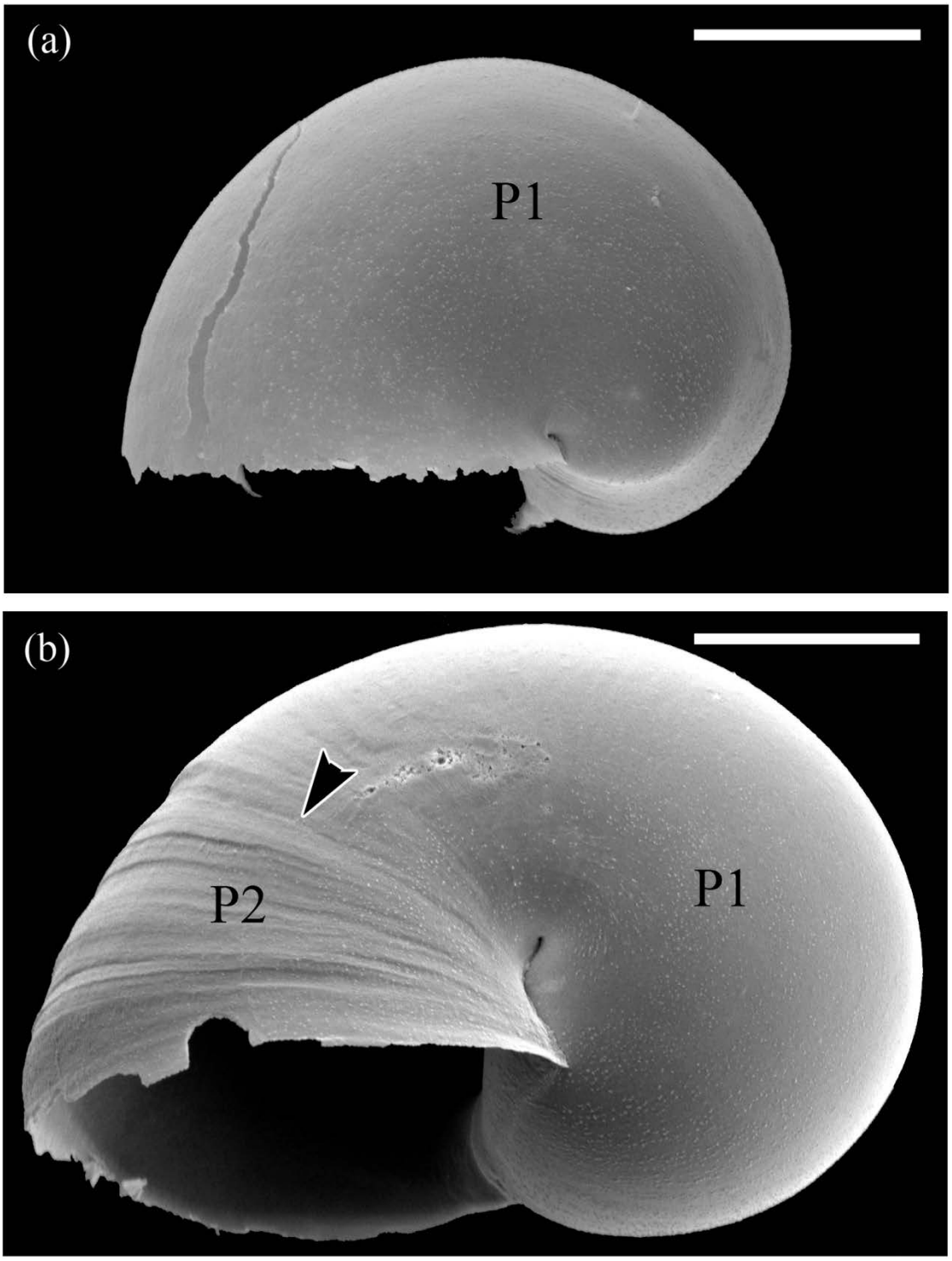

Figure 24. *Nassarius mendicus*; SEM of embryonic and larval shells. **(a)** Left side view of protoconch I (P1) from an 8 day post-oviposition embryo; crack is an artifact resulting from extreme fragility of the shell at this stage. **(b)** Right side view of protoconch I (P1) and the begining of protoconch II (P2) from a newly hatched larva; arrowhead indicates transition between the two phases of shell secretion. Scale bars 50 μm.

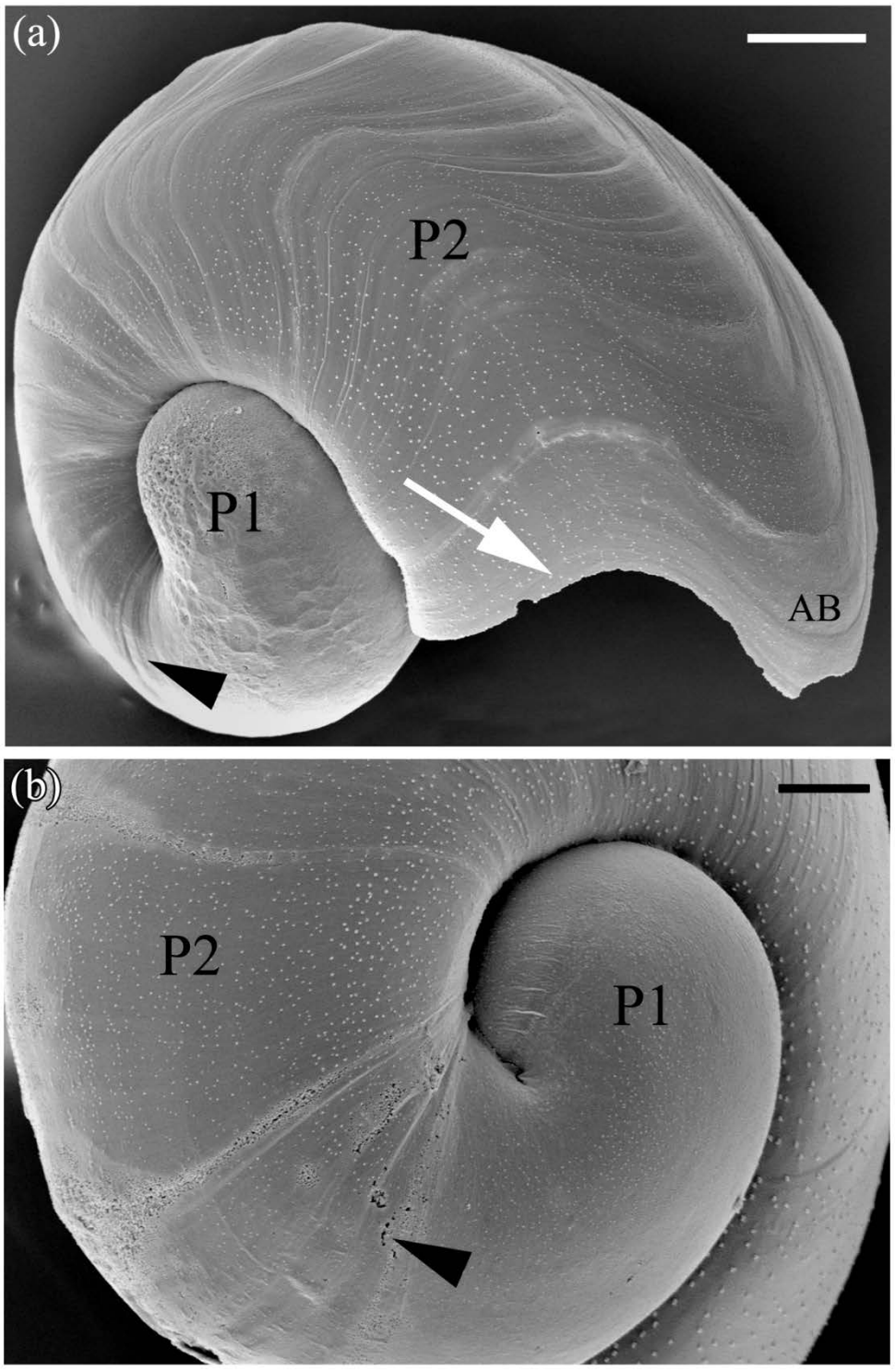

Figure 25. *Nassarius mendicus*; SEM of shells from 20 dph larvae. **(a)** Right side view of showing protoconch I (P1) and protoconch II (P2); transition between these phases of shell growth indicated by arrowhead. Note velar notches (white arrow) and apertural beak (AB). Scale bar 50 µm. **(b)** Right side view of transition region between protoconch I (P1) and protoconch II (P2) with arrowhead indicating approximate site of transition. Scale bar 25 µm.

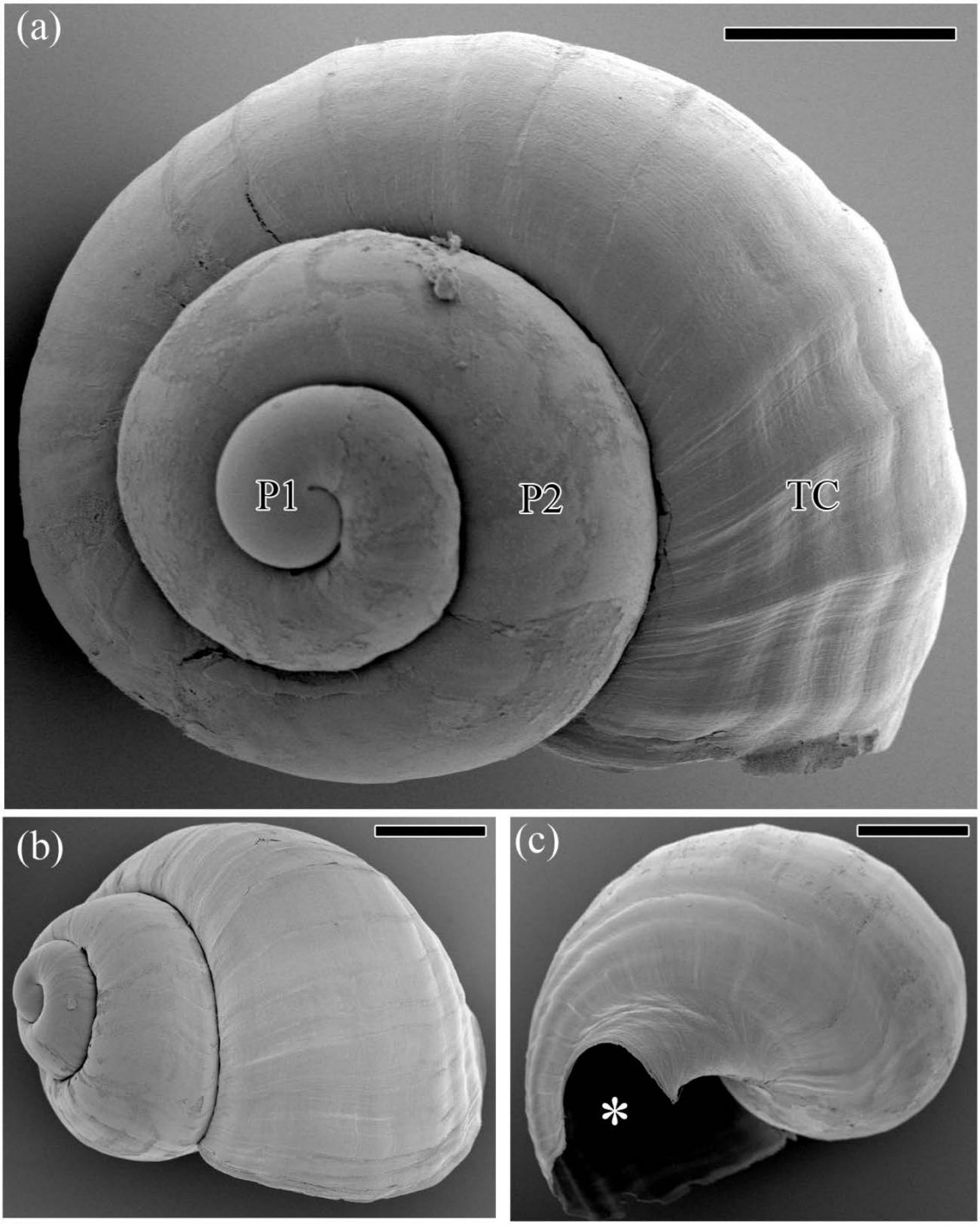

Figure 26. *Nassarius mendicus*; SEM of juvenile shells. **(a)** Right side of juvenile shell showing embryonic protoconch I (P1), larval protoconch II (P2) and juvenile teleoconch (TC). Scale bar 100 µm. **(b)** Juvenile teleoconch; note the absence of velar notches in the apertural rim. Scale bar 250 µm. **(c)** Basal view of juvenile teleoconch showing siphonal canal (asterisk). Scale bar 250 µm.

3.4.b *Nassarius mendicus* – embryonic stage

Embryos of *N. mendicus* were fixed and sectioned at 8 days post-oviposition to describe the cells involved in the active secretion of the embryonic shell, the protoconch I. Although the periostracum of the protoconch I in these embryos was not easily seen in light micrographs of histological sections (Fig. 27a), transmission electron micrographs showed the periostracum as a faint profile of material defining a shallow cup at the posterior end of the embryo (Fig. 27b).

Details of the cells underlying and presumably secreting the peripheral margin of the initial sheet of periostracum in an embryo are shown in Figs. 27b, 28 and 29b). The peripheral margin of the periostracum began at the apical surface of cytoplasmic extensions from presumed growing edge cells. These cytoplasmic extensions overlapped so as to define narrow subsurface spaces.

The cells directly adjacent to the GE cells and situated under the periostracum are the proximal (Pr) cells. These cells gave rise to short apical microvilli that impinged directly on the inner surface of the periostracum (Figs. 27b, 29b, c). The cells on the opposite side of the GE cells (i.e. exposed to the environment outside the space defined by the cup of growing periostracum) correspond in position to the microvilli-bearing cells in other species and stages of development described here. In *N. mendicus* at 8 days post-oviposition, the first row of MV cells, directly bordering the GE cells, are secretory cells containing vacuoles filled with a fibrillar material (Fig. 28).

Electron dense granules were not observed in the Pr, GE or MV cells of *N. mendicus* embryos at 8 days post-oviposition.

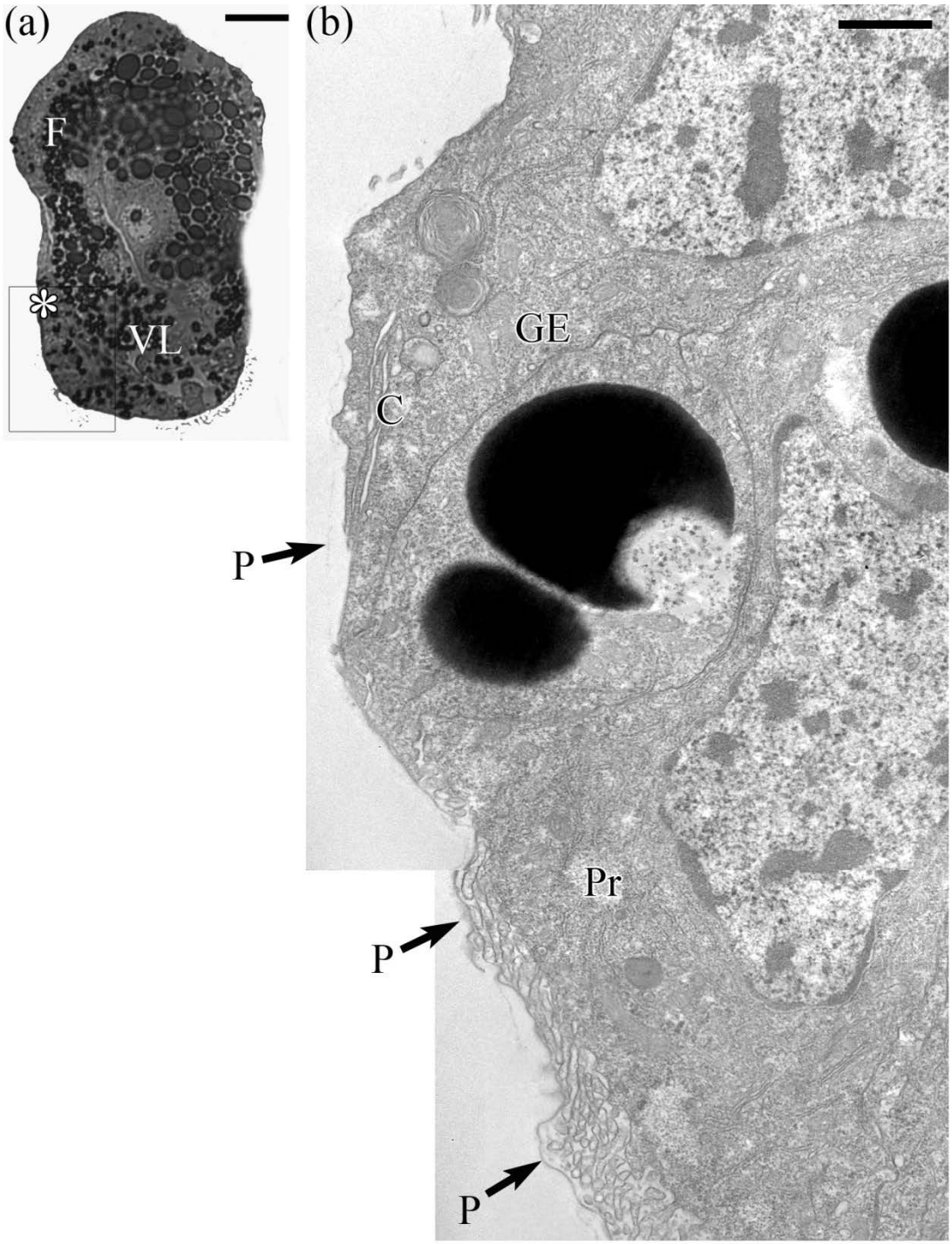

Figure 27. *Nassarius mendicus*; embryo at 8 d post-oviposition. **(a)** Histological longitudinal section showing the foot rudiment (F) and visceral lobe (VL). The initial protoconch I lies within the area outlined by the box; asterisk marks area shown in Fig. 27b. Scale bar 25 μm. **(b)** TEM of ventral peripheral margin of protoconch I showing growing edge (GE) and proximal cells (Pr). The delicate periostracum (P) overlies proximal cell and ends at cytoplasmic extensions (C) from the GE cells. Scale bar 1 μm.

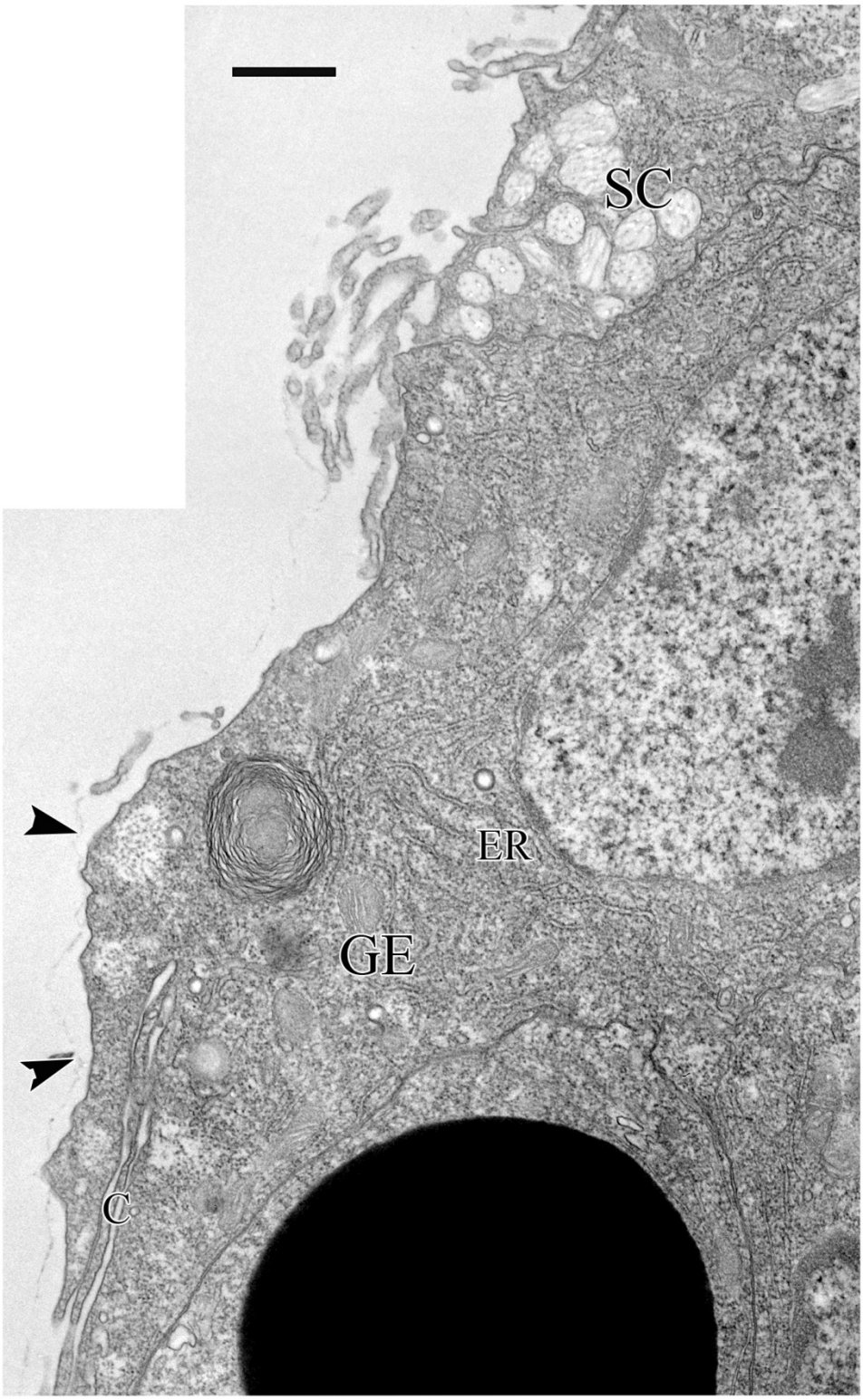

Figure 28. *Nassarius mendicus*; embryo at 8 days post-oviposition. TEM detail of growing edge cell (GE) with endoplasmic reticulum (ER) and cytoplasmic extensions (C) underlying delicate periostracum (arrowheads). Also note secretory cell beyond GE cell. Scale bar 0.5 μm.

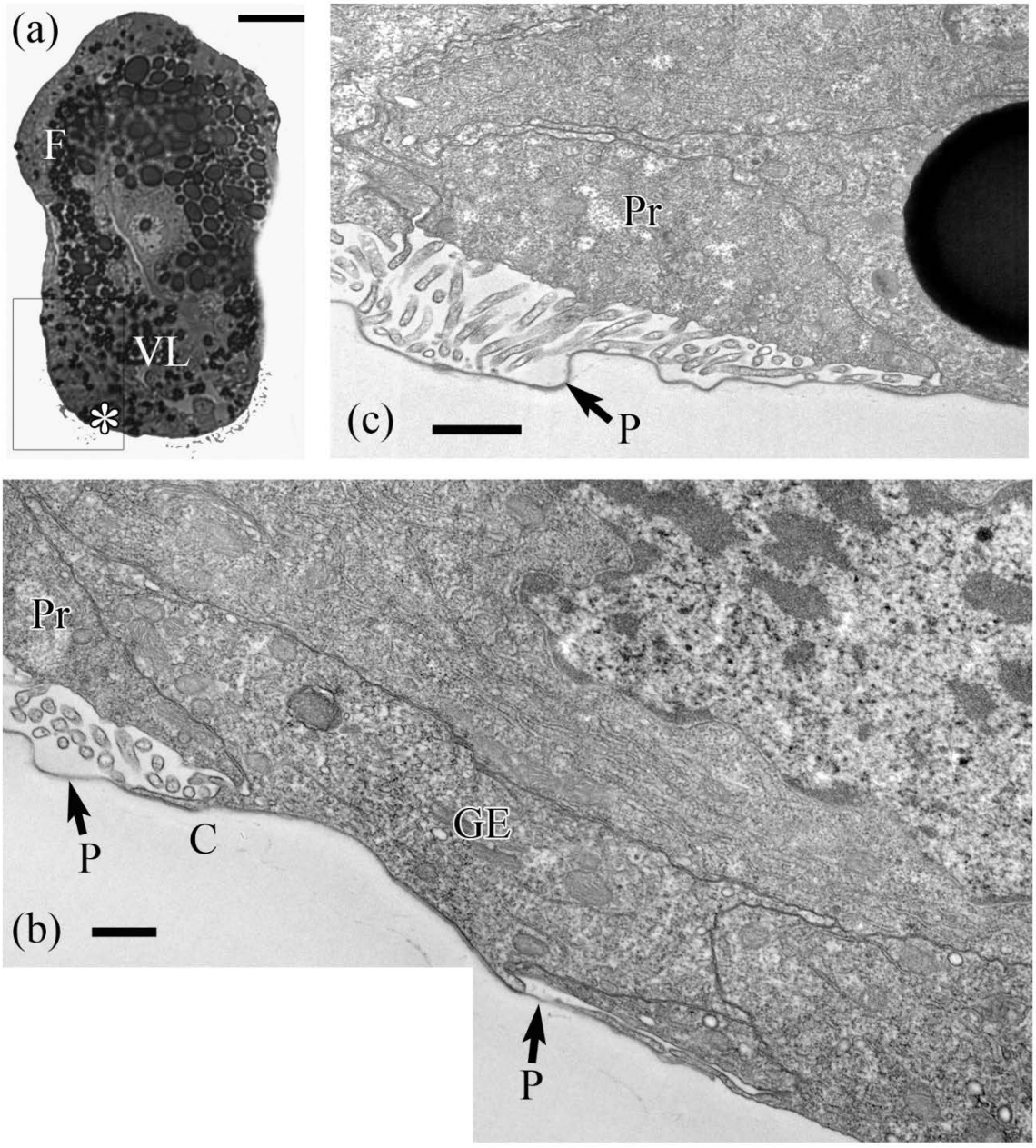

Figure 29. *Nassarius mendicus*; embryo at 8 days post-oviposition. **(a)** Histological longitudinal section through foot rudiment (F) and visceral lobe (VL). The initial protoconch I lies within the area outlined by the box; asterisk marks area shown in Figs. 29b and c. Scale bar 25 µm. **(b)** TEM showing dorsally directed edge of enlarging protoconch I. Note periostracum (P) emerging from cytoplasmic extensions (C) of growing edge cells (GE). Scale bar 0.5 µm. **(c)** TEM showing microvilli from proximal cell (Pr) closely associated with periostracum (P). Scale bar 1 µm.

3.4.c *Nassarius mendicus* – 20 days post-hatching larva

At 20 days post-hatching (dph), the protoconch II of larvae of *N. mendicus* was steadily enlarging by accretion of shell material along the apertural rim. Longitudinal sections through larvae of this age that were examined by light microscopy and low magnification electron microscopy showed that the periphery of the mantle fold was not directly attached to the periostracum of the decalcified protoconch II (Figs. 30a, b). However, transmission electron microscopy showed that the GE cells at the periphery of the mantle fold extended very long cytoplasmic processes that reached up to the organic matrix that lay immediately beneath the periostracum (Fig. 31). In life, these cytoplasmic extensions, if they adhered to the inner wall of the mineralized shell, would have acted to seal off the extrapallial space from surrounding seawater. Fusion among the cytoplasmic extensions from the GE cells delineated an intercellular space at the apex of the GE cells (Figs. 31, 32).

The cells bordering either side of the GE cells in 20 dph larvae of *N. mendicus* were similar to the corresponding cells observed in embryos. That is, the presumed Pr cells were filled with large vacuoles containing a flocculent material. Fortuitous sections showed this material undergoing exocytosis into the extrapallial space (Fig. 32). On the other side of the GE cell, the first row of MV cells was a type of secretory cell, possibly secreting mucous (Fig. 31).

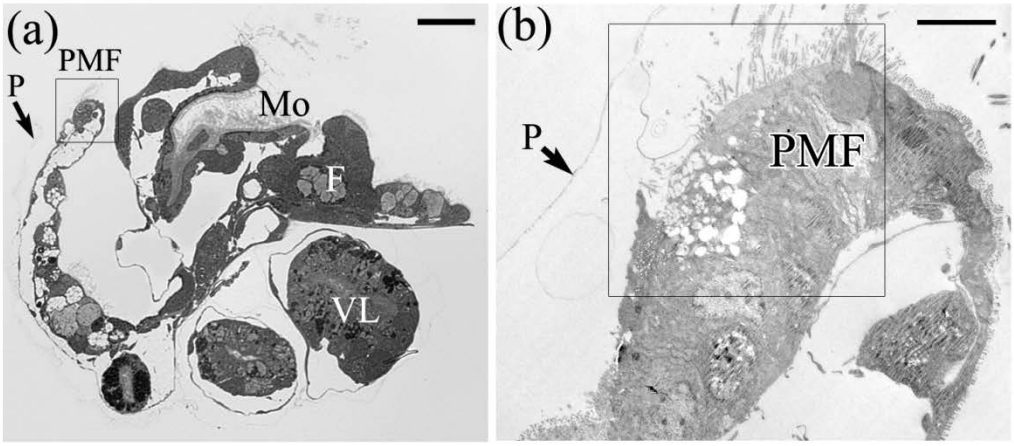

Figure 30. *Nassarius mendicus*; 20 dph larva. **(a)** Light micrograph of mid-sagittal section; boxed area highlights the periphery of the mantle fold (PMF) that secretes protoconch II. Foot (F), mouth (Mo),visceral lobe (VL). Scale bar 50 μm. **(b)** TEM at low magnification showing periphery of the mantle fold (PMF), which is not closely attached to the edge of the periostracum (P). Scale bar 5 μm.

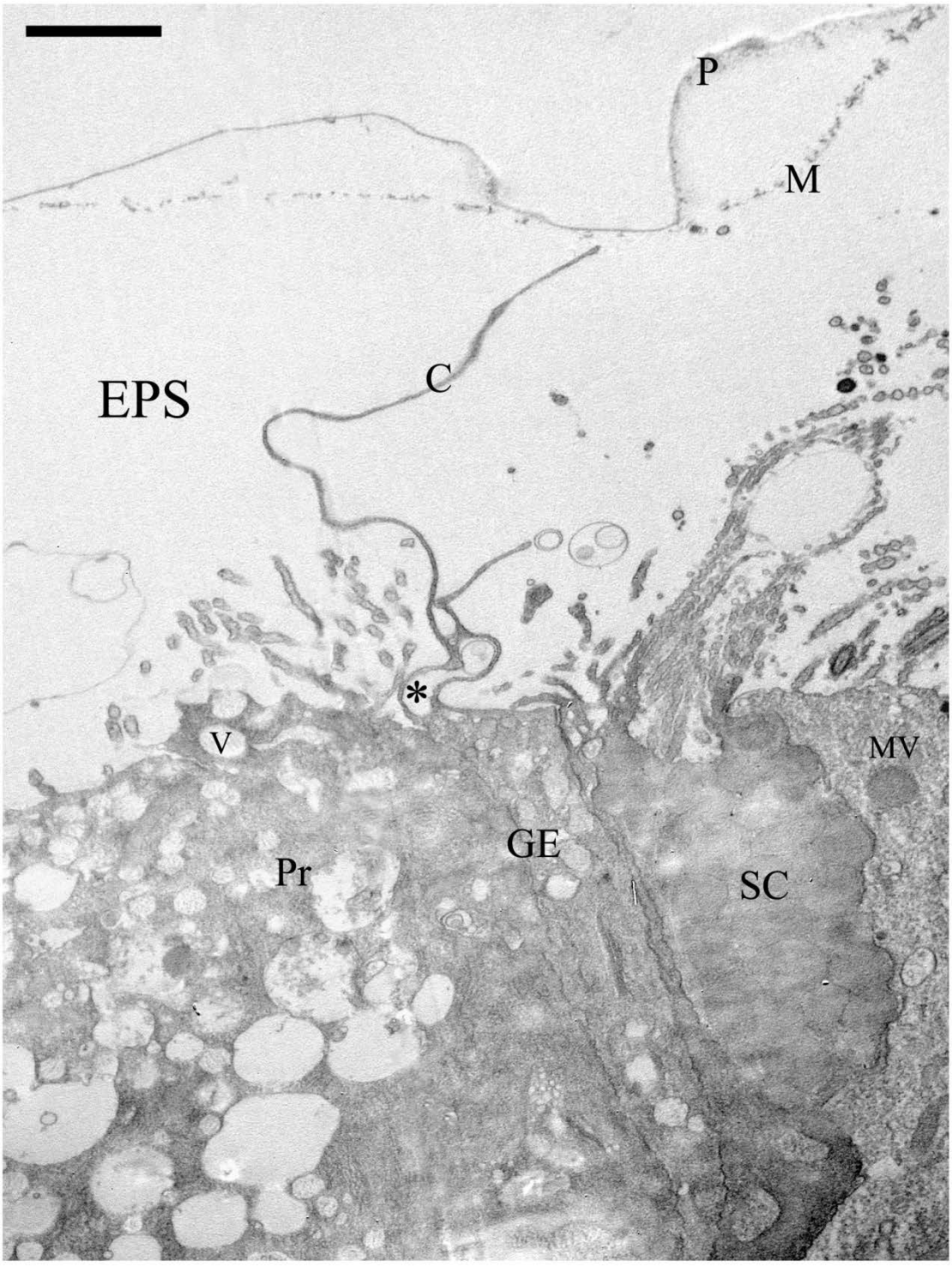

Figure 31. *Nassarius mendicus;* 20 dph larva. TEM of periphery of the mantle fold showing a long cytoplasmic extension (C) from the growing edge cell (GE) projecting toward the periostracum (P) and organic matrix (M) of protoconch II. The cytoplasmic extensions form an intercellular space (asterisk). The growing edge cells (GE) are flanked by the proximal cell (Pr), which is filled with vacuoles (V), and a secretory cell (SC). Extrapallial space (EPS) and microvilli-bearing cell (MV). Scale bar 2 µm.

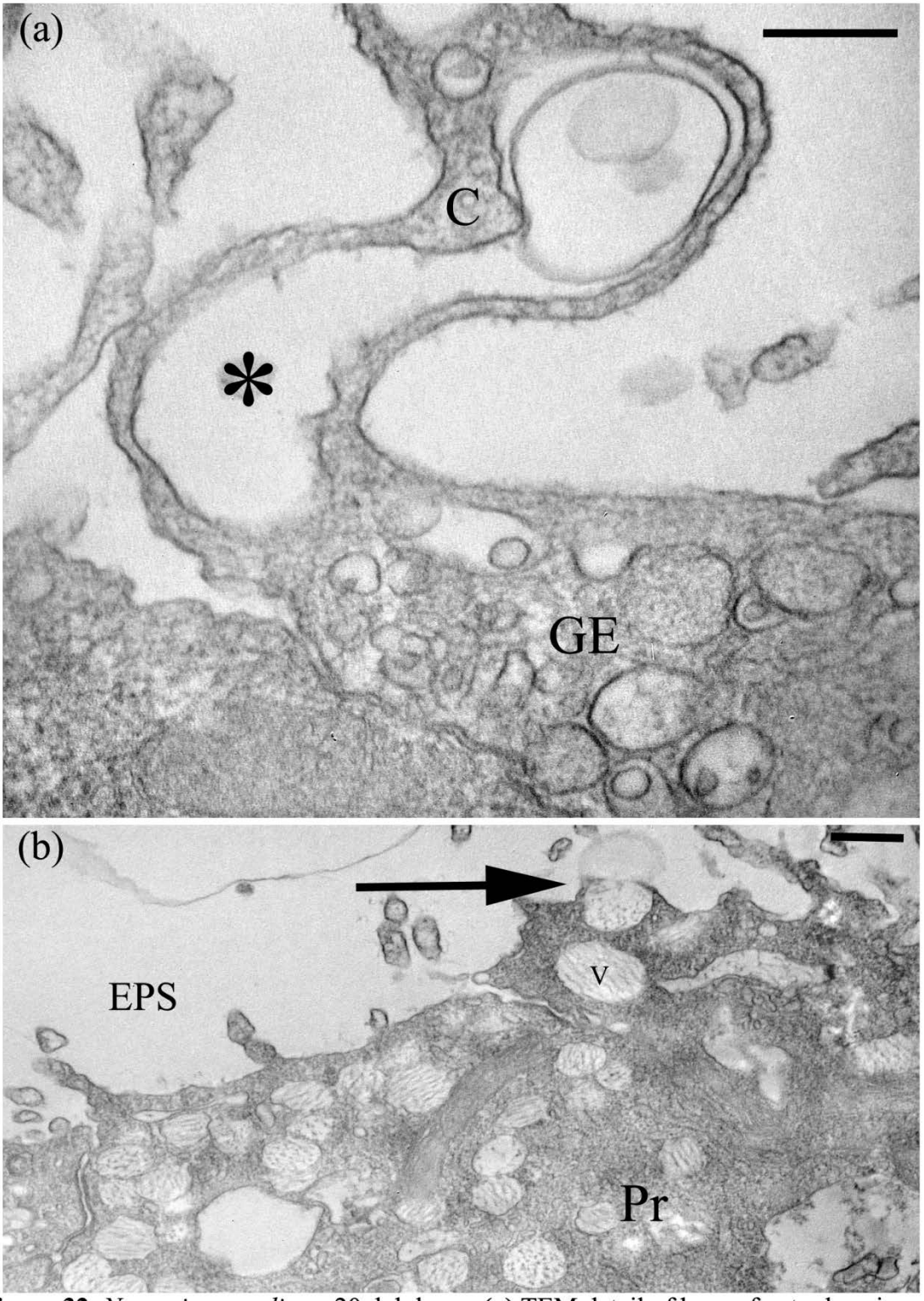

Figure 32. *Nassarius mendicus*; 20 dph larva. **(a)** TEM detail of base of cytoplasmic extensions (C) originating from the GE cell. Intercellular space (asterisk) created by the cytoplasmic extensions. Scale bar 0.25 µm **(b)** Detail of proximal cell (Pr) with numerous vacuoles (V) and detail of vacuole rupturing (arrow) into extrapallial space (EPS). Scale bar 0.5 µm.

3.4.d *Nassarius mendicus* – one month-old juvenile

One month-old *N. mendicus* juveniles show the edge of the periostracum detached from the periphery of the mantle fold (Fig. 33). The proximal (Pr) cell bears short microvilli at its apical surface. The growing edge (GE) cell bears long cytoplasmic extensions, which appear slightly stacked or folded over each other, to create an intercellular space (Fig. 33). The GE cell contained a small number of electron dense granules and mitochondria in its apical region. Neighbouring the GE cell towards the inner mantle epithelium is a secretory cell (secreting into the external environment). Highly vacuolated proximal cells comparable to those observed in the embryonic and larval stage were not seen in juveniles of *N. mendicus*.

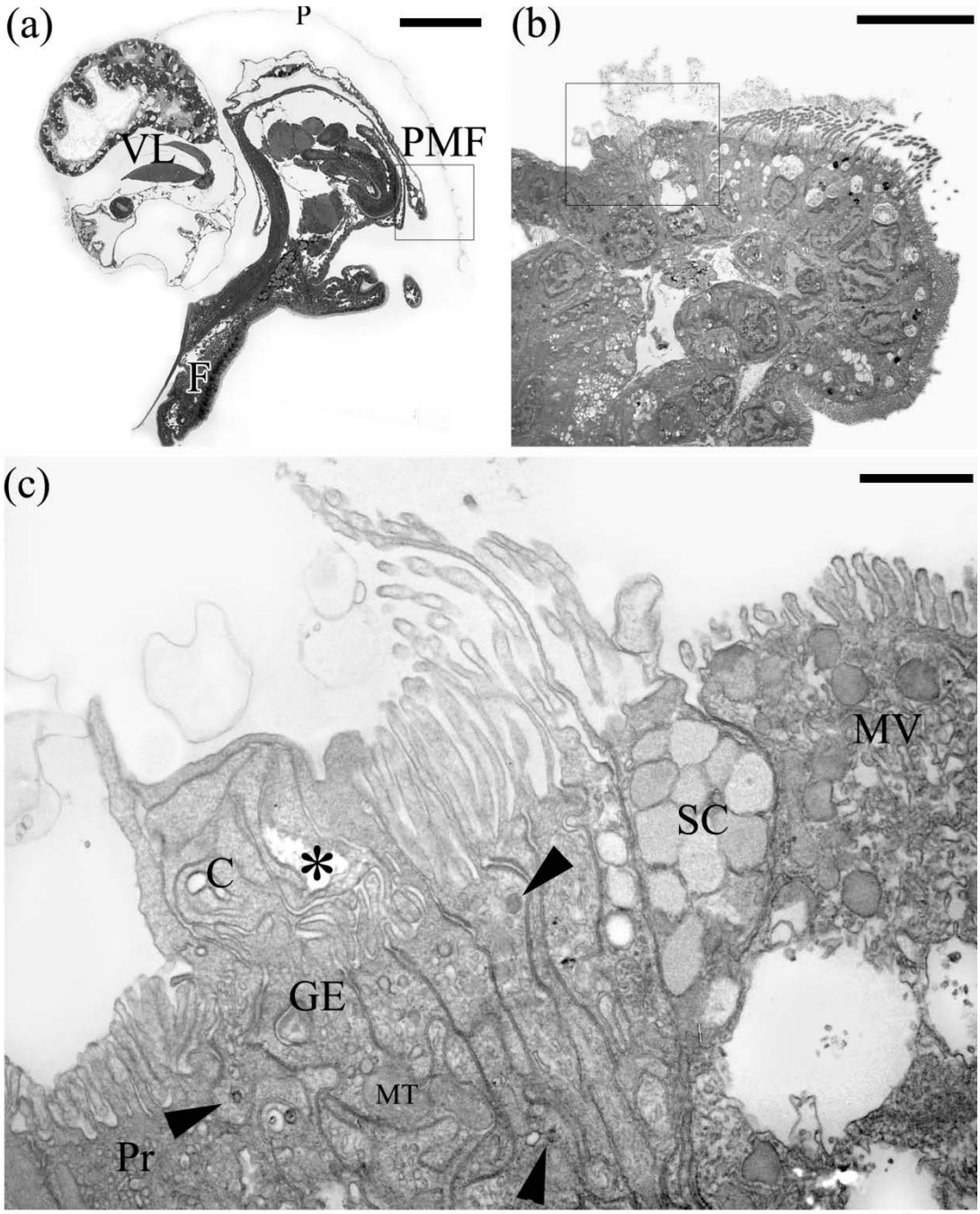

Figure 33. *Nassarius mendicus*; juvenile. **(a)** Light micrograph of mid-sagittal section showing the periphery of the mantle fold (PMF) not closely attached to the teleoconch, as marked by the periostracum (P). Visceral lobe (VL), foot (F). Scale bar 200 µm. **(b)** TEM of PMF at low magnification; boxed area is shown in Fig. 33c. Scale bar 10 µm. **(c)** TEM detail of area highlighted in Fig. 33b showing apical regions of the proximal (Pr), growing edge (GE), and microvilli-bearing (MV) cells. Elaborate cytoplasmic extensions (C) originate from the GE cells, some of which create an intercellular space (asterisk). Small number of electron dense granules (arrowheads). A secretory cell (SC) lies between the GE and MV cells. Scale bar 1 µm.

Discussion

4.1 Gastropod shell secretion during development – filling gaps in information

Molluscs have extraordinary control over all aspects of the biomineralization process, including: the site of biomineral formation, the type of mineral deposited, the orientation of mineral crystals, and the overall shape of the mineralized component (reviewed by Lowenstam and Weiner, 1989; Simkiss and Wilbur, 1989; Addadi *et al*., 2006). The mechanism of this control, which results in the combination of organic and inorganic elements to form a composite material having remarkable material properties, has motivated a great deal of recent research by bioengineers that seek to manufacture mimetics (Meyers *et al*., 2006). Biologists, on the other hand, are more interested in the functional attributes of the form and composition of molluscan shells and how changes in these parameters have evolved through time. For example, extensive previous research has documented the adaptive value of particular shell features of adult gastropods for resisting shell crushing predators (e.g. Palmer, 1979; Vermeij, 1982; West and Cohen, 1996; Hoso and Hori, 2008). The shell of gastropod molluscs is also interesting from the standpoint of evolution of development, because different life history stages produce different phases of shell secretion and the shell produced by each stage may have different evolutionary histories, different underlying constraints, and different opportunities for adaptation. For example, the adult shells (teleoconchs) of vetigastropods are extraordinarily diverse, ranging from the flat, ear-shaped shells of abalone, the volcano-shaped shells of key hole limpets, and the plump spirals of trochoideans, yet the

form of the embryonic shell (protoconch) is very similar among species of vetigastropods (Haszprunar *et al*., 1995). The beautiful surface sculpturing described here for the protoconch of *Calliostoma ligatum* represents an extreme degree of embellishment among vetigastropod protoconchs, but even here the overall shape of the protoconch is still similar to that of other vetigastropods.

The potential value of the shell of gastropod molluscs as a model system for questions about evolution of development cannot be realized without much more information about the mechanism of biomineralization during each developmental stage and the functional role of the mantle cells responsible for depositing the shell biomineral. Previous studies employing ultrastructural techniques to examine the cells that manufacture the shell have concentrated on either adult molluscs (see reviews by Wilbur and Saleuddin, 1983; Simkiss and Wilbur, 1989; Lowenstam and Weiner, 1989) or on the earliest stages of shell secretion in bivalve or gastropod embryos (Carriker and Palmer, 1979; Kniprath, 1979; 1980; Eyster, 1983; 1986, Eyster and Morse, 1984; Mouëza *et al*., 2006; Jardillier *et al*., 2008). Remarkably few studies have examined ultrastructural details of shell-secreting mantle cells in gastropod larval stages (but see Mouëza *et al*., 2006).

The major contribution of this thesis has been to provide information, previously missing, on the ultrastructure of shell-secreting cells during all life history stages, including the larva, for representatives from four different major clades of gastropods: the Patellogastropoda, Vetigastropoda, Heterobranchia, and Caenogastropoda. These data can now be compared to previous information on the morphology of shell-secreting cells in molluscs and integrated with recently revised interpretations of the biochemical and

biophysical process of biomineral deposition in order to gain new insights about the different developmental stages of shell secretion.

4.2 Functional interpretations of cellular structure

Traditionally, the embryonic shell-secreting tissue of molluscs is called the “shell gland”, although Eyster (1983) suggested that “shell field invagination” (SFI) is a preferable term for this tissue. Over the course of development, cells of the SFI become the so-called mantle or pallial epithelium of larval and adult molluscs. Unfortunately, at present there are no unambiguous morphological criteria that distinguish “shell field cells” from “mantle cells”. Similarly, there are no criteria that clearly distinguish the embryonic shell or protoconch I from a protoconch II or teleoconch. The definition of these phases of shell growth is typically coupled to the events of hatching and metamorphosis. However, this is unsatisfactory because time of hatching relative to overall developmental events is highly variable among molluscs, including gastropods (Haszprunar *et al*., 1995). Haszprunar *et al*. (1995) suggested that shells secreted by embryos differed from shells secreted by later life history stages because biomineralization of embryonic shells occurs rapidly and simultaneously throughout the whole shell at some threshold developmental time point, presumably after organic elements of the embryonic shell had been secreted. However, this proposal is not consistent with results showing that calcium carbonate within embryonic shells is deposited gradually as the periostracum is extended during embryogenesis, beginning with the earliest formed region of the periostracum and extending to the later-formed regions (Eyster, 1986; Collin and Voltzow, 1998; Jardillier *et al.*, 2008).

Regardless of the uncertainty about possible differences in details of shell secretion during different life history stages, it is clear that throughout development, the molluscan shell consists of an overlying layer of proteinaceous periostracum and the biomineral itself that consists of calcium carbonate deposits within a framework of organic matrix. The organic matrix, which becomes entombed within the mineral phase, constitutes only 1-5% by weight of the biomineral, although it is essential for control of the biomineralization process. All three of these shell components: periostracum, organic matrix, and mineral ions, are presumably secreted or actively transported by cells at the periphery of the shell field or mantle fold. Previous work, notably studies by Eyster (1983, 1985, 1986; Eyster and Morse, 1984) have identified three types of cells at the periphery of the shell field of molluscs. In most cases, I was able to distinguish these three cell types within the periphery of the mantle fold in embryos, larvae, and juveniles of the four species that I examined. In light of additional information about the process of molluscan shell formation that has accumulated during the 25 years since Eyster's work, it is worthwhile to revisit the topic of possible roles for these three cell types in the manufacture of periostracum, organic matrix, and in transport of mineral ions.

Growing edge cells and periostracum:

A major frustration for an ultrastructural study of biomineral-secreting tissues, comes from the fact that the mineral phase must be completely removed before thin-sectioning of tissue for transmission electron microscopy is possible. Not surprisingly, the most conspicuous structure remaining after the mineral is removed is the periostracum. In Eyster's (1983) early study on shell secretion by the shell field of a

nudibranch embryo, she referred to this electron-dense material as “organic shell” and suggested that it formed the template for deposition of the mineral phase of the shell. However, as more information on molluscan shell structure accumulated, it became clear that this electron-dense lamina was periostracum – comparable to the proteinaceous periostracum that covers the external surface of adult molluscan shells (Page, 1997; Mouëza *et al*., 2006; Jardillier *et al.*, 2008). In embryos of the nudibranch gastropod *Aeolidia papillosa* (Eyster, 1983), the vetigastropod *Haliotis kamtschatkana* (L.R. Page, unpublished observations), the bivalve *Chione cancellata* (Mouëza *et al.*, 2006, Fig. 21), and in embryos of three species that I studied (embryos of *Siphonaria denticulata* were not examined), the peripheral growing edge of the embryonic periostracum is consistently associated with cells having an intercellular space created by anastomosing cytoplasmic extensions (Table 2). Eyster (1983) called these the ‘growing edge cells’ (GE cells), a term that I have also used. The functional significance of this space is currently unknown.

Table 2. Occurrence of an intercellular space and electron dense granules within growing edge cells in life history stages of four gastropod species. Presence of the intercellular space is indicated by a √; absence of intercellular space indicated by ---. Presence of electron dense granules is indicated by: + few granules, ++ moderate amount of dense granules, or +++ many dense granules.

		Intercellular space	Electron dense granules
Tectura scutum	embryo	√	+
(Patellogastropoda)	larva	---	+
	juvenile	√	++
Calliostoma ligatum	embryo	√	+
(Vetigastropoda)	larva	√	+++
	juvenile	√	++
Siphonaria denticulata	young larva	√	+
(Heterobranchia)	old larva	---	---
	juvenile	√	+
Nassarius mendicus	embryo	√	no
(Caenogastropoda)	larva	√	no
	juvenile	√	+

Vesicles having an electron-dense content are a second feature often noted for GE cells (Table 2). It is tempting to suggest that the vesicles contain precursor of periostracum material. This interpretation is consistent with the presence of GE cells containing electron dense granules in embryos of the *Coryphella salmonacea*, a direct developing nudibranch that generates an embryonic periostracum but not a calcified embryonic shell (Eyster, 1985). If this interpretation is correct, and electron dense granules within GE cells are precursor of periostracum, then it seems anomalous that the greatest density of dense granules within GE cells was found in larvae of *Calliostoma ligatum*, when the shell was not enlarging (Fig. 12c). Possibly, during the arrest of shell

growth that occurs during the larval phase of this species, periostracum precursor builds-up in these cells but is not exocytosed until formation of the teleoconch is initiated at metamorphosis.

Proximal cells, organic matrix and mineral:

While the periostracum may be essential for facilitating biomineralization and protecting the shell from dissolution, it is not part of the actual mineralized shell. The shell proper of molluscs consists of mineral, usually aragonite, deposited within an organic matrix. I found that, whereas the periostracum was usually conspicuous in sections of all developmental stages, the organic matrix was evident only in post-metamorphic stages and in larvae of *Nassarius mendicus* at 20 dph. This result is not surprising given that the organic matrix constitutes only 1-5% by mass of the shell and is visible in sections of decalcified specimens only because, given sufficient shell mass, the organic matrix collapses as a conspicuous sheet of fibrillar material. The thin, delicate shells of embryos and larvae probably contain insufficient organic matrix to leave behind a "ghost" of the shell after decalcification.

If the GE cell secretes the periostracum, then the proximal (Pr) cells may be responsible for secreting organic matrix and mineral along the peripheral margin of pre-existing biomineral so as to extend this marginal rim during shell growth. A notable feature of the Pr cells from specimens that were fixed during periods of active shell growth was a close association between the apices of stubby microvilli arising from the Pr cells and the inner surface of the periostracum or organic matrix of the shell (when visible) (Table 3).

Table 3. Close association between microvilli arising from proximal edge cells and the periostracum or organic matrix of the shell. Presence of association is indicated by √; absence indicated by ---. NA (not applicable) is indicated for those specimens where the mantle periphery was retracted from the apertural rim of the shell during a period of developmental arrest of shell growth.

		association between Pr microvilli and periostracum (P) or organic matrix (M)
Tectura scutum	embryo	√ (P)
(Patellogastropoda)	larva	NA
	juvenile	√ (M)
Calliostoma ligatum	embryo	√ (P)
(Vetigastropoda)	larva	NA
	juvenile	√ (M)
Siphonaria denticulata	young larva (6dph)	√ (P)
(Heterobranchia)	old larva (14 dph)	NA
	juvenile	√ (P & M)
Nassarius mendicus	embryo	√ (P)
(Caenogastropoda)	larva	---
	juvenile	---

The original epitactic matrix model for molluscan shell biomineralization proposed that constituents of the organic matrix (ß-chitin, silk fibroin, and acidic protein) were secreted into the extrapallial space where they self-assembled into envelopes. Calcium and carbonate ions were then transported into fluid of the extrapallial space and precipitation of mineral crystals was nucleated by the organic matrix. Recent studies have forced revision of this model. Although constituents of the organic matrix may indeed self-assemble within the extrapallial space, it appears that mineral may be directly

applied to the matrix as pre-formed aggregates of amorphous calcium carbonate (ACC) that subsequently reorganizes as aragonite crystals (reviewed by Addadi *et al*., 2006). I suggest that the close association between microvilli of Pr cells and the periostracum (and presumably an underlying layer of organic matrix) in embryos and with the organic matrix in juveniles may be the morphological correlate of direct application of ACC to the organic matrix.

The ultrastructural data gained from this study and used to make these functional interpretations has been simplified and summarized in Fig. 34. The shell growth regions of all stages studied from each representative and the important features including: the presence of an intercellular space, the relationship of the periostracum to the growing edge (GE) cells and the association of the periostracum to the proximal (Pr) cells, have been illustrated (Fig. 34).

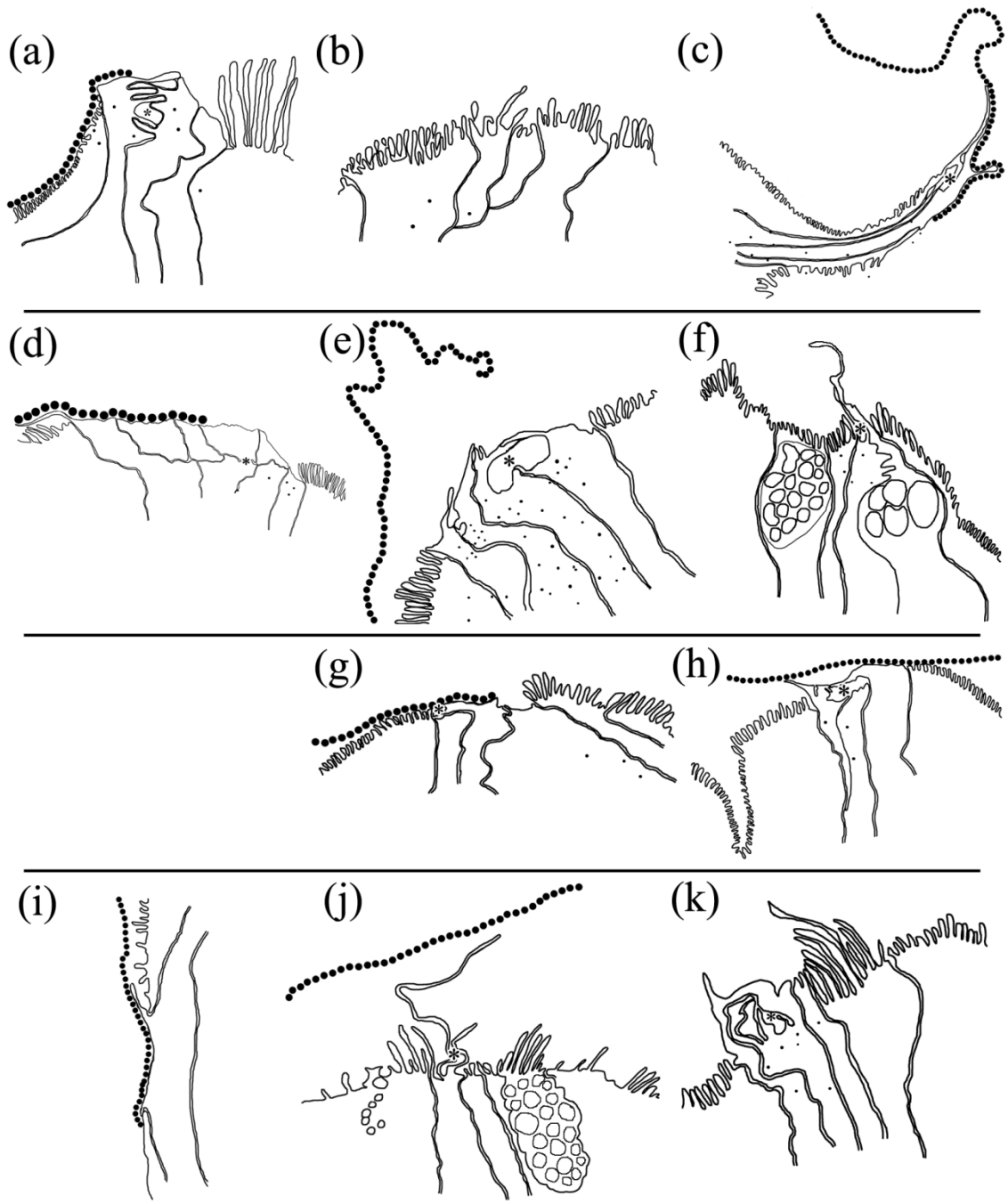

Figure 34. Illustrations of simplified ultrastructural features of shell growth regions (Pr, GE and MV cells) of stages and species examined in this study. Note association of growing edge of periostracum with GE cells, relationship between inner surface of periostracum with Pr cells, electron dense granules and intercellular spaces (asterisk). **(a)** *Tectura scutum* embryo, **(b)** *T. scutum* larva, **(c)** *T. scutum* juvenile. **(d)** *Calliostoma ligatum* embryo, **(e)** *C. ligatum* larva, **(f)** *C. ligatum* juvenile. **(g)** *Siphonaria denticulata* 6dph larva, **(h)** *S. denticulata* juvenile. **(i)** *Nassarius mendicus* embryo. **(j)** *N. mendicus* larva, **(k)** *N. mendicus* juvenile. Illustrations not to scale. (Note: *S. denticulata* older larva at 14 dph omitted from figure.)

4.3 Evolution of a novelty by manipulating timing of a developmental module

This study was an effort to test two hypotheses about the evolutionary origin of a novel phase of shell secretion during the life history of gastropods with a feeding larval stage. Non-feeding gastropod larvae, which are typical of members of the Patellogastropoda and Vetigastropoda, are presumably the ancestral larval type for gastropods. Non-feeding larvae do not grow and have only two phases of shell secretion: the embryonic shell (protoconch) and the post-metamorphic shell (teleoconch). By contrast, feeding larvae do grow during the larval stage and require a shell that also grows. Gastropods with feeding larvae are found within the Heterobranchia and the Caenogastropoda. Increase in size of the larval body and larval shell is particularly marked in caenogastropods, whereas growth is relatively more modest among heterobranchs. Nevertheless, for both these clades, a growing larval shell is a novel acquisition during development.

Hypothesis #1: Heterobranch protoconch II is an extended protoconch phase of non-feeding larvae.

One hypothesis that my observations tested is the suggestion that the protoconch II of heterobranchs originated during evolution by prolongation of the embryonic phase of shell secretion. This hypothesis interprets the protoconch II of heterobranch larvae as being the result of the heterochronic process of hypermorphosis (i.e.: a change in timing of developmental events where the rate of development stays the same, but the length of time is extended) (Hall, 1999). Two previous observations inspired this hypothesis. First, the larvae and therefore the larval shells of heterobranch larvae typically do not attain

large size relative to caenogastropod larvae; indeed the size range for final larval shell sizes among heterobranchs broadly overlaps the size range for the protoconchs of patellogastropod and vetigastropod larvae (Hadfield and Miller, 1987). Second, the periphery of the mantle fold detaches and retracts from the apertural rim of the shell in both non-feeding larvae of patellogastropods and vetigastropods and in feeding larvae of heterobranchs. This morphogenetic event signals the end of shell growth until after metamorphosis.

My ultrastructural observations are at least consistent with this hypothesis. The patellogastropod and vetigastropod embryos that I fixed during the phase of protoconch secretion both showed the growing edge of the periostracum intimately connected with the growing edge (GE) cells at the periphery of the mantle fold. Immediately proximal to the growing edge cells, the microvilli of the proximal (Pr) cells impinged directly on the inner surface of the periostracum. Both these features were also recorded for young larvae of the heterobranch, *Siphonaria denticulata,* but were evident only during the embryonic phase of protoconch I formation in the caenogastropod, *Nassarius mendicus*. Furthermore, the same features were observed in ultrastructural sections through the mantle fold of young larvae of the heterobranch, *Melibe leonina* (Page, 1994).

Hypothesis #2: Caenogastropod protoconch II is a precocious teleoconch.

This hypothesis also invokes heterochronic transformation of a developmental module to explain the novelty of a growing larval shell (protoconch II) in a clade of gastropods having a feeding larva. In this case, however, the heterochronic process may be pre-displacement - earlier onset of teleoconch secretion relative to the ancestral

condition (Hall, 1999). The inspiration for this hypothesis comes from the fact that the protoconch II of many caenogastropods does not have a developmentally programmed endpoint for enlargement – shell growth continues throughout the larval stage (mantle retraction does not occur prior to the attainment of metamorphic competence) and often continues during the "optional" period of delay of metamorphosis.

My observations on the form and surface sculpturing of the protoconch II and the teleoconch of the caenogastropod, *Nassarius mendicus*, made by scanning electron microscopy, are consistent with this hypothesis. The overall shape of protoconch II was similar to that of the teleoconch, suggesting similar shell coiling parameters in both life history stages. The surface sculpturing of the protoconch II was also similar to that of the teleoconch and the protoconch II also acquired a siphonal canal prior to metamorphosis. However, the sinuous outline of the apertural rim was unique to late stages of protoconch II growth and is likely a feature to accommodate a uniquely larval characteristic of the soft anatomy – greatly enlarged velar lobes in older larvae.

Although features of the shell itself were consistent with predictions of hypothesis #2, I was unable to find significant support from ultrastructural features of the shell-secreting cells at the periphery of the mantle fold in *N. mendicus*. The periphery of the mantle fold in larvae of *N. mendicus* showed a unique type of Pr cell that was not seen in any other specimens that I examined, including juveniles of this species. These cells had a large number of vacuoles filled with a flocculent material.

4.4 Conclusions and suggestions for future research

As previously mentioned, there is been a gap in our knowledge of the mechanisms of biomineralization and the functional role of the shell-secreting cells at the periphery of the mantle fold in the developmental stages of gastropod molluscs. The ultrastructural observations and functional interpretations made for the shell-secreting cells of the representative species used in this study, have hopefully opened a small window into the process of ontogenetic shell growth in the groups of the Gastropoda. The ultrastructural features of these cells that appear to have a close relationship with the growing edge of the periostracum and material presumed to be the organic matrix, appear to maintain these features throughout development and are consistent with characteristic features observed in other studies highlighting the shell growth region (Eyster, 1983; 1985; 1986; Mouëza *et al.*, 2006). The growing edge cells may secrete growing periostracum (possibly present in the cell as electron dense granule precursors) and the proximal cells (whose stubby microvilli often closely associate with the inner surface of the periostracum and organic matrix material) may pre-form and secrete the components of the organic matrix. Further investigation using more specimens (as only 2-3 specimens were sectioned per stage), more species from the four major groups of gastropods, and more ontogenetic stages to fill in the morphological development of these shell-secreting cells is needed.

The potential value of the shell of gastropod molluscs as a model system for questions about evolution of development within the Gastropoda remains to be explored. Though this study was not able to add support to the hypothesis that the larval shell secreted by the Caenogastropoda is a post-metamorphic shell with an early onset of

secretion (heterochronic pre-displacement), it does add to the support to the possibility that within the Heterobranchia, the feeding larval stage may have evolved by hypermorphosis (a heterochronic event whereby there is an extension of a developmental phase). Further investigation into both of these hypotheses using a more detailed study of the shells and other morphological features related to the shell of different and potentially more appropriate representatives from the groups of gastropods is required before any conclusions can be made.

Literature Cited

Addadi, L., D. Joester, F. Nudelman, and S. Weiner. 2006. Mollusk shell formation: A source of new concepts for understanding biomineralization processes. Chemistry - A European Journal 12: 980-987.

Aktipis, S.W., G. Giribet, D.R Lindberg, and W.F. Ponder. 2008. Gastropoda. Pp 201-237 *in* W.F. Ponder and D.R. Lindberg, eds. Phylogeny and Evolution of the Mollusca. University of California Press, Berkeley.

Bielefeld, U., and W. Becker. 1991. Embryonic development of the shell in *Biomphalaria glabrata* (Say). International Journal of Developmental Biology 35: 121-131.

Carriker, M.R., and R.E. Palmer. 1979. Ultrastructural morphogenesis of prodissoconch and early dissoconch valves of the oyster *Crassostrea virginica*. Proceedings of the National Shellfisheries Association 69: 103-128.

Collin, R., and J. Voltzow. 1998. Initiation, calcification, and form of larval "archaeogastropod" shells. Journal of Morphology 235: 77-89.

Collins, A.G., and J.W. Valentine. 2001. Defining phyla: evolutionary pathways to metazoan body plans. Evolution & Development 3(6): 432-442.

Currey, J.D. 1980. Mechanical properties of mollusc shell. Symposia of the Society for Experimental Biology 34: 75-97.

Davidson, E.H., K.J. Peterson, and R.A. Cameron. 1995. Origin of bilaterian body plans: evolution of developmental regulatory mechanisms. Science 270: 1319-1325.

Degnan, S.M., and B.M. Degnan. 2006. The origin of the pelagobenthic metazoan life cycle: what's sex got to do with it? Integrative and Comparative Biology 46(6): 683-690.

Eyster, L.S. 1983. Ultrastructure of early embryonic shell formation in the opisthobranch gastropod *Aeolidia papillosa*. Biological Bulletin 165: 394-408.

Eyster, L.S. 1985. Origin, morphology and fate of the nonmineralized shell of *Coryphella salmonacea*, an opisthobranch gastropod. Marine Biology 85: 67-76.

Eyster, L.S. 1986. Shell inorganic composition and onset of shell mineralization during bivalve and gastropod embryogenesis. Biological Bulletin 170: 211-231.

Eyster, L.S., and M.P. Morse. 1984. Early shell formation during molluscan embryogenesis, with new studies on the surf clam, *Spisula solidissima*. American Zoologist 24: 871-882.

Falini, G., S. Albeck, S. Weiner, and L. Addadi. 1996. Control of aragonite or calcite polymorphism by mollusk shell macromolecules. Science 271: 67-69.

Guillard, R.R.L. 1975. Culture of phytoplankton for feeding marine invertebrates. Pp. 29 40 *in* W.L. Smith and M.H. Chanley, eds. Culture of Marine Invertebrate Animals. Plenum Press, New York.

Hadfield, M.G., and Miller S.E. 1987. On developmental patterns of opisthobranchs. American Malacological Bulletin 5: 197-214.

Hadfield, M.G., E.J. Carpizo-Ituarte, K. del Carmen, and B.T. Nedved. 2001. Metamorphic competence, a major adaptive convergence in marine invertebrate larvae. American Zoologist 41: 1123-1131.

Hall, B.K. 1999. Evolutionary Developmental Biology. Kluwer Academic Publishers, Boston.

Haszprunar, G. 1992. The types of homology and their significance for evolutionary biology and phylogenetics. Journal of Evolutionary Biology 5: 13-24.

Haszprunar, G., L. v. Salvini-Plawen, and R.M. Rieger. 1995. Larval planktotrophy – a primitive trait in the Bilateria? Acta Zoologica 76(2): 141-154.

Hoso, M., and M. Hori. 2008. Divergent shell shape as an antipredator adaptation in tropical land snails. American Naturalist 172(5): 726-732.

Jablonski, D., and R.A. Lutz. 1980. Molluscan larval shell morphology - ecological and paleontological applications. Pp. 323-377 *in* D.C. Rhoads and R.A. Lutz, eds. Skeletal Growth of Aquatic Organisms. Plenum Press, New York.

Jablonski, D., and R.A. Lutz. 1983. Larval ecology of marine benthic invertebrates: paleobiological implications. Biological Revue 58: 21-89.

Jägersten, G. 1972. Evolution of the Metazoan Life Cycle - A comprehensive theory. Academic Press, London.

Jardillier, E., M. Rousseau, A. Gendron-Badou, F. Fröhlich, D.C. Smith, M. Martin, M.-N. Helléouet, S. Huchette, D. Doumenc, and S. Auzoux-Bordenave. 2008. A morphological and structural study of the larval shell from the abalone *Haliotis tuberculata*. Marine Biology 154: 735-744.

Kempf, S.C. 1981. Long-lived larvae of the gastropod *Aplysia juliana*: do they disperse and metamorphose or just slowly fade away? Marine Ecology Progress Series 6: 61-65.

Kniprath, E. 1977. Zur ontogenese des schalenfeldes von *Lymnaea stagnalis*. Development Genes and Evolution 181(1): 11-30.

Kniprath, E. 1979. The functional morphology of the embryonic shell-gland in the conchiferous molluscs. Malacologia 18: 549-552.

Kniprath, E. 1980. Larval development of the shell and the shell gland in *Mytilus* (Bivalvia). Development Genes and Evolution 188(3): 201-204.

Kniprath, E. 1981. Ontogeny of the molluscan shell field: a review. Zoologica Scripta 10: 61-79.

Lesoway, M.P., and L.R. Page. 2008. Growth and differentiation during delayed metamorphosis of feeding gastropod larvae: signatures of ancestry and innovation. Marine Biology 153: 723-734.

Lowenstam, H.A., and S. Weiner. 1989. On Biomineralization. Oxford University Press, New York.

Marin, F., and G. Luquet. 2004. Molluscan shell proteins. Comptes rendus Palevol 3: 469-492.

Mayr, E. 1960. The emergence of evolutionary novelties. Pp 349-380 *in* S. Tax, ed. Evolution after Darwin. University of Chicago Press, Chicago.

Meyers, M.A., A.Y.M. Lin, Y. Seki, P.Y. Chen, B.K. Kad, and S. Bodde. 2006. Structural biological composites: an overview. JOM (Journal of Materials) 58: 35-41.

Moczek, A.P. 2008. On the origins of novelty in development and evolution. BioEssays 30: 432-447.

Mouëza, M., O. Gros, and L. Frenkiel. 2006. Embryonic development and shell differentiation in *Chione cancellata* (Bivalvia, Veneridae): an ultrastructural analysis. Invertebrate Biology 125(1): 21-33.

Müller, G.B. 1990. Developmental mechanisms at the origin of morphological novelty: a side-effect hypothesis. Pp 99-130 *in* M.H. Nitecki, ed. Evolutionary Innovations. University of Chicago Press, Chicago.

Müller, G.B., and S.A. Newman. 2005. The innovation triad: an EvoDevo agenda. Journal of Experimental Zoology Part B: Molecular and Developmental Evolution 304: 487-503.

Müller, G.B., and G.P. Wagner. 1991. Novelty in evolution: restructuring the concept. Annual Review of Ecology, Evolution, and Systematics 22: 229-256.

Nielsen, C., and A. Nørrevang. 1985. The trochaea theory: an example of life cycle

phylogeny. Pp. 28-41 *in* S. Conway Morris, J.D. George, R. Gibson and H.M. Platt, eds. The Origin and Relationships of Lower Invertebrate Groups. Oxford University Press, Oxford.

Nützel, A., O. Lehnert, and J. Fryda. 2006. Origin of planktotrophy – evidence from early molluscs. Evolution & Development 8(4): 325-330.

Page, L.R. 1994. The ancestral gastropod larval form is best approximated by hatching-stage opisthobranch larvae: evidence from comparative developmental studies. Pp. 206-223 *in* W.H. Wilson, S.A. Stricker, and G.L. Shinn, eds. Reproduction and Development of Marine Invertebrates. Johns Hopkins University Press, Baltimore and London.

Page, L.R. 1995. Similarities in form and developmental sequence for three larval shell muscles in nudibranch gastropods. Acta Zoologica 76(3): 177-191.

Page, L.R. 1997. Ontogenetic torsion and protoconch form in the archaeogastropod *Haliotis kamtschatkana*: evolutionary implications. Acta Zoologica 78(3): 227-245.

Page, L.R. 2009. Molluscan larvae: pelagic juveniles or slowly metamorphosing larvae? Biological Bulletin 216: 216-225.

Palmer, A.R. 1979. Fish predation and the evolution of gastropod shell sculpture: experimental and geographic evidence. Evolution 33(2): 697-713.

Pearse, V., J. Pearse, M. Buchsbaum, and R. Buchsbaum. 1987. Living Invertebrates. Boxwood Press, USA.

Ponder, W.F., and D.R. Lindberg. 1997. Towards a phylogeny of gastropod molluscs: an analysis using morphological characters. Zoological Journal of the Linnean Society 199: 83-265.

Richardson, K.C., L. Jarett, and E.H. Finke. 1960. Embedding in epoxy resins for ultrathin sectioning in electron microscopy. Stain Technology 35: 313-323.

Ruppert, E.E., R.S. Fox, and R.D. Barnes. 2004. Invertebrate Zoology: A Functional Evolutionary Approach. Brooks/Cole – Thomson Learning Inc, USA.

Saleuddin, A.S.M., and H.P. Petit. 1983. The mode of formation and the structure of the periostracum. Pp 199-234 *in* A.S.M. Saleuddin and K.M. Wilbur, eds. The Mollusca, Vol. 4. Physiology, Part 1. Academic Press, New York.

Shen, X., A.M. Belcher, P.K. Hansma, G.D. Stucky, and D.E. Morse. 1997. Molecular cloning and characterization of Lustrin A, a matrix protein from shell and pearl nacre of *Haliotis rufescens*. The Journal of Biological Chemistry 272 (51): 32472-32481.

Silberglied, R.E. 1984. Visual communication and sexual selection among butterflies. Pp 207-223 *in* R.I. Vane-Wright and P.R. Ackery, eds. The Biology of Butterflies. Academic Press, London.

Simkiss, K., and K.M. Wilbur. 1989. Biomineralization - Cell Biology and Mineral Deposition. Academic Press, Inc., San Diego.

Strathmann, M.F. 1992. Reproduction and Development of Marine Invertebrates of the Northern Pacific Coast. University of Washington Press, Seattle.

Thorson, G. 1950. Reproductive and larval ecology of marine bottom invertebrates. Biological Reviews 25: 1-45.

True, J.R., and E.S. Haag. 2001. Developmental system drift and flexibility in evolutionary trajectories. Evolution & Development 3(2): 109-119.

Vermeij, G.T. 1982. Unsuccessful predation and evolution. The American Naturalist 120(6): 701-720.

Weiner, S., W. Traub, and S.B. Parker. 1984. Macromolecules in mollusc shells and their functions in biomineralization. Philosophical Transactions of the Royal Society of London B: 425-434.

Weiss, I.M., N. Tuross, L. Addadi, and S. Weiner. 2002. Mollusc larval shell formation:

amorphous calcium carbonate is a precursor phase for aragonite. Journal of Experimental Zoology 293: 478-491.

West, K., and A. Cohen. 1996. Shell microstructure of gastropods from Lake Tanganyika, Africa: adaptation, convergent evolution, and escalation. Evolution 50(2): 672-681.

Wilbur, K.M., and A.S.M. Saleuddin. 1983. Shell formation. Pp. 236-288 *in* A.S.M. Saleuddin and K.M. Wilbur, eds. The Mollusca, Vol. 4, Part 1. Academic Press, New York.

Wilt, F.H., C.E. Killian, and B.T. Livingston. 2003. Development of calcareous skeletal elements in invertebrates. Differentiation 71: 237-250.

Wolpert, L. 1999. From egg to adult to larva. Evolution & Development 1(1): 3-4.

Appendix: Glossary of Terms

amorphous calcium carbonate (ACC): non-crystalline form of calcium carbonate (least stable form)

apertural beak: protruding anterior margin of the shell formed as a result of the velar notches of the aperture

aragonite: less stable crystal polymorph of calcium carbonate, primary polymorph used in the formation of larval gastropod shells

biomineral: mineral produced by a living organism

calcite: most stable crystal polymorph of calcium carbonate

delay of metamorphosis: occurs during late stage of larval development, describes the ability of a larva to maintain metamorphic competence and survive in the absence of the environmental cues required to trigger metamorphosis

extrapallial space (EPS): space delineated by the outer mantle epithelium and periostracum, sealed off from the outer environment to allow shell formation

growing edge (GE) cell: cell of the shell growth region associated with the growing edge of the periostracum, often bearing cytoplasmic extensions from the apical surface and containing electron dense granules

heterochrony: a change in rate or timing of the onset or termination of a developmental event

hypermorphosis: the development of a character that extends beyond the point at which it stopped in the ancestor

intercellular space: space created by cytoplasmic extensions originating from the GE cells

mantle: epithelium covering the dorsal surface of the snail (covering the visceral mass) and is responsible for the secretion of the molluscan shell

metamorphic competence: the stage when larvae can undergo the morphological transformation that will allow them to assume the lifestyle of the benthic juvenile

microvilli-bearing (MV) cell: cell of the shell growth region neighbouring the GE cells and bear long, densely packed microvilli extending from the apical surface

ontogenetic torsion: morphogenetic movement where the head and foot rotate by 180˚ relative to the shell, mantle and visceral lobe

organic matrix: organic macromolecules controlling mineral composition, crystal orientation, and shape of shell biomineral

periostracum: proteinaceous outer layer covering the molluscan biomineralized shell, protecting the shell from dissolution

pre-displacement: a process in which the character begins to develop earlier in the descendant than in the ancestor

protoconch: shell secreted during the embryonic phase of gastropod development (embryonic shell)

protoconch II: shell secreted during the larval phase of gastropod development (larval shell)

proximal (Pr) cell: cell of the shell growth region neighbouring the GE cells, proximal to the shell field invagination in early development and facing the extrapallial space later in development

shell field: thickening of cells in the dorsal ectoderm of an embryo that appears after the completion of gastrulation

shell field invagination: in the early embryo, brings together the cells of the shell growth region that are responsible for secreting the early beginnings of the periostracum

shell growth region: term used to describe the cells at the periphery of the mantle fold responsible for the secretion of the shell

siphonal canal: an extension of the shell near the aperture that allows for the protection of the extended siphon, the organ that is used (post-metamorphosis) by the snail for chemoreception and to bring water in and out of the mantle cavity

teleoconch: shell secreted during the post-metamorphic juvenile phase of gastropod development (juvenile shell)

velar lobes (velum): ciliated organ used by molluscan larvae for swimming and feeding (in planktotrophic larvae) that is lost at metamorphosis

velar notches: indentations at the apertural margin of larval shell that aid in accommodating large velar lobes of planktotrophic larvae

visceral mass: the region of a gastropod's body that includes most of the visceral organs: stomach, digestive gland, posterior esophagus, intestine, nephridia (or single

nephridium), and heart. Adult gastropods also have a gonad included within the visceral mass.